The parasitic nematode *Strongyloides ratti* exists as populations of long-lived asexual lineages.

Rebecca Cole[1], Nancy Holroyd[2], Alan Tracey[2], Matt Berriman[2] and Mark Viney[1,3]

1. School of Biological Sciences, University of Bristol, Bristol, BS8 1TQ, UK.

2. Wellcome Trust Sanger Institute, Wellcome Trust Genome Campus, Hinxton, CB10 1SA, UK.

3. Department of Evolution, Ecology and Behaviour, University of Liverpool, Liverpool L69 7ZB, UK.

Abstract

Nematodes are important parasites of people and animals and in natural ecosystems they are a major ecological force. *Strongyloides ratti* is a common parasitic nematode of wild rats and we have investigated its population genetics using single worm, whole genome sequencing. We find that *S. ratti* populations in the UK consist of mixtures of asexual lineages that are widely dispersed across a host population. These parasite lineages are likely very old and may have originated in Asia from where rats originated. Genes that underly the parasitic phase of the parasite's life cycle are hyperdiverse, compared with the rest of the genome, and this may allow the parasites to maximise their fitness in a diverse host population. These patterns of parasitic nematode population genetics have not been found before and may also apply to *Strongyloides* spp. that infect people, which will affect how we should approach their control.

Introduction

Parasitic nematodes are important parasites of humans, livestock and other animals. In humans, parasitic nematodes are responsible for four of the twenty World Health Organization-defined Neglected Tropical Diseases (WHO 2021). In natural ecosystems parasitic nematodes are highly abundant and so a major force affecting host populations (Lafferty *et al.,* 2005; Kuris *et al*., 2008), so understanding parasites' biology is critical in understanding wider ecological patterns and processes. Study of the population genetics of parasitic nematodes can give important insights into their biology and patterns of transmission in host populations. This has been studied extensively in nematodes parasitizing livestock, for example finding that they exist with very large effective population sizes, showing limited population genetic substructure, likely due to the high rate of livestock movement (Blouin *et al.* 1985; Redman *et al*., 2015; Sallé *et al*., 2019). The population genetics of parasitic nematodes infecting humans has also been investigated to understand their host range and zoonotic potential (Criscione *et al.*, 2007; Thiele *et al*., 2018). In contrast, there has been much more limited study of the population genetics and genomics of nematodes infecting natural, unmanaged species (Cole and Viney, 2018).

Strongyloides spp. are a genus of parasitic nematodes, with two species – *S. stercoralis* and *S. fuelleborni* – infecting some 100-600 million people worldwide (Bethany *et al.,* 2006; Buonfrate *et al*. 2020). *S. ratti* is a common parasite of rats, *Rattus norvegicus* (Fisher and Viney, 1998). In the *Strongyloides* spp. life cycle hosts are infected by parasitic female worms only that reproduce parthenogenetically (Viney, 1994), producing eggs that pass out of the host in its faeces. Outside of the hosts, larvae can develop directly into infective larvae that then infect new hosts. Alternatively, and facultatively, larvae outside of the host can develop into a single generation of free-living adult males and females that reproduce sexually (Viney *et al*., 1993), with their progeny then also developing into infective larvae to infect new hosts. Genetically, this means that *Strongyloides* reproduces by obligatory mitotic parthenogenesis inside the host and by facultative sexual reproduction outside of the host. The choice between asexual, direct development and sexual, indirect development is affected by environmental conditions (particularly the host immune response and the temperature outside of the host), but genotypes also differ in their propensity for these two developmental routes (Viney *et al.* 1992; Harvey *et al.* 2000).

Strongyloides' mode of reproduction is very likely to affect its population genetics. If reproduction is exclusively by mitotic parthenogenesis, then the only source of genetic variation is mutation, and such a population would consist of an assemblage of different genetic lineages. In this scenario the mutation rate of a species is key in determining the extent of variation within a population. The occurrence of some sexual reproduction would allow genetic lineages of parasites to recombine, though the extent to which this will happen depends on the frequency with which sexual reproduction occurs. A three locus study of *S. ratti* in the UK found that it consists of one interbreeding population, likely mainly reproducing by direct, asexual reproduction (Fisher and Viney, 1998).

S. ratti has a compact 43 Mbp genome, consisting of 2 autosomes and an X chromosome, and its genome assembly is among the most contiguous for any nematode. This facilitates

the population genomic analysis of wild *S. ratti.* Further, genomic, transcriptomic and proteomic analyses have identified genes that are putatively critical to *Strongyloides'* parasitic lifestyle. These were characterised in two ways: genes whose expression was significantly greater in the parasitic female stage compared with the free-living female stage; and genomic clusters of genes belonging to one of three families (encoding astacin-like metallopeptidases, CAP domain-containing proteins, acetylcholinesterases), which are gene families that have expanded as *Strongyloides* evolved to become parasites (Hunt *et al*., 2016).

In many, but not all, host-parasite systems, parasites can locally adapt to their host population, which enhances the fitness of those parasite genotypes (Greischar *et al.,* 2007). The genes and gene products underlying parasite local adaption are not well known. In *Strongyloides* the genes that have been shown to be central to its parasitism are at the interface between the parasite and its host and therefore may play a role in such adaptation. In such a scenario these genes could be under different selection pressures compared with the rest of the genome and so may have population genetic patterns that differ from the rest of the genome.

Here we report the whole-genome, fine-scale population genomics of *S. ratti* in a wild rat population, describing how parasite genotypes are distributed among individual hosts. We find that *S. ratti* populations in the UK exist as a mixture of asexual lineages and that these lineages are likely very long lived. Comparison of these lineages with historical, geographically dispersed samples shows that some of these lineages may be very widely spatially dispersed. We find that genes and gene clusters critical to the parasitic phase of the *S. ratti* life cycle are genetically hyperdiverse, compared with the rest of the genome. This hyperdiversity may contribute to *S. ratti*'s local adaption to its hosts within the context of it existing as long-lived asexual lineages.

Results

S. ratti is a common parasite of rats

We sampled rat faecal pellets from three sites in the southwest UK (**Figure 1**), from which we isolated 10,471 *S. ratti* infective larvae from 114 pellets (from a sample of 308). The proportion of infected faecal pellets significantly differed among the three sites (13, 47 and 62 % at sites CA, AM and LA respectively; χ^2 = 48.9, *df* = 2, P < 0.0001) (**Figure 1; Supplementary Table 1**), but is consistent with a previous report of a high prevalence of *S. ratti* in wild rats in the UK (Fisher and Viney, 1998). The number of *S. ratti* larvae per pellet ranged from 1 – 1,730 (**Supplementary Figure 1**). While culturing these faeces for *S. ratti* we did not observe any sexual free-living adults. We genotyped rat faecal pellets to assign these to individual rats finding that 132 genotyped pellets belonged to 112 rats.

S. ratti is partially genetically clustered at sample sites

We investigated the population genetics of *S. ratti* by analysing whole genome sequence of 90 individual infective larvae collected from the three sites. We identified 170,666 SNPs, giving an average density of 4.1 SNPs per kb. A total of 614 SNPs were tri-allelic, the remainder bi-allelic, with a ratio of 1.77 of transitions to transversions. Considering all SNPs together, the 90 parasites were in HWE (χ^2 = 13.65, *df* = 19.35, P = 0.48) but this varied among SNPs. Overall, there was more heterozygosity than expected; specifically, allele frequencies predicted that 28% of SNP loci would be heterozygous in individual worms, whereas 36% (range 28-58%) were.

We analysed the pattern of parasite population genetic variation (i) within and among rat hosts, and (ii) within and among sampling sites, finding evidence of some differentiation of the parasites among the sample sites. The pairwise relatedness (Φ) among the 90 parasites was non-normal (Shapiro-Wilkes test for normalcy W = 0.902, P < 0.0001), suggesting genetic clustering among the worms at some level (**Supplementary Figure 2**). *S. ratti* parasitic females reproduce by mitotic parthenogenesis (Viney, 1994) and so siblings will be genetically identical save for individual-specific mutations. We did not detect putative sibling parasites within individual rats, despite sampling up to 4 parasites from each rat. (**Supplementary Figure 3**). This suggests that faecal pellets commonly contained larvae of more than 4 genotypes. In faecal pellets containing $\geq$ 10 larvae, if there indeed had only been 4 genotypes present then our chance of detecting the 4 would have been $\leq$ 0.19. It is more likely that faecal pellets contained worms of more than 4 genotypes. Specifically, we had a $\geq$ 0.50 chance of detecting 4 unique genotypes when: $\geq$ 6 genotypes were actually present in pellets containing 12-18 larvae; $\geq$ 7 genotypes were present in pellets containing 19-31 larvae. The average relatedness among pairs of parasites from the same rat and among parasites from different rats (Φ = 0.22 and 0.214, respectively), was not significantly different (t = -0.32, *df* = 108.81, P = 0.75). Thus, we conclude that individual rats contain genetically diverse parasites (consistent with our *S. ratti* RFLP genotyping, see Materials and Methods section), meaning that genetic clustering of parasites is not at the level of the rat.

Figure 1. **Map of sampling sites.** Showing site LA near Bristol, AM on the English coast of the Bristol Channel, and CA on the Welsh coast of the Bristol Channel. Road bridges crossing the channel are shown as dotted lines; a train tunnel is not shown.

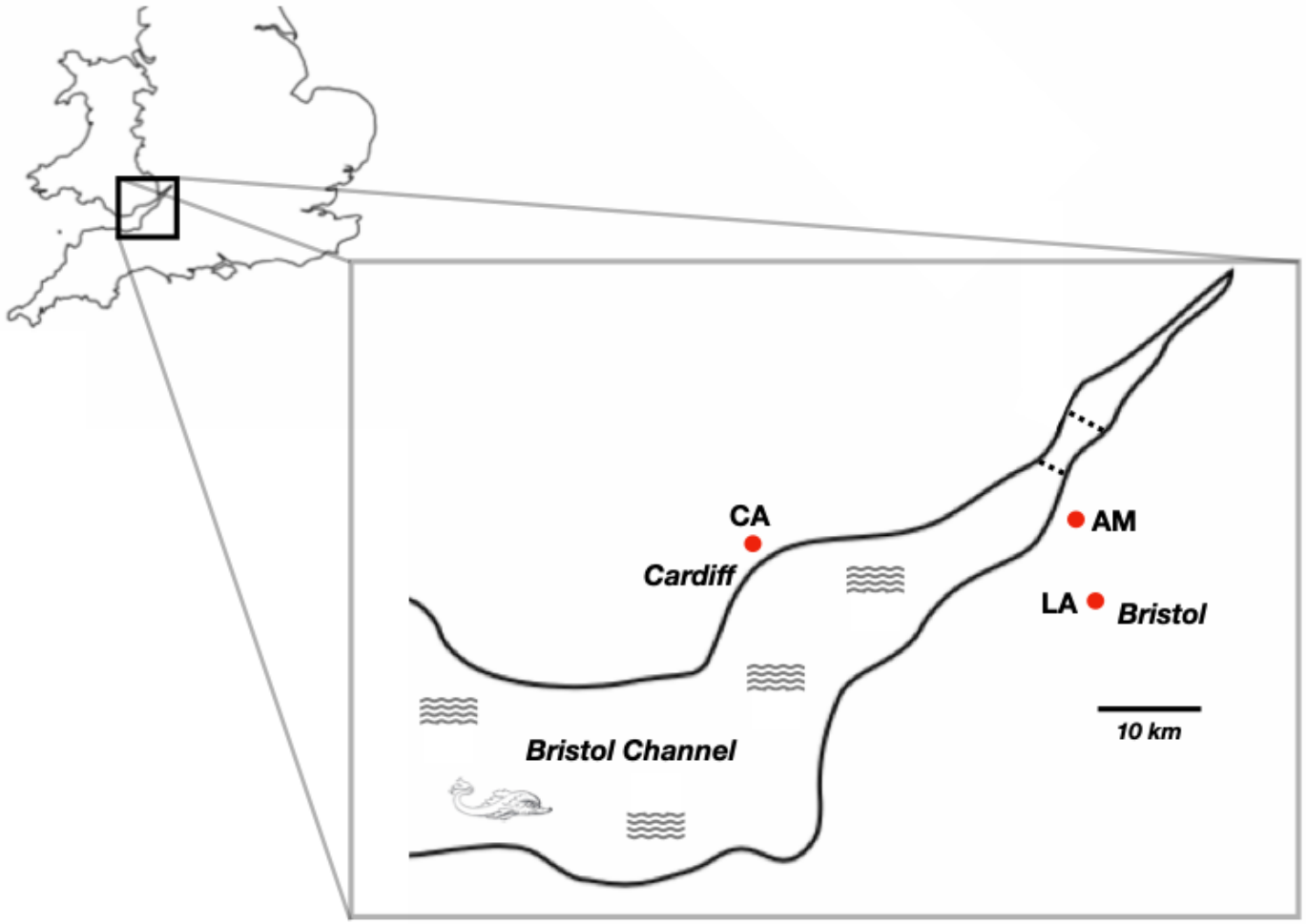

However, parasites from the same sample site were more closely related (mean same site $\Phi = 0.225$; single, same site Φ, CA = 0.128, LA = 0.258, AM = 0.227) than parasites from different sample sites ($\Phi = 0.206$) ($t = -3.68$, $df = 3975.9$, $P \leq 0.001$) (**Figure 2**). Overall, F_{ST} was very low (0.02), and indeed zero between parasites at the two English sample sites (**Figure 2**). Together, these results show that there is some genetic clustering of *S. ratti* at the level of the sampling site, but not at the level of individual rats.

S. ratti consists of divergent genetic clades that are widely distributed

We examined the parasite diversity more closely by constructing neighbour-joining dendrograms. This revealed five parasite clades, with most worms (78 of the 90) in one of three clades (clades 1 – 3) (**Figure 3A**). Maximum likelihood trees also confirmed the existence of these clades (**Figure 3B**; **Supplementary Figure 4**). We examined the admixture among the 90 parasites, which most reliably grouped the parasites into five genetic groups, corresponding to the five clades defined by the neighbour-joining tree (**Figure 3C; Supplementary Figure 5**). Moreover, even under other subdivision scenarios there is no evidence for gene flow (**Supplementary Figure 5**).

Parasites belonging to the three main clades were present in all three sampling sites, in ratios expected based on the number of sequenced parasites from each sampling site (Fisher's exact test, $P = 0.14$). Individual rats contained parasites from multiple clades; specifically, 11 rats contained parasites from two clades, and 3 rats contained parasites from three clades. Principal Component Analysis produced similar results, showing clustering of parasites within clades, and that these clades were dispersed across the three sampling sites (**Supplementary Figure 6**).

Analysis of Φ and F_{ST} within and among clades 1 – 3 is consistent with *S. ratti* being structured into sympatric, genetically distinct clades, with the three clades dispersed across the three sampling sites. Specifically, Φ was high within clades, especially clades 1 and 3 (0.43 and 0.45, respectively), but lower between clades; F_{ST} among the clades was 0.3 and similar (0.22 – 0.35) between clades (**Table 1**). Given that we did not observe any free-living sexual stages of *S. ratti* this further suggests that these clades are asexually derived and maintained.

The population genetic structure of *S. ratti's* mitochondrial genome consists of three divergent genetic clades that are not strongly associated with sampling sites, which is consistent with the nuclear genome results. Specifically, in the mitochondrial genome we identified 156 SNPs (average density 9.3 SNPs per kb) identifying 58 haplotypes among the 90 parasites. There was a strong, positive correlation between the pairwise similarities of mitochondrial and nuclear genomes (Mantel test, $r = 0.76$, $P < 0.01$), and between minimum spanning maps of mitochondrial haplotypes and neighbour-joining trees of nuclear genomes (**Supplementary Figure 7**). The number of mitochondrial SNPs in same sampling site and different sampling site comparisons (23.6 and 24.2, respectively) were not significantly different ($t = -0.98$, $df = 3771$, $P = 0.33$).

Figure 2. Physical and genetic differences among parasite and host populations. A schematic view of (A) Geographical distance among the sample sites, where direct distances between the sites are AM-LA = 9.2 km, CA-AM = 31.5 km, CA-LA = 33.5 km. (B) average pairwise relatedness (shown as 1-Φ) where Φ AM-LA = 0.244, CA-AM = 0.157, CA-LA = 0.162, (C) F_{ST} among parasites, from the three sample sites where, AM-LA = 0, CA-AM = 0.03, CA-LA = 0.03 and (D) ${}^{S}H_{UA}$ among rats where, AM-LA = 0.21, CA-AM = 0.22, CA-LA = 0.15. Note, the scales of the metrics varies among the panels.

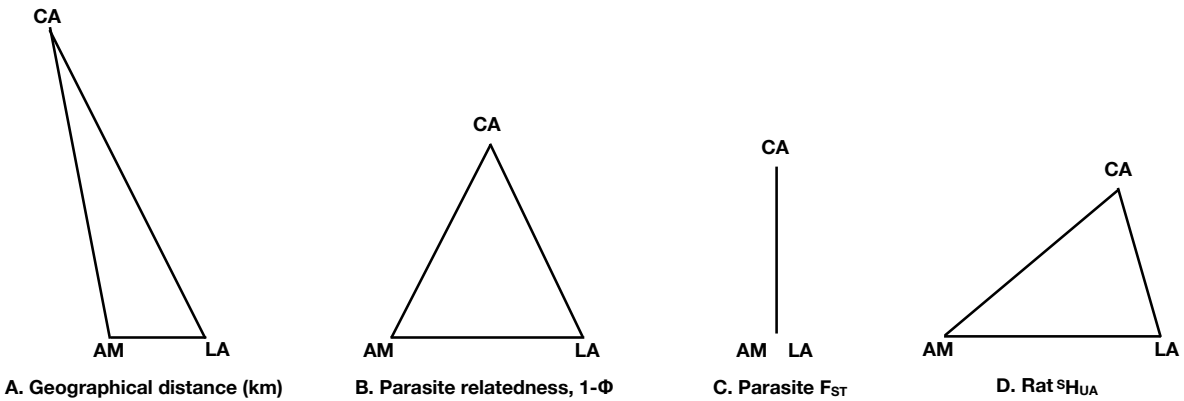

Figure 3. *S. ratti* consists of distinct genetic clades that are widely distributed. (A) A neighbour-joining dendrogram showing the five clades; (B) a maximum likelihood tree based on chromosome 1 where individuals are colour coded according to their clade membership in the neighbour-joining tree; the scale bar is 2 x 10^{-4} substitutions per site; chromosome specific trees are shown in **Supplementary Figure 4**; (C) the admixture of the 90 larvae for K = 5, which is the most strongly supported value of K; the order of individual worms and their neighbour-joining tree clade membership is shown in **Supplementary Figure 5.** Note, the colour coding in (C) does not correspond to (A) or (B).

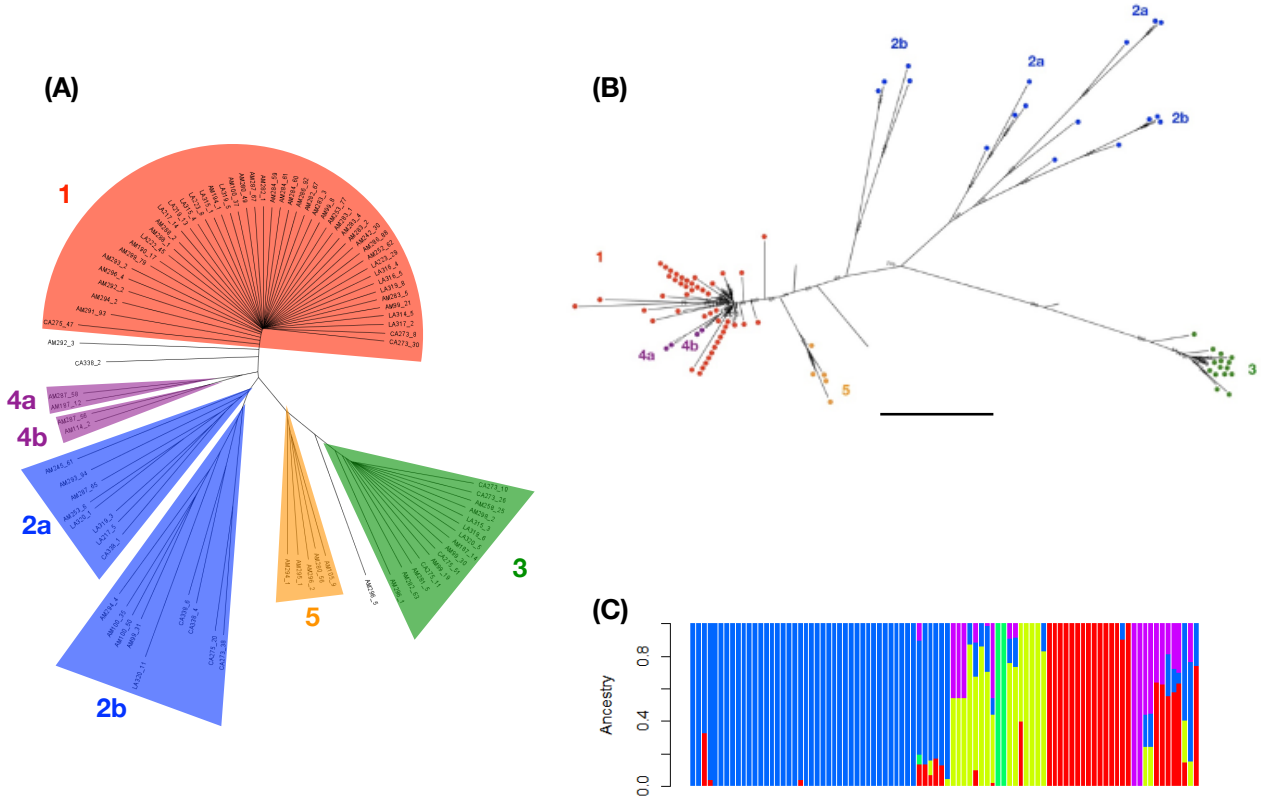

We wanted to investigate if the rat host population genetic structure enforced a population genetic structure on the parasites because of the partitioning of parasites among individual hosts. To do this we investigated the population genetics of the rats by genotyping faecal pellets at nine microsatellite locus (**Supplementary Table 2**). These loci were generally not in Hardy-Weinberg equilibrium (HWE); specifically 8, 3 and 5 of the 9 loci at sites CA, AM and LA, respectively, were not (**Supplementary Table 3**). Rat allele frequencies differed markedly among sampling sites, consistent with restricted rat gene flow among the sites. The pairwise relatedness among rats was higher within sites than among sites (average Ritland and Lynch relatedness values 0.06 and -0.06, respectively), and the distribution of these relatedness values at each site had a right-hand skew (**Supplementary Figure 8**), showing more closely related pairs of individual rats within sites than expected by chance. We could assign rats to each sample site based on allele frequencies with 89% accuracy. Shannon's mutual information index ($^{S}H_{UA}$), which does not assume HWE (Hedrick, 2005; Jost *et al.,* 2018), shows that there is moderate genetic differentiation among rats from the three sites (**Figure 2**). Together these results – differences in allele frequencies among sample sites, higher within-site than among-site relatedness, high accuracy in assignment to sample site, moderate values of $^{S}H_{UA}$ – show that there is genetic differentiation among rats at the three sampling sites. The evidence of moderate genetic differentiation among rats at sample sites is broadly consistent with the geographical separation of the three sites, and with limited migration of rats among the sites (**Figure 1**), as has been observed with urban rats (Combs *et al.* 2017). Notably, the genetic structure of the *S. ratti* populations does not mirror that of its rat hosts.

We sought to understand the age of the *S. ratti* clades. We did this using the ML trees of chromosomes 1 and 2 to calculate the number of substitutions per site that have occurred since the last common ancestor (LCA) of (i) clade 3 and (ii) clades 1 and 3. Assuming neutrality and the *C. elegans* mutation rate of 2.7 x 10^{-9} per site per generation (Denver *et al.,* 2009), we calculate that there were an average of 18,401 (range 17,037 – 20,195) and 322,011 (range 213,185 – 393,589) generations since the LCA of clade 3 and of clades 1 and 3, respectively. To convert these generations to years we assumed, conservatively, that there are two *S. ratti* generations per year in the wild, noting that *S. ratti* parasitic females have a maximum lifespan of a year when infecting immunodeficient laboratory rats (Gardner *et al.* 2006). On this basis the LCA of clade 3 existed approximately 9,000 years ago (*i.e.* 1200 CE) and the LCA of clades 1 and 3 approximately 161,000 years ago, which is the Middle Pleistocene (now renamed the Chibanian). Given the dates, it is a reasonable scenario that the LCA of these *S. ratti* clades evolved outside of the UK and arrived in the UK with their hosts. *R. norvegicus* is thought to have arrived in mainland Europe from Asia about 1,800 years ago (*c.* 200 CE) and into the British Isles from *c.*1750 CE (Lever 1977; Zeng *et al*. 2018), where the black rat (*R. rattus*) had likely been since *c.* 1100 CE. Clades 1 and 3 may well have emerged in Asia where *R. norvegicus* originated, and the LCA of clade 3 perhaps in mainland Europe.

We also investigated the spatial and temporal extent of the *S. ratti* clades by examining whole genome sequences of 10 *S. ratti* isofemale lines derived from rats sampled from the UK and Japan between 1989 and 2012 (**Supplementary Table 4**). A neighbour-joining

252 dendrogram of these isofemale lines and the 90 wild parasites (sampled in 2017/18) showed
253 that these isofemale lines are not genetically distinct from the 90 parasites, occurring in
254 clades 1, 2 and 4 (**Supplementary Figure 9**). This observation – particularly of the two
255 Japanese isofemale lines – is consistent with an Asian ancestry of the 90 contemporary UK
256 genotypes, and more generally with the idea that *S. ratti* genotypes exist as long lived,
257 asexually maintained lineages.
258
259 In summary, these results show that *S. ratti* populations consist of mixtures of different
260 genetic clades consisting of asexually maintained lineages that are likely very long lived –
261 over thousands and tens of thousands of years – and widely distributed across the global
262 host population. The *S. ratti* life cycle is obligately mitotically parthenogenetic (Viney 1994),
263 with facultative sexual reproduction (Viney *et al.,* 1993); the population genetic structure that
264 we have observed suggests that sexual reproduction occurs vary rarely, if at all, in these
265 populations. We observe no obvious geographical localisation of the different parasite
266 clades, which might be expected with geographically-based host local adaptation. Indeed,
267 given the likely asexual reproduction of these populations it would therefore appear that *S.*
268 *ratti* cannot genetically adapt to its local host populations except through mutational
269 processes.
270
271 ***S. ratti* genes involved in parasitism are highly diverse**
272 We next investigated the diversity of genes that *S. ratti* uses in the parasitic phase of its life
273 cycle. We focussed on two sets of genes: (i) "parasitism genes", which are genes whose
274 expression is at least one $\log_2$-fold greater in the parasitic female morph compared with the
275 free-living female morph, and (ii) "expansion clusters", which are genomic regions containing
276 four or more genes encoding members of either astacin-like metallopeptidase, CAP domain-
277 containing protein, or acetylcholinesterase families, which previous analyses have identified
278 as having expanded with the evolution of parasitism in *Strongyloides* (Hunt *et al.,* 2016).
279
280 Genetic diversity in *S. ratti* is not evenly distributed across the *S. ratti* genome
281 (**Supplementary Figure 14**), and we identified high SNP diversity regions, consisting of $\geq$
282 200 SNPs per 10 kb. We first asked how often parasitism or free-living (which are *vice versa*
283 compared with parasitism genes) genes occurred in these high SNP diversity regions. We
284 found that parasitism genes were significantly overrepresented within these high diversity
285 regions, compared with their representation in highly conserved genomic regions ($\leq$ 4 SNPs
286 per 10 kb region), or across the genome as a whole (**Figure 4A; Supplementary Table 5**).
287 In contrast, free-living genes were represented at the same rate in high diversity regions,
288 highly conserved regions, and across the genome as a whole (**Figure 4A**).
289
290 Furthermore, two classes of genes – those encoding astacin-like metallopeptidases and
291 CAP domain-containing proteins, both of which are associated with parasitism in *S. ratti* –
292 were more common in these high diversity regions, compared with the genome as a whole.
293 Specifically, 5.6 and 11.8 % (95% confidence intervals 2.6-10.3 and 6.3-16.4 %,
294 respectively) of genes in these regions encode astacin-like metallopeptidase and CAP
295 domain-containing proteins, which is higher than their representation across the whole
296 genome (1.5 and 0.7 %, respectively).

Figure 4. *S. ratti* genes involved in parasitism are highly diverse. (A) The percentage of genes in high diversity regions (≥ 200 SNPs per 10 kb), conserved regions (≤ 4 SNPs per 10 kb), or across the whole genome as a whole, that are parasitism or free-living genes. There were 100 genes in the variable regions, 137 in the conserved regions, and 12,464 across the whole genome. Parasitism and free-living genes are as defined by Hunt *et al.,* 2016. Errors bars are 95 % confidence intervals. (B) The number of SNPs per kb (+1 SD) in parasitism genes (range 0-85.9), free-living genes (0-41.5) or across the genome as a whole. The SNP density for parasitism and free-living genes is calculated from coding sequence only; for the whole genome, all sequence data are used and so no SD is given. (C) The density of SNPs of different effect in parasitism and free-living genes. (D) The density of SNPs of different effect in expansion clusters and flanking regions.

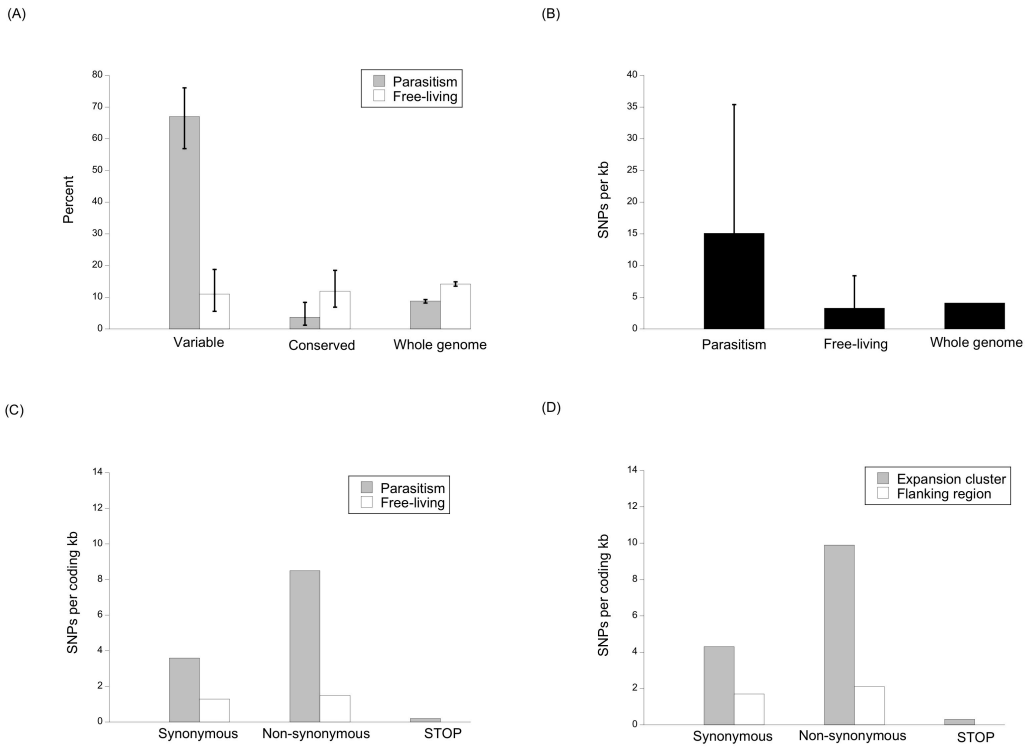

306 We compared the SNP density among the hundred most parasitic and most free-living
307 genes, though we excluded six of the parasitism genes due to concerns about their
308 underlying sequence assembly, leaving 94 parasitic genes (**Supplementary Tables 6 and**
309 **7**). Parasitism gene SNP density was approximately four times that of free-living genes, or
310 that of the genome as a whole (**Figure 4B**). The SNPs in these parasitism genes mainly
311 code for non-synonymous substitutions, rather than synonymous substitutions, which
312 contrasts with free-living genes, where the rate of both types of SNPs occurred with similar
313 frequency (**Figure 4C**).
314
315 We also found evidence of high genetic diversity in *S. ratti*'s expansion clusters, compared
316 with the flanking regions (**Supplementary Table 8**). SNPs were three times more dense in
317 the expansion clusters than in the flanking regions (SNP density (SD) per kb 15.9 (18.3) and
318 4.6 (7.2), in expansion clusters and flanking regions, respectively). Strikingly, SNPs within
319 expansion clusters were approximately twice as likely to code non-synonymously, rather
320 than synonymously, unlike the flanking regions where these rates were similar (**Figure 5D**);
321 a pattern also seen for each individual expansion cluster, except clusters 1 and 8
322 (**Supplementary Table 5**).
323
324 We thought about possible reasons for the elevated genetic diversity in genes involved in
325 *S. ratti*'s parasitism. Parasites can locally adapt to their hosts to maximise parasite fitness,
326 and we hypothesised that evolution of the expansion clusters, independent of the rest of the
327 genome, could be a means by which host local adaptation occurs, where the expansion
328 clusters evolve differently from the rest of the genome. To investigate this, we created
329 neighbour-joining trees based on individual expansion clusters to see if they strongly
330 diverged from the whole genome-based trees. However, in these expansion cluster-specific
331 trees, the whole genome-defined clades 1 and 3 were still strongly evident (**Supplementary**
332 **Figure 15**). We next measured the selection in the expansion clusters and their flanking
333 regions, but could also find no consistent evidence for diversifying selection in the expansion
334 clusters compared with their flanking regions (**Supplementary Table 9**). These results
335 therefore do not support the idea that the expansion clusters are locally adapting to host
336 genotypes.
337
338 Together, these observations – that highly variable genomic regions have an over-
339 representation of parasitism genes, and of astacin-like metallopeptidase and CAP domain-
340 containing coding genes; that parasitism genes have SNP densities that are higher than
341 those of free-living genes; that parasitism genes have a comparative excess of non-
342 synonymous-coding SNPs; that expansion clusters have higher SNP densities and an
343 excess of non-synonymous-coding SNPs – shows that in *S. ratti* there is a concentration of
344 genetic diversity within genes and genomic regions that very likely play a key role in the
345 parasitic phase of its life cycle.

Discussion

Parasitic nematodes are ubiquitous parasites of animals and are partitioned among individual hosts between which they must transmit, and so parasite and host biology can affect their population genetic structure ((Blouin *et al.* 1985; Cole and Viney, 2018). Understanding the population genetics of parasitic nematodes can give an insight into their population biology, which is poorly known outside of species infecting humans and livestock (Cole and Viney, 2018).

For the facultatively sexual parasite of rats *S. ratti* we have discovered that in the UK its population consists of a mixture of genetically diverse clades, where those clades are widely dispersed across host populations (and possibly on a global scale), with very little evidence of structuring across three host populations. By estimating the age of the last common ancestor of these clades we find that these parasites lineages are very long lived, existing over some thousands to tens of thousands of years. This result does raise the question of whether these different lineages should be consider as different species or sub-species. Considering the age of these lineages with the history of the spread of the brown rat from Asia into mainland Europe and then to the British Isles, a plausible scenario is that the *S. ratti* lineages originated in Asia and spread to the UK, and likely the world. It is notable that the neighbour-joining dendrograms shows Japanese-derived *S. ratti* isofemale lines among the UK-derived genotypes. More extensive global sampling of *S. ratti* genetic diversity is now warranted.

This is a pattern of population genetic variation that has not, as far as we are aware, been observed in a parasitic nematode before. The life cycle of *S. ratti* contains an obligatory asexual parthenogenetic stage (Viney, 1994), as well as a facultative sexual stage (Viney *et al*., 1993). We observed no sexual stages during our work, suggesting that sexual reproduction is very rare, or even absent, in these UK populations, consistent with previous observations (Viney *et al.* 1992; Fisher and Viney, 1998). The population genetics of the populations that we studied is also consistent with the absence of sexual reproduction. Other lines of *S. ratti* (from Japan and a long-term lab adapted line originally isolated from the United States) show some development of free-living males and females, suggesting that some sexual reproduction may occur in wild *S. ratti* populations beyond the UK (Viney *et al.,* 1992). Even low levels of sexual reproduction can be effective in the spread od alleles in a population, especially with strong selection (Hartfield, 2016).

In contrast to the parasites' population genetic patterns, the host rat populations did show some evidence of population genetic differentiation among the different sample sites, consistent with restricted movement of rats between the sites. Studies of the population genetics of rats in cities have also shown evidence of limited dispersal of rats and so population genetic differentiation among rats in different city regions (Gardner-Santana *et al.,* 2009).

Understanding a parasite's population genetic structure can be important in understanding the host range of a parasite, which is of applied interest for parasites of humans. For example, population genetic analysis has been used to understand the possibly changing

host range of Guinea worm (*Dracunculus medinensis*) in human and dog hosts during sustained control efforts in human populations (Durrant *et al*., 2020). There is considerable interest in understanding the host range of *S. stercoralis* that infects people; specifically, *Strongyloides* in dogs has been considered to be a source of human infection (Jaleta *et al.,* 2017). If the population genetic structure we have observed with *S. ratti* – a mixture of asexually maintained clones widely distributed across host populations – also pertains in *S. stercoralis*, then there is likely to be considerable complexity in understanding the population genetics and host range of *S. stercoralis* genotypes. Where a species exits as a collection of asexually maintained lineages, then each lineage could diverge genetically, which raises the possibility that *S. stercoralis* could exist as a mixture of lineages each with different host ranges, for example some able only to infect people, some only able to infect dogs and some intermediate. Current approaches to studying the host range of *S. stercoralis* have commonly only used single or a few loci, which cannot resolve more complex patterns of population genetic variation. Whole genome analysis (following whole genome amplification) of *S. stercoralis* from people in Japan and Myanmar found differences between parasites from these two sources (Kikuchi *et al.,* 2016). If population genetic structure similar to *S. ratti's* also occurs in *Strongyloides* spp. infecting people and livestock, then there will be consequences for the evolution of anthelminthic resistance. In the absence of sexual reproduction, anthelmintic resistance could evolve separately in different *Strongyloides* lineages, but would not be passed among them. The effect of this might be to slow the development of anthelminthic resistance in *Strongyloides* populations, compared with obligatory sexually reproducing nematodes, though with *Strongyloides* sustained anthelminthic use would, of course, select against anthelminthic sensitive genotypes.

Genomic analyses of *Strongyloides* have discovered genes and gene families that play a critical role in the parasitic phase of its life cycle. We have discovered that in wild *S. ratti* both parasitism genes and genes in expansion clusters are highly diverse compared with other genes. Of particular note, many of these SNPs in the parasitism genes and genes in expansion clusters we observed are predicted to code for non-synonymous substitutions, meaning that this genetic diversity may cause functional differences in the gene products. The parasitism genes and genes in expansion clusters are dominated by large gene families. Large families can allow genetic diversity to accumulate among gene family members because any potential negative fitness consequence of a mutation in one gene of a family, could be effectively ameliorated by others in that family. In this way, large gene families can allow the exploration of genetic space.

Our observation of comparatively high genetic diversity in these genes is particularly interesting in light of recent observations of genetic diversity in the free-living nematode *Caenorhabditis* spp. Specifically, analysis of worldwide populations of *C. elegans* find that genetic variation is concentrated in a number of genomic regions (56 and 19 kb mean and median size, respectively), with evidence suggesting that diversity in these regions is maintained by balancing selection (Lee *et al*., 2021). In the *C. tropicalis* genome, genetic variation is also distributed heterogeneously across its genome, for example with some 140 high genetic diversity classified regions extending for more than 30 kb (Noble *et al*., 2021). While there is a superficial similarity between the patterns of genomically concentrated genetic diversity in two *Caenorhabditis* species and in *S. ratti*, the mechanisms generating

these patterns might be different. Notably, in *S. ratti* we did not find any evidence of diversifying selection in the expansion cluster genes. What these two *Caenorhabditis* studies and the present study do demonstrate is that detailed, whole genome analysis of wild individuals is uncovering hitherto un-expected patterns of genomic diversity, which are likely to exit in other taxa too, and which need to be investigated.

Parasites have commonly been found to locally adapt to their host populations (Lively *et al*., 2004; Greischar and Koskella, 2007). If such a phenomenon was occurring in *S. ratti* then it may be manifest as geographical clustering of parasite genotypes *per se* or geographical clustering of parasitism gene genotypes and / or expansion cluster genotypes. However, the dispersion of *S. ratti* genotypes and of the genetic diversity in parasitism genes and expansion clusters that we have observed does not show any suggestive signatures of such local adaptation to hosts.

Alternatively, mindful that the products of the parasitism genes and genes in expansion clusters interface with the host, some variants of these genes may give a parasite a fitness advantage when infecting certain host genotypes, compared with parasites with other variants. Each individual parasite's suite of these genes may therefore represent a combination of different variants that have been selected for as these parasite lineages have over their history infected a range of host genotypes. In this scenario, these parasites are not locally adapted to their host genotypes *pe se*, but rather have available a set of gene variants that are appropriate for a wide range of already-encountered host genotypes. This idea – the so-called grey pawn hypothesis – that the aggregate effect of a large number of diverse genes is selected so as to cover a large phenotypic space has previously been suggested in trying to understand the very large number of *Caenorhabditis* spp. chemoreceptor-coding gene families in (Thomas and Robertson, 2008); this idea has also been applied to hookworm parasites (Schwarz *et al*., 2015). It is clear that that further research is needed to understand the evolution of large gene families, as well as the full biological significance of high levels of genetic diversity in genes underlying *S. ratti*'s parasitism.

Our whole-genome, single worm analysis of wild *S. ratti* is a non-destructive method of sampling parasite genetic diversity, and the hope must be that these approaches are now expanded to other parasitic nematodes. Such analyses will likely uncover different patterns of population genetic variation in other species, and understanding this will more fully illuminate the interactions between parasites and hosts, and so underpin a better understanding of the rich ecology of parasites. If *Strongyloides* infecting people has a similar population genetic structure, then this may have consequences for understanding *Strongyloides* host range and so zoonotic potential, as well as for the evolution of anthelmintic resistance.

Materials and Methods

Parasite and rat sampling

We sampled at three sites in the southern UK – Avonmouth (AV), Cardiff (CA) and Long Ashton (LA) (**Supplementary Table 10, Figure 1**), collecting fresh rat faecal pellets, which were cultured at 19°C and visually inspected for *S. ratti* infective third stage larvae (Viney and Lok, 2007), which were washed twice in distilled water, once in 1 % w/v SDS, and then twice more in distilled water, before being stored at -80°C. We genotyped rat faecal pellets at 9 dinucleotide repeat microsatellite loci (**Supplementary Table 2**) that had previously been used with wild rats (Desvars-Larrive *et al.,* 2017; Giraudeau *et al*., 1999; Gardner-Santana *et al.,* 2009; Steen *et al*., 1999), preparing DNA using the QIAamp DNA Stool Mini Kit (Qiagen) (Cole, 2020).

S. ratti genotyping

Of the more than 10,000 *S. ratti* larvae that we isolated from wild rats, we had to select a sub-sample for whole genome sequencing. We did this mindful that *S. ratti* parasitic females reproduce by mitotic parthenogenesis (Viney, 1994), such that in pellets containing more than one larva, that those larvae may be genetically identical siblings. Alternatively, a rat may be infected with multiple genotypes of *S. ratti* in which case there will also be a genetically different larvae in individual faecal pellets. We used RFLP genotyping to initially assess the genetic diversity among larvae within individual faecal pellets (Cole 2020). This showed that *S. ratti* infrapopulations are typically composed of multiple, genetically distinct parasitic adults and so we concluded that whole genome sequencing of multiple infective larvae from the same faecal pellet was unlikely to result in extensive resequencing of genetically identical siblings, and as such would be informative both for measuring the genetic diversity within sampling sites as a whole, and for assessing the extent of genetic variation within infrapopulations (Cole 2020)

For whole genome sequencing larvae were lysed and DNA prepared (Cole 2020). Samples were quantified with Biotium Accuclear Ultra high sensitivity dsDNA Quantitative kits using Mosquito LV liquid platform, Bravo WS and BMG FLUOstar Omega plate reader and cherrypicked to 200 ng / 120 µL using a Tecan liquid handling platform. Cherrypicked plates were sheared to 450 bp using a Covaris LE220 instrument and post-sheared samples purified using Agencourt AMPure XP SPRI beads on Agilent Bravo WSLibraries were constructed using the NEB Ultra II custom kit on an Agilent Bravo WS automation system. PCRs were set-up using KapaHiFi Hot start mix and IDT 96 iPCR tag barcodes on an Agilent Bravo WS automation system, and then purified using Agencourt AMPure XP SPRI beads on Beckman BioMek NX96 liquid handling platform. Libraries were quantified with Biotium Accuclear Ultra high sensitivity dsDNA Quantitative kit using Mosquito LV liquid handling platform, Bravo WS and BMG FLUOstar Omega plate reader. Libraries were pooled in equimolar amounts on a Beckman BioMek NX-8 liquid handling platform and libraries normalised to 2.8 nM ready for cluster generation on a c-BOT and loading on the Illumina X Ten platform. Sequencing reads from the libraries were aligned to the *S. ratti* reference assembly version 5_0_4 (Hunt *et al.* 2016, taken from WormBase ParaSite release WBPS7) using Bowtie 2 version 2.2.9 (Langmead and Salzberg, 2012) with default settings. We initially whole genome sequenced 225 *S. ratti* infective larvae at low depth of coverage and

524 calculated the proportion of reads that aligned to the *S. ratti* genome, and used this metric
525 to choose 90 libraries for further deep sequencing.
526
527 **Sequence analysis**
528 We used BCFtools (Li 2011) to identify SNPs using the criteria that they (i) fell on a
529 nucleotide covered by at least 1,000 reads (cumulative across all samples), (ii) had a mean
530 mapping quality of at least 20, and (iii) had a QUAL score of at least 50. Among the 90 *S.*
531 *ratti* genome sequences, nucleotides that were identical among all samples (but different
532 from the ED321 reference genome) were removed. We sequenced to an average coverage
533 of 96 % of nucleotides (range 75.8-99.3 %), and an average read depth of 68 (range 20-
534 246; just 5 larvae had mean read depths of less than 30).
535
536 We noticed that the mean read depth on the X chromosome was 67.9 % of the mean read
537 depth on the two autosomes. We concluded that this was due to the GC content because
538 (i) there was a significant correlation between read depth and GC content (**Supplementary**
539 **Figure 16**) and (ii) that the X chromosome has a slightly lower GC content (19.7 %)
540 compared with the autosomes (22 %) (Hunt *et al*., 2016).
541
542 Basic genetic diversity and population genetic statistics were calculated using VCFtools
543 version 0.1.12 (Danecek *et al.*, 2011). Hardy-Weinberg equilibrium (HWE) was calculated
544 considering only biallelic SNPs. Φ relatedness values (Manichaikul *et al.,* 2010) of each pair
545 of larvae were calculated using VCFtools and we used t-tests to compare Φ values. We also
546 measured the differentiation among sites using the fixation index, F_{ST}.
547
548 We generated neighbour-joining dendrograms using TASSEL 5.0 (Bradbury *et al.,* 2007),
549 and visualised these in FigTree Version 1.4.3. Clades within the neighbour-joining trees
550 were identified by eye. Fisher's exact tests, performed in R, were used to determine whether
551 there were significant differences in the frequencies of these clades among sampling sites
552 or sampling seasons.
553
554 We constructed maximum likelihood trees of the 90 parasites, producing consensus fasta
555 sequences for each individual, but where an individual was heterozygous the reference
556 allele was applied, with sequences aligned with MAFFT version 7 (Katoh *et al.* 2009) using
557 strategy FF-NST-1 for fast alignment, and maximum likelihood tree estimation performed
558 using RaxML version 8.1.15 (Stamatakis 2006), using the general time reversible gamma
559 model of substitution rate heterogeneity, and rapid bootstrapping with 100 replicates. We
560 generated separate maximum likelihood trees for chromosome 1, the first 80 Mb of
561 chromosome 2, the remainder of chromosome 2 and the two largest contigs of the X
562 chromosome.
563
564 We conducted Principal Component Analysis using the R package pcadapt version 4.1.0
565 (Luu *et al.* 2017) using only loci with a minor allele frequency greater than 0.05. We
566 investigated the admixture among the 90 parasite genotypes using ADMIXTURE version
567 1.3.0 (Alexander and Large 2011). Due to computational constraints, for the 90 parasites
568 SNP data were first thinned so that no two SNPs were within 500 bp of each other, leaving
569 a dataset of 35,559 SNPs. ADMIXTURE was run separately for k values 2-15.

570
571 We measured linkage disequilibrium (LD) among the 90 samples for the two autosomes and
572 the two largest X chromosome scaffolds. We initially phased the genotype data into
573 haplotypes using Beagle version 5.0 (Browning and Browning, 2007; Browning *et al.,* 2018),
574 where we used 100 burn-in iterations to generate an initial estimate of haplotype frequency,
575 and a further 100 iterations were used to estimate genotype phase for each SNP in each
576 sample. Phasing is influenced by the effective population size (Ne), which isn't known for *S.*
577 *ratti*, but we estimated this as 50,000; otherwise, default Beagle parameters were used. We
578 also undertook phasing using Shapeit version 2-r900 (O'Connell *et al.* 2014), where we used
579 100 burn-in iterations, 100 phasing iterations, and an estimated Ne of 50,000. For both we
580 used a window size of 0.5 Mb to estimate haplotypes. Only biallelic loci were used in Shapeit,
581 but triallelic loci were also included in Beagle. We report the results from phasing using
582 Beagle; Shapeit gave similar results.
583
584 To reduce computational time during linkage decay analysis, phased VCF files were thinned
585 so that no two remaining loci were within 100 bp of one another. To perform linkage decay
586 analysis, VCFTools was used to compare each SNP to each other SNP within a 50 kb
587 window of it, with Pearson's coefficient of correlation, r^2, calculated for each pair. To
588 measure LD across the whole genome we further thinned the phased data so that no two
589 SNPs were within 500 bp of each other, when the analysis was repeated as above, except
590 that this time each SNP was compared to every other SNP in the entire genome. We also
591 repeated these analyses for sub-sets of parasites within the clades that we identified.
592
593 We also analysed the mitochondrial genomes (excluding one individual from site AM due to
594 unexpectedly low mitochondrial read depth), and used Analysis of Molecular Variance
595 (AMOVA) which was conducted in GenAlEx version 6.5 (Peakall and Smouse 2006, 2012).
596 Haplotype maps were generated in PopART version 1.7 (Leigh and Bryant 2015) using the
597 minimum spanning network method (Bandelt *et al*. 1999), and maximum likelihood trees
598 based on unique haplotypes were generated with RaxML version 8.1.15 (Stamatakis 2006),
599 using the general time reversible gamma model of substitution rate heterogeneity, and rapid
600 bootstrapping with 100 replicates was applied. We calculated the proportion of SNPs shared
601 among all pairs or worms and compared this to the nuclear Φ relatedness using a Mantel
602 test.
603
604 We also used whole genome sequence data of 10 isofemale lines derived from wild *S. ratti*
605 (**Supplementary Table 4**), which we obtained from the European Variant Archive, study
606 code PRJEB41 https://www.ebi.ac.uk/ena/data/view/PRJEB4163. Among the 90 wild *S. ratti*
607 and 10 isofemale lines there were 235,393 SNPs of which 928 were tri-allelic, the remainder
608 bi-allelic, with a ratio of 1.8 of transitions to transversions.
609
610 **Rat population genetic analysis**
611 We only used data for faecal pellets that were successfully genotyped at 6 or more loci,
612 resulting in 132 genotyped faecal pellets. Locus D12Rat42 was excluded from further
613 population genetic analyses due to the low number of rats successfully genotyped at this
614 locus. We used GenAlEx's (version 6.5; Peakall and Smouse 2006, 2012) pairwise
615 relatedness function) to detect pellets with identical multi-locus genotypes, which we took to

616 have come from the same individual rat. We calculated Ritland and Lynch pairwise
617 relatedness (Lynch and Ritland 1999), where each individual was compared with each other
618 individual, and doubled these values to give a possible range of -1 to 1 from which we
619 calculated the mean within-sample-site and mean among-sample-site relatedness. We
620 determined the log-likelihood of the rat originating from each sampling site using GenAlEx
621 to assign pellet genotypes to each sample site by comparing the multilocus genotype of
622 each rat with the allele frequencies of each of the sampling sites (excluding the rat currently
623 being investigated).
624
625 We used Shannon's mutual information index ($^{S}H_{UA}$) to quantify the differences in allele
626 frequencies among sampling sites and to estimate the number of effective migrants per
627 generation. $^{S}H_{UA}$ measures and is valid despite deviations from HWE within subpopulations
628 (Hedrick, 2005; Sherwin *et al.,* 2006). $^{S}H_{UA}$ ranges from 0 (indicating unhindered gene flow)
629 to 1 (indicating a complete lack of gene flow).
630
631 We ensured (beyond visual identification) that none of the faecal pellets that we had
632 genotyped were from species other than *R. norvegicus* by seeking to amplify the nine rat
633 microsatellite loci from DNA isolated from other species that may potentially produce
634 contaminating faecal material, specifically that from black rats (*R. rattus*), moles (*Talpa*
635 *europaea*), and squirrels (*Sciurus carolinensis*). With one exception, none of these
636 microsatellite loci successfully amplified from these species (the exception was locus
637 D12Rat42 that did amplify *R. rattus* DNA) confirming that all successful genotypes were
638 from *R. norvegicus*. As positive controls we used primer pairs (i) Scv1 previously used to
639 amplify *Sciurus* sp. DNA (Hale *et al*., 2001), which successful amplified our *Sciurus* sp. DNA,
640 and weakly amplified *R. norvegicus* DNA, and (ii) RodActin previously used to amplify *R.*
641 *rattus* DNA (Apte *et al*., 2007), which successfully amplified our *R. rattus* and *R. norvegicus*
642 DNA.
643
644 **Parasitism and free-living genes and expansion clusters**
645 We followed previous work that identified "parasitism genes" (Hunt *et al.*, 2016). We
646 excluded parasitism genes if they were part of an expansion cluster (below) and the
647 underlying genome assembly was poor. We calculated 95% confidence intervals for
648 percentages from www.sample-size.net.
649
650 We define an "expansion cluster" as a genomic region containing four or more genes coding
651 for members of one of three protein families (astacin-like metallopeptidases, CAP domain-
652 containing proteins, or acetylcholinesterases), where there is not more than one other gene
653 between any two genes of those families. This definition differs somewhat from, and is more
654 conservative than that used by (Hunt *et al.*, 2016). As controls we used "flanking regions",
655 which we define as the genomic region directly adjacent to the expansion cluster that is the
656 same size as the cluster itself. Each expansion cluster has two flanking regions.
657
658 Lists of genes belonging to these three gene families were collated from Hunt *et al.*, 2016
659 and from this we initially identified 15 expansion clusters. Because clusters 10 and 11 were
660 very close to each other, cluster 10's right flanking region was shortened to end where
661 expansion cluster 11 began, and expansion cluster 11 was considered to not have a left

flanking region. Similarly, to avoid overlap of cluster 11's right flanking region and cluster 12's left flanking region we shortened cluster 12's left flanking region to the start of cluster 11's right flanking region. Across all expansion clusters there were 135 genes in total, of which 126 belonged to one of the three gene families: 46 encoding CAP domain-containing proteins, 70 encoding astacin-like metallopeptidases, and 10 encoding acetylcholinesterases, representing 51.7%, 38% and 33.3% of CAP domain-containing proteins, astacin-like metallopeptidase and acetylcholinesterase encoding genes, respectively, in the genome as a whole. Flanking regions collectively contained 216 protein-coding genes the products of which had varying predicted functional descriptions.

Mindful that these expansion cluster regions were repetitive in nature we checked their original reference genome assembly by realigning the sequencing reads originally used to build the reference assembly back to the reference, available at NCBI, BioProject code PRJEB2398, and then assessed the quality of these alignments using Gap5 (Bonfield and Whitman 2010). Repetitiveness of the sequence was examined *via* Dotplots with the software package Dotter (Sonnhammer and Durbin, 1995). Gene annotation schematics were retrieved from Ensembl's 'Region in Detail' tool (Hubbard *et al.,* 2002), accessed via WormBase Parasite (Howe *et al.,* 2017) version 12 (https://parasite.wormbase.org/index.html) and added to the graphics produced by Gap5. Regions with poor mapping quality, unusually large distances between mate pairs and the occurrence of mate pairs facing opposite directions are suggestive of high rates of sequence misalignment. Peaks in read depth and fragment depth above background levels were evidence that multiple copies of a repetitive sequence were collapsed in the reference assemblies. Where expansion cluster genes or genes in flanking regions fell in poorly resolved reference assembly areas, these genes were excluded from further analysis.

Using this approach, we excluded expansion clusters 4, 11 and 13, and their flanking regions entirely and other genes within various clusters, resulting in 196 genes remaining, of which 61 were in expansion clusters and 135 were in flanking regions (**Supplementary Table 8**). Expansion clusters 6, 7, 8, 12 and 14 had no genes excluded. Three expansion clusters had genes that did not belong to one of the three target gene families, and were excluded from analyses. Of the remaining 58 in the expansion cluster genes, 29 encoded CAP domain-containing proteins, 27 encoded astacin-like metallopeptidases, and 2 encoded acetylcholinesterases.

Data Deposition

The genome data of the 90 larvae are deposited in the European Variation Archive, study PRJEB32744, https://www.omicsdi.org/dataset/eva/PRJEB32744.

Acknowledgements

We would like to thank the land owners for access to the sample sites; Benito Wainwright, Amy Williams Schwartz, and Bristol Zoo Gardens for the provision of mammalian tissue; Andrea Betancourt for substantial help with mutation rate analyses; and Vicky Hunt for helpful discussions. RC was funded by a NERC studentship. The sequence data for this project were produced by the Wellcome Sanger Institute with funding from the Wellcome Trust grant 206194.

Competing interests

The authors declare that they have no competing interests.

References

Alexander D. H. and Large K. (2011). Enhancements to the ADMIXTURE algorithm for individual ancestry estimation. *BMC Bioinformatics* **12:**246.

Apte U., Thompson M. D., Cui S., Liu B., Cieply B. and Monga S. P. S. (2007). Wnt/β-catenin signaling mediates oval cell response in rodents. *Hepatology* **47:**288-295.

Bandelt H., Forster P. and Röhl A. (1999). Median-joining networks for inferring intraspecific phylogenies. *Molecular Biology and Evolution* **16:**37-48.

Bethany J., Brooker S., Albonico M., Geiger S.M., Loukas A., Diemert D. and Hotez P.J. (2006). Soil-transmitted helminth infections: ascariasis, trichuriasis, and hookworm. *Lancet* **367**:1521-1532.

Blouin M.S., Yowell C.A., Courtney, C.H. and Dame, J.B. (1995). Host movement and the genetic structure of populations of parasitic nematodes. *Genetics* **141**:1007-1014.

Bonfield J.K. and Whitwham, A. (2010). Gap5 - editing the billion fragment sequence assembly. *Bioinformatics* **26:**1699-1703.

Bradbury P. J., Zhang Z., Kroon D. E., Casstevens T. M., Ramdoss Y. and Buckler E. S. (2007). TASSEL: Software for association mapping of complex traits in diverse samples. *Bioinformatics* **23:**2633-2635.

Browning S. R. and Browning B. L. (2007). Rapid and accurate haplotype phasing and missing data inference for whole genome association studies by use of localized haplotype clustering. *American Journal of Human Genetics* **81:**1084-1097.

Browning B. L., Zhou Y. and Browning S. R. (2018). A one-penny imputed genome from next generation reference panels. *American Journal of Human Genetics* **103:**338-348.

Buonfrate D., Bisanzio D., Giorli G., Odermatt P., Fürst T., Greenaway C., French M., Reithinger R., Gobbi F., Montresor A. and Bisoffi, Z. (2020). The global prevalence of *Strongyloides stercoralis* infection. *Pathogens* **9**:468.

Cole, R.L. (2020). The distribution of genetic diversity within and among the *Strongyloides ratti* genome. PhD thesis, University of Bristol, UK. https://research-information.bris.ac.uk/en/studentTheses/the-distribution-of-genetic-diversity-within-and-among-the-strong

Cole R. and Viney M. (2018). The population genetics of parasitic nematodes of wild animals. *Parasites and Vectors* **11:**590.

Combs M., Puckett E. E., Richardson J., Mims D. and Munshi-South J. (2017). Spatial population genomics of the brown rat (*Rattus norvegicus*) in New York City. *Molecular Ecology* **27:**83-98.

Criscione, C.D., Anderson, J.D., Sudimack, D., Peng, W., Jha, B., Willilams-Blangero, S. and Anderson T.J.C. (2007). Disentangling hybridization and host colonization in parasitic roundworms of humans and pigs. *Proceedings of the Royal Society B* **274**:2669-2677.

765 Danecek P., Auton A., Abecasis G., Albers C. A., Banks E., DePristo M. *et al*. (2011). The
766 variant call format and VCFtools. *Bioinformatics* **27:**2156-2158.
767
768 Denver, D.R., Dolan, P.C., Willhelm, L.J., Sung, W., Lucas-Lledó, J.I., Howe DK, *et al.*
769 (2009). A genome-wide view of *Caenorhabditis elegans* base-substitution mutation
770 processes. *Proceedings of the National Academy USA* **106**:16301-16314.
771
772 Desvars-Larrive A., Pascal M., Gasqui P., Cosson J.-F., Benoit E., Lattard V., Crespin L. *et*
773 *al.* (2017). Population genetics, community of parasites, and resistance to rodenticides in
774 an urban brown rat (*Rattus norvegicus*) population. *PLoS One* **12:**e0184015.
775
776 Durrant, C., Thiele, E.A., Holroyd, N., Doyle, S.R., Sallé, G., Tracey, A., *et al.* (2020).
777 Population genomic evidence that human and animal infections in Africa come from the
778 same populations of *Dracunculus medinensis*. *PLoS Neglected Tropical Diseases*
779 **14:**e0008623.
780
781 Fisher M.C. and Viney M.E. (1998). The population genetic structure of the facultatively
782 sexual parasitic nematode *Strongyloides ratti* in wild rats. *Proceedings of the Royal Society*
783 *of London B* **265:**703-709.
784
785 Gardner, M.P., Gems, D. and Viney, M.E. (2006). Extraordinary plasticity in aging in
786 *Strongyloides ratti* implies a gene-regulatory mechanism of lifespan evolution. *Aging Cell*
787 **5**:315-323.
788
789 Gardner-Santana L. C., Norris D. E., Fornadel C. E., Hinson E. R., Klein S. L. and Glass
790 G.E. (2009). Commensal ecology, urban landscapes, and their influence on the genetic
791 characteristics of city-dwelling Norway rats (*Rattus norvegicus*). *Molecular Ecology*
792 **18:**2766-2778.
793
794 Giraudeau F., Apiou F., Amarger V., Kaisaki P. J., Bihoreau M.-T., Lathrop M. *et al.* (1999).
795 Linkage and physical mapping of rat microsatellites derived from minisatellite loci.
796 *Mammalian Genome* **10:**405-409.
797
798 Greischar M. and Koskella B. (2007). A synthesis of experimental work on parasite local
799 adaptation. *Ecology Letters* **10**:418-433.
800
801 Hale M. L., Bevan R. and Wolff K. (2001). New polymorphic microsatellite markers for the
802 red squirrel (*Sciurus vulgaris*) and their applicability to the grey squirrel (*S. carolinensis*).
803 *Molecular Ecology Resources* **1:**47-49.
804
805 Hartfield, M. (2016). Evolutionary genetic consequences of facultative sex and outcrossing.
806 *Journal of Evolutionary Biology* **29:**5-22.
807
808 Harvey S.C., Gemmill A.W., Read A.F. and Viney M.E. (2000). The control of morph
809 development in the parasitic nematode *Strongyloides ratti. Proceedings of the Royal Society*
810 *of London B* **267:**2057-2063.
811
812 Hedrick P. W. (2005). A standardized genetic differentiation measure. *Evolution* **59:**1633-
813 1638.
814

Howe K. L., Bolt B. J., Shafie M., Kersey P and Berriman M. (2017). WormBase ParaSite − a comprehensive resource for helminth genomics. *Molecular and Biochemical Parasitology* **215:**2-10.

Hubbard T., Barker D., Birney E., Cameron G., Chen Y., Clark L. *et al.* (2002). The Ensembl genome database project. *Nucleic Acids Research* **30:**38-41.

Hunt V.L., Asai I.J., Coghlan A., Reid A.J., Holroyd N., Foth B.J., *et al.* (2016). The genomic basis of parasitism in the *Strongyloides* clade of nematodes. *Nature Genetics* **48:**299-307.

Jaleta, T.G., Zhou, S., Bemm, F.M., Schär, F., Khieu, V., Muth, S. *et al.* (2017). Different but overlapping populations of *Strongyloides stercoralis* in dogs and humans – Dogs as a possible source for zoonotic strongyloidiasis. *PLoS Neglected Tropical Diseases* **11:**e0005752.

Jost L., Archer F., Flanagan S., Gaggiotti O., Hoban S and Latch E. (2018). Differentiation measures for conservation genetics. *Evolutionary Applications* **11:**1139-1148.

Kikuchi T., Hino, A., Tanaka, T., Aung, M.P.P.T.H.H., Afrin, T., Nagayasu, E. *et al*. (2016). Genome-wide analyses of individual *Strongyloides stercoralis* (Nematoda: Rhabditoidea) provide insights into population structure and reproductive life cycles. *PLoS Neglected Tropical Diseases* **10**:e0005253.

Katoh K., Asimenos G. and Toh H. (2009). Multiple alignment of DNA sequences with MAFFT. *Methods in Molecular Biology* **537:**39-64.

Kuris, A.M., Hechinger, R.F., Shaw, J.C., Whitney, K.L., Aguirre-Macedo, L. *et al.* (2008). Ecosystem energetic implications of parasite free-living biomass in three estuaries. *Nature* **454:**515-518.

Lafferty, K.D., Dobson, A.P. and Kuris, A.M. (2006) Parasites dominate food web links. *Proceedings of the National Academy of Sciences* **103**:11211-11216.

Langmead B. and Salzberg S. (2012). Fast gapped-read alignment with Bowtie 2. *Nature Methods* **9:**357-359.

Lee, D., Zdraljevic, S., Stevens, L., Wang, Y., Tanny, R.E., Crombie, T.A., *et al*. (2021). Balancing selection maintains hyper-divergent haplotypes in *Caenorhabditis elegans*. *Nature Ecology and Evolution* **5**:794-807.

Leigh JW and Bryant D. (2015). PopART: Full-feature software for haplotype network construction. *Methods in Ecology and Evolution* **6:**1110-1116.

Lever C. (1977). The naturalized animals of the British Isles. Hutchinson, 600 pp.

Li H. (2011). A statistical framework for SNP calling, mutation discovery, association mapping and population genetical parameter estimation from sequencing data. *Bioinformatics* **27:**2987-2993.

Lively CM., Dybdahl MF., Jokela J., Osnas EE. and Delph LF. (2004). Host sex and local adaptation by parasites in a snail-trematode interaction. *American Naturalist* **164:**S6-S18.

867 Luu K., Bazin E. and Blum M. G. (2017). pcadapt: an R package to perform genome scans
868 for selection based on principal component analysis. *Molecular Ecology Resources* **17:**67-
869 77.
870
871 Lynch M. and Ritland K. (1999). Estimation of pairwise relatedness with molecular markers.
872 *Genetics* **152:**1753-1766.
873
874 Manichaikul A., Mychaleckyj J. C., Rich S. S., Daly K., Sale M., Chen W. M. (2010). Robust
875 relationship inference in genome-wide association studies. *Bioinformatics* **26:**2867-28773.
876
877 Noble, L.M., Yuen, J., Stevens, L., Moya, N., Persaud, R., Moscatelli, M., *et al.* (2021).
878 Selfing is the safest sex for *Caenorhabditis tropicalis. eLife* **10**:e62587.
879
880 O'Connell J., Gurdasani D., Delaneau O., Pirastu N., Ulivi S., Cocca M. *et al.* (2014). A
881 general approach for haplotype phasing across the full spectrum of relatedness. *PLoS*
882 *Genetics* **10:**e1004234.
883
884 Peakall R. and Smouse P. E. (2006). GENALEX 6: genetic analysis in Excel. Population
885 genetic software for teaching and research. *Molecular Ecology Notes* **6:**288-295.
886
887 Peakall R. and Smouse P. E. (2012). GenAlEx 6.5: genetic analysis in Excel. Population
888 genetic software for teaching and research-an update. *Bioinformatics* **28:**2537-2539.
889
890 Redman, E., Whitelaw, F., Tait, A., Burgess, C., Bartley, Y., Skuce, P.J., Jackson, F. and
891 Gilleard J. (2015). The emergence of resistance to the benzimidazole anthelminthics in
892 parasitic nematodes of livestock is characterised by multiple independent hard and soft
893 selective sweeps. *PLoS Neglected Tropical Diseases* **9**:e0003494.
894
895 Sallé G., Doyle S. R., Cortet J., Cabaret J., Berriman M, Holyroyd N. *et al.* (2019). The global
896 diversity of *Haemonchus contortus* is shaped by human intervention and climate. *Nature*
897 *Communications* **10:**4811.
898
899 Schwarz, E. M., Hu, Y., Antoshechkin, I., Miller, M. M., Sternberg, P. W. and Aroian, R. V.
900 (2015). The genome and transcriptome of the zoonotic hookworm *Ancylostoma ceylanicum*
901 identify infection-specific gene families. *Nature Genetics* **47**:416-422.
902
903 Sherwin W. B., Jabot F., Rush R. and Rossetto M. (2006). Measurement of biological
904 information with applications from genes to landscapes. *Molecular Ecology* **15:**2857-2869.
905
906 Sonnhammer E.L.L and Durbin R. (1995). A dot-matrix program dynamic threshold control
907 suited for genomic DNA and protein sequence analysis. *Gene* **167:**GC1-10.
908
909 Stamatakis A. (2006). RAxML-VI-HPC: maximum likelihood-based phylogenetic analyses
910 with thousands of taxa and mixed models. *Bioinformatics* **22:**2688-2690.
911
912 Steen R. G., Kwitek-Black A. E., Glenn C., Gullings-Handley J., Van Etten W., Atkinson O.
913 *et al.* (1999). A high-density integrated genetic linkage and radiation hybrid map of the
914 laboratory rat. *Genome Resources* **9:**AP1-8.
915
916 Thiele, E., Eberhard, M.L., Cotton, J.A., Durrant, C., Berg, J., Hamm, K. and Ruiz-Tiben, E.
917 (2018). Population genetic analysis of Chadian Guinea worms reveals that human and non-

human hosts share common parasite populations. *PLoS Neglected Tropical Diseases* **12**:e006747.

Thomas, J.H., and Robertson, H.M. (2008) The *Caenorhabditis* chemoreceptor gene families. *BMC Biol*ogy **6:**42.

Viney M.E. and Lok J.B. (2007). *Strongyloides* spp. WormBook, ed. The C. elegans Research Community, *WormBook*, doi/10.1895/wormbook.1.7.1, http://www.wormbook.org

Viney M.E. (1994). A genetic analysis of reproduction in *Strongyloides ratti*. *Parasitology* **109**:511-515.

Viney M.E., Matthews B.E. and Walliker, D. (1992). On the biological and biochemical nature of cloned populations of *Strongyloides ratti*. *Journal of Helminthology* **66**:45-52.

Viney M.E**.,** Matthews B.E. and Walliker D. (1993). Mating in the parasitic nematode *Strongyloides ratti*: Proof of genetic exchange. *Proceedings of the Royal Society of London Series B* **254:**213-219.

WHO (2021) www.who.int/neglected_diseases/diseases/en/

Zeng, L., Ming, C., Li, Y., Su L-Y., Su, L-H., Otecko, N.O. *et al.* (2018). Out of southern east Asia of the brown rat revealed by large-scale genome sequencing. *Molecular Biology and Evolution* **35**:149-158.

Table 1. F_{ST} and Φ among *S. ratti* clades 1, 2 and 3. Pairwise F_{ST} is shown in italics above the diagonal, and Φ on and below the diagonal in non-italic text.

	Clade 1	**Clade 2**	**Clade 3**
Clade 1	0.43	*0.22*	*0.35*
Clade 2	0.18	0.23	*0.23*
Clade 3	0.06	0.05	0.45

SUPPLEMENTARY INFORMATION

SUPPLEMENTARY TABLES

1. The occurrence of *S. ratti* in rat faecal pellets.
2. Rat microsatellite loci.
3. Population genetics of rat microsatellite loci.
4. Isofemale lines of *S. ratti* that were whole genome sequenced.
5. Genes in highly variable 10 kb regions.
6. The hundred most parasitic genes.
7. The hundred most free-living genes.
8. *S. ratti* expansion clusters, revised after further inspection of genome assembly in the cluster region.
9. dN/dS ratios of expansion clusters and their flanking regions.
10. Sampling sites and times.

SUPPLEMENTARY FIGURES

1. Frequency distribution of the number of *S. ratti* infective larvae isolated from infected rat faecal pellets.
2. Histogram of Φ relatedness values among 90 *S. ratti* larvae.
3. The frequency distribution of the pairwise number of SNP differences among the 90 parasites.
4. Maximum likelihood trees of the 90 parasites.
5. ADMIXTURE analysis of the 90 parasites.
6. PCA analysis of *S. ratti* parasites.
7. Minimum spanning *S. ratti* mitochondrial haplotype maps.
8. Ritland and Lynch pairwise relatedness values of rats within sampling sites.
9. *S. ratti* neighbour-joining dendrograms of 10 isofemale lines and 90 larvae collected from the three sample sites.
10. Linkage disequilibrium in the *S. ratti* genome.
11. Linkage disequilibrium in the *S. ratti* genome for clade 1 and 3 parasites.
12. Heatmaps of linkage disequilibrium in the *S. ratti* genome for clade 1 and 3 parasites.
13. Heatmaps of linkage disequilibrium in the *S. ratti* genome.
14. The distribution of SNPs across the *S. ratti* genome.
15. Neighbour-joining dendrograms based on five expansion clusters.
16. Correlation of read depth and GC content for 90 *S. ratti* larvae.

985

SUPPLEMENTARY TABLES

986 **Supplementary Table 1. The occurrence of *S. ratti* in rat faecal pellets.** The proportion of infected pellets did not differ significantly
987 among the seasons when the faecal pellets were collected (χ^2 = 6, *df* = 3, P = 0.11).
988

Site and season	Number of pellets collected	Number (and %) of infected pellets	Number of larvae collected	Mean (SD) number of larvae per infected pellet
CA, Spring	35	7 (20%)	244	34.9 (24.3)
CA, Summer	32	5 (15.6%)	89	17.8 (22.1)
CA, Autumn	19	2 (10.5%)	256	128 (7.1)
CA, Winter	26	1 (3.8%)	6	6 (0)
CA, All seasons	**112**	**15 (13.4%)**	**595**	**39.7 (42.1)**
AM, Spring	11	8 (72.7%)	137	17.1 (23.5)
AM, Summer	75	23 (30.7%)	428	18.6 (29.3)
AM, Autumn	27	15 (55.6%)	3,044	202.9 (185)
AM, Winter	21	17 (81%)	5,067	298.1 (500.3)
AM, All seasons	**134**	**63 (47%)**	**8,676**	**137.7 (296.5)**
LA, Spring	27	14 (51.9%)	211	15.1 (23.1)
LA, Summer	11	7 (63.6%)	40	5.7 (3.7)
LA, Autumn	7	6 (85.7%)	360	60 (46.8)
LA, Winter	13	9 (69.2%)	589	65.4 (83.8)
LA, All seasons	**58**	**36 (62.1%)**	**1,200**	**33.3 (52.8)**
All sites, Spring	73	29 (39.7%)	592	20.4 (24.3)
All sites, Summer	118	35 (29.7%)	557	15.9 (25)
All sites, Autumn	53	23 (43.4%)	3,660	159.1 (162.4)
All sites, Winter	60	27 (45%)	5,662	209.7 (412.4)
Total	**304**	**114 (37.5%)**	**10,471**	**91.9 (226.9)**

989

990 **Supplementary Table 2. Rat microsatellite loci.** The forward primers are listed first and all primers are 5' to 3'; Length refers to the length
991 in bp of the region amplified by the given primer sequences as determined from Rnor 6.0 (1.7.2014) release of the *R. norvegicus* genome;
992 Fluorophore indicates the fluorophore used to label forward primers and thus PCR products.
993

Locus	Primer sequences	Length	Fluorophore	Reference
D3Rat159	CCAGGGATGAGTCCAAGGTA CTGGTCTGCTTCCTCCAGTC	243	VIC	Steen *et al*., 1999
D4Rat59	GCAGTGTGTTTGGGGTAGCT GCGGAATGATAGTTACTACGGC	180	FAM	Steen *et al*., 1999.
D6Cebr1	GGTTTGGTTGGGGAGAA GTGCTGTCAGGGAAAGATGTA	223	NED	Giraudeau *et al*., 1999
D8Rat162	TCACTGGCAGCAATTTACCA TCTGAGACCTCTTCAACTCTGTTG	249	VIC	Steen *et al*., 1999.
D10Rat105	ATCCAGCCAGAAAGCAAAAC CTGGCTGAGTCCTGTCACAA	100	FAM	Steen *et al*., 1999.
D12Rat42	CAACCCAGTGTGTCAAACGT GGGTTGGTGAAGCATTTTCA	128	VIC	Steen *et al*., 1999.
D14Rat110	AACATTGTCTTGCTTAGCCTCA CTCCACCCACACACCACG	280	NED	Steen *et al*., 1999.
D18Rat11	GCCCAGGAGCTAAGTCTGATT CCAGCCTCAGAGCCAATAAG	133	FAM	Steen *et al*., 1999.
D19Rat62	GTGCTAATGTGGGTGGCTTT TGAATTCTACCATGCATCACAG	112	NED	Steen *et al*., 1999.

994

Supplementary Table 3. Population genetics of rat microsatellite loci. A. Genetic diversity of loci. Rats genotyped is the number of individual rats in which genotyping was successful; Allele number is the number of alleles identified at the locus; He and Ho are expected and observed heterozygosity, respectively; Site diversity is the proportion of allelic diversity that partitions within sites, as opposed to among sites, according to $^{S}H_{UA}$. locus D12Rat42 was not used in analyses due to the low genotyping success rate. **B. HWE of loci.** Locus shows the loci; Site is the sampling site; Rats genotyped is the number of rats that were genotyped; Alleles is the number of alleles detected; X^2 is the statistic testing whether the observed genotype frequencies match HWE expectations with the degrees of freedom (df) in parentheses. Those still significant after Bonferroni correction are shown in bold.

A.

Locus	Rats genotyped	Allele number	He	Ho	Site diversity (%)
D3Rat159	103	14	0.779	0.756	18
D4Rat59	105	12	0.822	0.652	8
D6Cebr1	109	14	0.752	0.356	13
D8Rat162	73	15	0.835	0.600	16
D10Rat105	112	8	0.696	0.617	13
D12Rat42	34	9	0.762	0.267	NA
D14Rat110	83	16	0.824	0.529	18
D18Rat11	112	10	0.686	0.319	19
D19Rat62	96	12	0.678	0.462	13

B.

Locus	Site	Rats genotyped	Alleles	X^2 (df)	Probability
D3Rat159	CA	45	7	41.8 (21)	0.01
	LA	17	11	89.9 (55)	0.01
	AM	**41**	**10**	**98.4 (45)**	**0.001**
D4Rat59	**CA**	**46**	**9**	**74.6 (36)**	**0.001**
	LA	15	9	39.1 (36)	0.03
	AM	44	10	67.2 (45)	0.05
D6Cebr1	**CA**	**45**	**11**	**100.7 (55)**	**0.001**
	LA	**18**	**10**	**87.6 (45)**	**0.001**
	AM	**46**	**6**	**105.1 (15)**	**0.001**
D8Rat162	**CA**	**25**	**10**	**120.1 (45)**	**0.001**
	LA	13	8	28.3 (28)	0.45
	AM	35	10	67.7 (45)	0.05
D10Rat105	**CA**	**47**	**5**	**89.6 (10)**	**0.001**
	LA	**19**	**6**	**64 (15)**	**0.001**
	AM	**46**	**7**	**94.2 (21)**	**0.001**
D12Rat42	**CA**	**15**	**9**	**71.8 (36)**	**0.001**
	LA	5	4	12 (6)	0.06
	AM	14	6	33.1 (15)	0.01
D14Rat110	**CA**	**34**	**11**	**112.4 (55)**	**0.001**
	LA	16	9	45.2 (36)	0.14
	AM	**33**	**11**	**113.6 (55)**	**0.001**
D18Rat11	**CA**	**47**	**8**	**66.6 (28)**	**0.001**
	LA	**19**	**5**	**34.5 (10)**	**0.001**

	AM	**46**	**9**	**141 (36)**	**0.001**
D19Rat62	**CA**	**39**	**9**	**115.2 (36)**	**0.001**
	LA	17	7	40.8 (21)	0.01
	AM	40	5	17.9 (10)	0.06

1008

1009 **Supplementary Table 4. Isofemale lines of *S. ratti* that were whole genome sequenced**.
1010

Isofemale line	Isolation year	Origin
ED36	1990	Hampshire, UK
ED43	1989	Edinburgh, UK
ED53	1990	Kagoshima, Japan
ED132	1990	Kagoshima, Japan
ED336	1995	Berkshire, UK
ED391	1989	Wiltshire, UK
ED399	1989	Sussex, UK
ED405	1989	Sussex, UK
ED428	2012	Bath, UK
ED438	2012	Bath, UK

1011

1012 **Supplementary Table 5. Genes in highly variable 10 kb regions.** Region lists the 61 regions (region 1 does not contain any genes);
1013 Gene gives the gene's designation; Predicted function is the WormBase ParaSite description of each gene, where Astacin-like
1014 metalloendopeptidase is abbreviated to Astacin; Coding SNPs per kb is the number of SNPs per kb within the coding sequence of that
1015 gene; SNP type is the absolute number of synonymous (S), nonsynonymous (NS) and STOP codon-causing SNPs; Expression is taken
1016 from Hunt *et al*., 2016, which compared the expression of genes between the parasitic female and free-living female morph, and where the
1017 expression is one $\log_2$ fold more in the parasitic female morph (Parasitic), free-living female morph (Free-living), not different (Same), or
1018 not listed (Unlisted); Expansion cluster is expansion cluster or associated flanking region a gene belongs to, if any. Some genes are marked
1019 as "discarded" because they had poor underlying assembly according to Gap5 analysis of expansion clusters and flanking regions and so
1020 were discounted from further analysis.
1021

Region	Gene	Predicted function	Coding SNPs per kb	SNP type (S/NS/STOP)	Expression	Expansion cluster
2	SRAE_0000058700	Kinesin, motor domain and P-loop-containing	26.7	3 / 3 / 0	Unlisted	None
3	SRAE_2000499400	Hypothetical protein	48.2	5 / 28 / 0	Parasitic	None
	SRAE_2000499500	Hypothetical protein	0	0 / 0 / 0	Parasitic	None
	SRAE_2000499600	Hypothetical protein	72.2	8 / 20 / 1	Parasitic	None
	SRAE_2000499700	Hypothetical protein	45.7	5 / 22 / 0	Parasitic	None
4	SRAE_0000058500	Hypothetical protein	3.3	0 / 1 / 0	Unlisted	None
5	SRAE_2000124300	CAP domain-containing	69	17 / 49 / 4	Parasitic	EC3
	SRAE_2000124400	CAP domain-containing	43.3	8 / 30 / 1	Parasitic	EC3
	SRAE_2000124500	CAP domain-containing	50.9	11 / 33 / 2	Parasitic	EC3
6	SRAE_X000232600	Reverse transcriptase domain and Aspartic peptidase domain-containing	45.8	62 / 51 / 1	Unlisted	None
	SRAE_X000232700	Integrase, catalytic core domain and Ribonuclease H-like domain-containing	22.2	5 / 1 / 1	Unlisted	None
	SRAE_X000232800	Hypothetical protein	32	6 / 6 / 0	Same	None
	SRAE_X000232900	Hypothetical protein	31.7	4 / 4 / 0	Unlisted	None

	SRAE_X000233000	Zinc finger, CCHC-type domain-containing	11.8	14 / 36 / 0	Unlisted	None
	SRAE_X000233100	Hypothetical protein	11.3	12 / 22 / 1	Unlisted	None
7	SRAE_0000057800	Hypothetical protein	28.5	1 / 9 / 0	Parasitic	None
8	SRAE_X000062200 **(discarded)**	Poly-glutamine tract binding protein 1	0	0 / 0 / 0	Unlisted	EC13
	SRAE_X000062300 **(discarded)**	Acetylcholinesterase	66.2	29 / 86 / 0	Same	EC13
9	SRAE_2000478200	Hypothetical protein	6.2	4 / 0 / 0	Unlisted	None
	SRAE_2000478300	Hypothetical protein	21.1	5 / 6 / 0	Same	None
	SRAE_2000478400	Hypothetical protein	90.7	10 / 29 / 1	Unlisted	None
	SRAE_2000478500	CAP domain-containing	89.3	17 / 47 / 0	Parasitic	None
10	SRAE_X000050900	Hypothetical protein	66.7	13 / 34 / 0	Parasitic	None
	SRAE_X000051000	Hypothetical protein	44.5	8 / 21 / 0	Parasitic	None
	SRAE_X000051100	Hypothetical protein	53	6 / 27 / 1	Parasitic	None
12	SRAE_X000026900	Hypothetical protein	51	5 / 19 / 0	Parasitic	None
	SRAE_X000027000	Hypothetical protein	15.8	3 / 4 / 0	Unlisted	None
13	SRAE_1000139800	Hypothetical protein	8	12 / 2 / 0	Unlisted	None
	SRAE_1000139900	Protein-tyrosine phosphatase-containing	54.6	42 / 145 / 1	Same	None
	SRAE_1000140000	Translation initiation factor SUI1 domain-containing	0	0 / 0 / 0	Same	None
	SRAE_1000140100	Hypothetical protein	0	0 / 0 / 0	Same	None
	SRAE_1000140200	Hypothetical protein	18.1	2 / 8 / 0	Same	None
14	SRAE_2000076600	CAP domain-containing	21.2	3 / 14 / 0	Parasitic	EC2
	SRAE_2000076700	CAP domain-containing	60.4	11 / 39 / 0	Parasitic	EC2

	SRAE_2000076800	CAP domain-containing	39.2	11 / 18 / 1	Parasitic	EC2
	SRAE_2000076900	CAP domain-containing	36.8	6 / 25 / 0	Parasitic	EC2
	SRAE_2000077000	CAP domain-containing	19	6 / 9 / 1	Parasitic	EC2
15	SRAE_2000499000	Hypothetical protein	55.9	2 / 25 / 1	Parasitic	None
	SRAE_2000499100	Hypothetical protein	35.8	7 / 12 / 0	Parasitic	None
16	SRAE_X000037500	Hypothetical protein	21.7	8 / 18 / 1	Unlisted	None
17	SRAE_X000066000	Trypsin Inhibitor-like	36.3	38 / 77 / 0	Parasitic	None
	SRAE_X000066100	Astacin	28.2	18 / 23 / 0	Parasitic	None
18	SRAE_X000032850	Hypothetical protein	69.2	4 / 18 / 0	Unlisted	None
	SRAE_X000032900	Hypothetical protein	54.6	8 / 11 / 0	Unlisted	None
	SRAE_X000033000	Hypothetical protein	78.6	9 / 20 / 0	Unlisted	None
	SRAE_X000033100	Hypothetical protein	46	4 / 12 / 0	Unlisted	None
19	SRAE_X000050700	Hypothetical protein	34.9	9 / 15 / 0	Parasitic	None
	SRAE_X000050800	Hypothetical protein	37	7 / 16 / 0	Parasitic	None
20	SRAE_0000074500	Aspartic peptidase domain-containing	46.4	93 / 116 / 6	Free-living	None
	SRAE_0000074600	Aspartic peptidase domain-containing	9.5	15 / 19 / 1	Unlisted	None
21	SRAE_X000145900	Astacin	82.7	27 / 76 / 1	Same	None
	SRAE_X000146000	Astacin	21.4	7 / 19 / 1	Para	None
22	SRAE_X000186500	Reverse transcriptase domain-containing	25.3	37 / 65 / 2	Free-living	None
	SRAE_X000186600	Cytochrome C oxidase subunit II	43.6	14 / 51 / 0	Same	None

23	SRAE_X000146300 **(discarded)**	Hypothetical protein	31.3	5 / 5 / 1	Unlisted	FR15L
	SRAE_X000146400 **(discarded)**	Hypothetical protein	6.4	2 / 1 / 0	Unlisted	FR15L
24	SRAE_0000074000	Hypothetical protein	16.7	3 / 6 / 1	Unlisted	None
	SRAE_0000074100	Hypothetical protein	10.4	2 / 6 / 0	Unlisted	None
	SRAE_0000074200	Aspartic peptidase domain-containing	42	86 / 74 / 0	Same	None
25	SRAE_2000460700	Hypothetical protein	52.4	20 / 112 / 1	Parasitic	None
	SRAE_2000460800	Hypothetical protein	4.6	1 / 1 / 0	Parasitic	None
	SRAE_2000460900	Hypothetical protein	6.7	1 / 3 / 1	Same	None
26	SRAE_X000063000 **(discarded)**	Acetylcholinesterase	15.2	9 / 18 / 0	Parasitic	EC13
	SRAE_X000063100 **(discarded)**	Poly-glutamine tract binding protein 1	0.4	0 / 1 / 0	Same	FR13R
27	SRAE_1000045700	E3 ubiquitin-protein ligase MYCBP2	4.9	51 / 20 / 0	Free-living	None
	SRAE_1000045800	Lipase, class 3 family-containing	15.2	7 / 8 / 0	Parasitic	None
	SRAE_1000045900	CAP domain-containing	76	19 / 67 / 0	Parasitic	None
	SRAE_1000046000	Speckle-type POZ	4.2	4 / 1 / 0	Same	None
28	SRAE_X000051500	CTP synthase 2	26.6	5 / 23 / 1	Unlisted	None
	SRAE_X000051600	CTP synthase 2	62.4	6 / 26 / 0	Unlisted	None
	SRAE_X000051700	Hypothetical protein	9.1	1 / 3 / 0	Parasitic	None
	SRAE_X000051800	CTP synthase 2	6,4	2 / 2 / 1	Unlisted	None
29	SRAE_0000058000	Reverse transcriptase domain-containing	40.7	19 / 46 / 0	Unlisted	None
	SRAE_0000058100	Integrase	38.9	18 / 21 / 3	Unlisted	None

	SRAE_0000058200	Hypothetical protein	26.5	3 / 3 / 1	Unlisted	None
	SRAE_0000058300	Reverse transcriptase domain-containing	3.3	2 / 8 / 0	Unlisted	None
30	SRAE_X000146200 **(discarded)**	Hypothetical protein	23.2	4 / 6 / 1	Unlisted	FR15L
31	SRAE_0000049800	Transposase, ISXO2-like domain-containing	24.9	2 / 6 / 2	Unlisted	None
	SRAE_0000049900	Integrase	9.6	4 / 20 / 2	Unlisted	None
32	SRAE_X000088600	Ras-like protein 3	0	0 / 0 / 0	Free-living	None
33	SRAE_X000195800	Hypothetical protein	0	0 / 0 / 0	Parasitic	None
	SRAE_X000195900	Hypothetical protein	30.7	2 / 6 / 0	Parasitic	None
	SRAE_X000196000	Hypothetical protein	12.4	1 / 6 / 0	Parasitic	None
	SRAE_X000196100	Hypothetical protein	31.1	2 / 4 / 1	Unlisted	None
34	SRAE_0000025500	Plasma membrane calcium-transporting ATPase 3	2.2	4 / 5 / 0	Free-living	None
	SRAE_0000025600	Transthyretin-like family-containing	103.9	11 / 37 / 0	Parasitic	None
	SRAE_0000025650	Hypothetical protein	26.3	2 / 9 / 1	Unlisted	None
	SRAE_0000025700	Transthyretin-like family-containing	0	0 / 0 / 0	Parasitic	None
	SRAE_0000025800	Protein argonaute-4	4.9	5 / 9 / 0	Parasitic	None
35	SRAE_0000007600	Amino acid transporter	2.5	4 / 0 / 0	Free-living	None
	SRAE_0000007700	Cathepsin L.1	13.4	9 / 4 / 0	Unlisted	None
	SRAE_0000007800	Cathepsin L.1	8.2	3 / 5 / 0	Free-living	None
	SRAE_0000007900	Hypothetical protein	29.5	14 / 20 / 0	Parasitic	None
	SRAE_0000008000	Hypothetical protein	37.5	10 / 32 / 1	Parasitic	None
36	SRAE_X000138600	Hypothetical protein	2.2	0 / 1 / 0	Same	None

	SRAE_X000138700	MAM domain and Concanavalin A-like lectin	2.3	4 / 0 / 0	Same	None
37	SRAE_X000236650	Hypothetical protein	24.4	3 / 18 / 1	Unlisted	None
	SRAE_X000236700	Ribonuclease H-like domain and AT hook-like family-containing	10	2 / 7 / 0	Unlisted	None
	SRAE_X000236800	Hypothetical protein	18.3	1 / 8 / 1	Unlisted	None
	SRAE_X000236900	Aspartic peptidase domain-containing	13.9	10 / 25 / 0	Unlisted	None
	SRAE_X000237000	Hypothetical protein	26.5	8 / 1 / 1	Unlisted	None
	SRAE_X000237100	Hypothetical protein	29.2	3 / 7 / 0	Unlisted	None
38	SRAE_0000057900	Hypothetical protein	42.9	3 / 10 / 0	Parasitic	None
39	SRAE_0000008000	Hypothetical protein	37.5	10 / 32 / 1	Parasitic	None
	SRAE_0000008100	Sulfotransferase family-containing	19.8	5 / 20 / 0	Parasitic	None
	SRAE_0000008200	Astacin-like metalloendopeptidase	4.3	4 / 1 / 0	Parasitic	None
40	SRAE_2000478600	CAP domain-containing	90	12 / 51 / 1	Parasitic	None
	SRAE_2000478610	Hypothetical protein	7.5	1 / 3 / 0	Unlisted	None
	SRAE_2000478700	Zinc finger, BED-type predicted domain-containing	8	8 / 8 / 0	Free-living	None
41	SRAE_2000499200	Hypothetical protein	75.7	8 / 27 / 2	Parasitic	None
	SRAE_2000499210	Hypothetical protein	40.7	5 / 17 / 0	Parasitic	None
	SRAE_2000499300	Hypothetical protein	15.5	2 / 6 / 0	Parasitic	None
42	SRAE_X000104500	Hypothetical protein	22.2	30 / 81 / 0	Parasitic	None
43	SRAE_X000038200	Hypothetical protein	25.2	8 / 5 / 0	Unlisted	None
	SRAE_X000038300	Synaptogyrin	3.1	2 / 1 / 0	Free-living	None
	SRAE_X000038400	EF-hand domain	2.9	2 / 0 / 0	Unlisted	None
	SRAE_X000038500	RUN domain-containing	4.9	4 / 5 / 0	Parasitic	None

44	SRAE_X000246300	Hypothetical protein	0	0 / 0 / 0	Same	None
45	SRAE_X000222600	Hypothetical protein	30.8	1 / 10 / 0	Parasitic	None
46	SRAE_X000158400	Astacin-like metalloendopeptidase	1.4	0 / 2 / 0	Free-living	None
	SRAE_X000158500	Acetylcholinesterase	8.7	1 / 14 / 0	Parasitic	None
47	SRAE_2000420700	CAP domain-containing	34.1	5 / 28 / 0	Parasitic	None
	SRAE_2000420800	Hypothetical protein	11.1	0 / 4 / 0	Unlisted	None
48	SRAE_X000221400	U1 small nuclear ribonucleoprotein 70 kDa	0	0 / 0 / 0	Same	None
	SRAE_X000221500	Hypothetical protein	5.8	0 / 2 / 0	Unlisted	None
	SRAE_X000221600	Hypothetical protein	46.4	7 / 9 / 0	Unlisted	None
49	SRAE_X000062400 **(discarded)**	Acetylcholinesterase	24.9	14 / 28 / 1	same	EC13
50	SRAE_X000201100	Astacin	29.8	17 / 27 / 1	Parasitic	None
	SRAE_X000201200	Hypothetical protein	12	1 / 5 / 0	Unlisted	None
	SRAE_X000201300	Hypothetical protein	0	0 / 0 / 0	Unlisted	None
51	SRAE_X000247200	Carboxylesterase	6.1	1 / 13 / 0	Free-living	None
	SRAE_X000247300	ShKT domain-containing	41.8	28 / 100 / 0	Parasitic	None
52	SRAE_1000127500	Amino acid transporter	48.2	41 / 34 / 0	Same	None
	SRAE_1000127600	Farnesyltransferase, CAAX box, beta	14	34 / 16 / 0	Same	None
	SRAE_1000127700	Hypothetical protein	2.6	1 / 1 / 0	Unlisted	None
53	SRAE_X000027100	Hypothetical protein	16.4	2 / 6 / 0	Parasitic	None
	SRAE_X000027200	Hypothetical protein	38.3	13 / 13 / 1	Parasitic	None
	SRAE_X000027300	Hypothetical protein	8.2	2 / 2 / 0	Parasitic	None

54	SRAE_X000144200	Astacin	39.5	24 / 24 / 1	Same	EC14
	SRAE_X000144210	Astacin	21.5	6 / 21 / 0	Parasitic	EC14
	SRAE_X000144220	Hypothetical protein	9.4	4 / 4 / 0	Same	FR14R
55	SRAE_X000199600	Hypothetical protein	11.8	2 / 9 / 0	Unlisted	None
	SRAE_X000199700	Integrase	8.7	5 / 11 / 0	Unlisted	None
	SRAE_X000199800	Hypothetical protein	19.5	2 / 5 / 1	Unlisted	None
	SRAE_X000199900	Zinc finger, CCHC-type domain-containing	24.5	9 / 14 / 0	Unlisted	None
	SRAE_X000200000	Reverse transcriptase domain-containing	38.4	25 / 20 / 1	Unlisted	None
	SRAE_X000200100	Hypothetical protein	34.2	22 / 16 / 1	Unlisted	None
56	SRAE_1000059600	Ground-like domain-containing	22.8	22 / 50 / 0	Same	None
	SRAE_1000059700	Phosphate-regulating neutral endopeptidase	14.6	10 / 13 / 0	Parasitic	None
	SRAE_1000059800	Phosphate-regulating neutral endopeptidase	11.3	6 / 10 / 0	Parasitic	None
	SRAE_1000059900	Phosphate-regulating neutral endopeptidase	12.5	9 / 9 / 0	Same	None
57	SRAE_X000168300	Hypothetical protein	46.3	8 / 22 / 0	Parasitic	None
	SRAE_X000168400	Hypothetical protein	23.8	2 / 7 / 0	Parasitic	None
58	SRAE_X000200200	Hypothetical protein	3.2	0 / 1 / 0	Unlisted	None
	SRAE_X000200300	Hypothetical protein	2	1 / 0 / 0	Parasitic	None
59	SRAE_0000065600	Hypothetical protein	69.8	28 / 30 / 3	Unlisted	None
	SRAE_0000065700	Hypothetical protein	24.8	3 / 6 / 0	Unlisted	None
	SRAE_0000065800	Hypothetical protein	12.6	1 / 3 / 0	Unlisted	None
	SRAE_0000065900	Ribonuclease H-like domain-containing protein	6.4	2 / 2 / 0	Unlisted	None

60	SRAE_2000325900 **(discarded)**	Astacin	25.3	13 / 20 / 0	Parasitic	EC5
	SRAE_2000326000	Astacin	7.6	3 / 7 / 0	Parasitic	EC5
61	SRAE_X000233200	Hypothetical protein	11.8	6 / 14 / 1	Unlisted	None
	SRAE_X000233300	Hypothetical protein	11.3	2 / 3 / 0	Unlisted	None
	SRAE_X000233400	Hypothetical protein	23.8	3 / 14 / 0	Unlisted	None
	SRAE_X000233500	Reverse transcriptase domain-containing	23.7	10 / 31 / 4	Unlisted	None
	SRAE_X000233600	Hypothetical protein	30.5	9 / 37 / 1	Unlisted	None
62	SRAE_2000124600	CAP domain-containing	8.7	3 / 5 / 0	Parasitic	EC3
	SRAE_2000124700	CAP domain-containing	5.2	0 / 4 / 1	Parasitic	EC3
	SRAE_2000124800	CAP domain-containing	6.5	4 / 2 / 0	Parasitic	EC3
	SRAE_2000124900	CAP domain-containing	6.6	2 / 4 / 0	Parasitic	EC3
	SRAE_2000125000 **(discarded)**	CAP domain-containing	2.2	1 / 1 / 0	Parasitic	EC3
	SRAE_2000125100 **(discarded)**	CAP domain-containing	38.6	9 / 25 / 2	Parasitic	EC3

1022

1023 **Supplementary Table 6. The hundred most parasitic genes.** Gene gives the gene's designation; Predicted function is the WormBase
1024 ParaSite description of each gene, where Astacin-like metalloendopeptidase is abbreviated to Astacin; Coding SNPs per kb is the number
1025 of SNPs per kb within the coding sequence of that gene; SNP type is the absolute number of synonymous (S), nonsynonymous (NS) and
1026 STOP codon-causing SNPs; Fold change is the $\log_2$ difference in expression of the gene between the parasitic female and free-living
1027 female morphs taken from Hunt *et al.,* 2016, here shown as positive values indicating greater expression in the parasitic female morph;
1028 Expansion cluster is expansion cluster or associated flanking region a gene belongs to, if any; Variable region is as defined in
1029 **Supplementary Table 5**. Some genes are marked as "discarded", because they had poor underlying assembly according to Gap5 analysis
1030 of expansion clusters and flanking regions and so were discounted from analyses.
1031

Gene	Predicted function	Coding SNPs per kb	SNP type (S/NS/STOP)	Fold Change	Expansion cluster	Variable region
SRAE_2000436100	Hypothetical protein	4.7	1 / 2 / 0	14.5	None	None
SRAE_X000014200	Hypothetical protein	15.2	0 / 6 / 1	13.4	None	None
SRAE_X000201000	Hypothetical protein	1.9	0 / 1 / 0	13	None	50
SRAE_1000182300	CAP domain-containing	0	0 / 0 / 0	12.9	EC1	None
SRAE_2000498800	Phloem filament PP1 domain-containing	0	0 / 0 / 0	12.7	None	None
SRAE_2000067500	Transthyretin-like family-containing	15.9	1 / 6 / 0	12.6	None	None
SRAE_X000201200	Hypothetical protein	12	1 / 5 / 0	12.1	None	None
SRAE_1000182700 **(discarded)**	CAP domain-containing	0	0 / 0 / 0	12.1	EC1	None
SRAE_2000420000	Astacin	1.7	0 / 1 / 1	12	None	None
SRAE_X000200300	Hypothetical protein	2	1 / 0 / 0	11.8	None	None
SRAE_X000124900	Hypothetical protein	0	0 / 0 / 0	11.8	None	None
SRAE_2000485600	Tissue inhibitor of metalloproteinase family	15	3 / 3 / 1	11.8	None	None
SRAE_X000222400	Hypothetical protein	73.8	7 / 20 / 0	11.7	None	45
SRAE_X000055800	Hypothetical protein	54.3	3 / 12 / 0	11.7	None	None
SRAE_2000498700	Hypothetical protein	27.8	4 / 9 / 0	11.7	None	None
SRAE_X000124800	Hypothetical protein	0	0 / 0 / 0	11.6	None	None
SRAE_X000037700	Hypothetical protein	0	0 / 0 / 0	11.6	None	None
SRAE_0000057900	Hypothetical protein	42.9	3 / 10 / 0	11.5	None	38
SRAE_2000457510	CAP domain-containing	13.8	4 / 6 / 0	11.4	None	None

SRAE_1000045800	Lipase, class 3 family-containing	15.2	7 / 8 / 0	11.4	None	27
SRAE_2000506800	Hypothetical protein	14.7	8 / 27 / 0	11.3	None	None
SRAE_0000045600	CAP domain-containing protein	9.5	3 / 4 / 0	11.3	None	None
SRAE_2000453600	Astacin	0	0 / 0 / 0	11.3	EC7	None
SRAE_2000522700	Trypsin Inhibitor-like	9	3 / 3 / 0	11.2	None	None
SRAE_0000071120	Metalloendopeptidase	1	0 / 1 / 0	11.2	None	None
SRAE_2000522300	Purple acid phosphatase	4.8	2 / 5 / 0	11.2	None	None
SRAE_2000465200	Hypothetical protein	0	0 / 0 / 0	11.1	None	None
SRAE_X000246200	Hypothetical protein	0	0 / 0 / 0	11.1	None	None
SRAE_2000475600	Hypothetical protein	34.9	3 / 10 / 0	11.1	None	None
SRAE_2000077400	CAP domain-containing	13	4 / 7 / 0	11.1	EC2	None
SRAE_2000465000	Hypothetical protein	0	0 / 0 / 0	11.1	None	None
SRAE_X000168300	Hypothetical protein	46.3	8 / 22 / 0	11	None	57
SRAE_2000499910	Hypothetical protein	7.5	2 / 2 / 0	11	None	None
SRAE_2000499810	Hypothetical protein	41.4	4 / 17 / 0	11	None	None
SRAE_0000057800	Hypothetical protein	28.5	1 / 9 / 0	11	None	7
SRAE_0000077300	Trypsin Inhibitor-like	6.3	1 / 1 / 1	11	None	None
SRAE_1000296600	Hypothetical protein	0	0 / 0 / 0	10.9	None	None
SRAE_2000499820	Hypothetical protein	1.6	1 / 0 / 0	10.9	None	None
SRAE_2000522600	Trypsin Inhibitor-like	25.6	10 / 7 / 0	10.9	None	None
SRAE_X000144210	Astacin	21.5	6 / 21 / 0	10.9	EC14	54
SRAE_2000486100	Tissue inhibitor of metalloproteinase family	51.9	7 / 17 / 0	10.9	None	None
SRAE_X000168800	Prolyl endopeptidase	0	0 / 0 / 0	10.9	None	None
SRAE_2000453500	Astacin	2.5	0 / 3 / 0	10.8	EC7	None
SRAE_2000485800	Tissue inhibitor of metalloproteinase family	0	0 / 0 / 0	10.8	None	None
SRAE_2000499500	Hypothetical protein	0	0 / 0 / 0	10.7	None	3
SRAE_X000065700	Prolyl endopeptidase	3.1	4 / 3 / 0	10.7	None	None
SRAE_2000461200	Hypothetical protein	25.2	3 / 13 / 0	10.7	None	None
SRAE_X000051700	Hypothetical protein	9.1	1 / 3 / 0	10.6	None	28

SRAE_2000456500	Metalloendopeptidase	2.3	2 / 1 / 0	10.6	None	None
SRAE_1000182400	CAP domain-containing	1.2	1 / 0 / 0	10.6	EC1	None
SRAE_2000460300	Zinc metalloproteinase	17.1	5 / 19 / 0	10.6	None	None
SRAE_2000525700 **(discarded)**	Astacin	29.4	3 / 22 / 0	10.6	EC11	None
SRAE_X000201100	Astacin	29.8	17 / 27 / 1	10.5	None	50
SRAE_0000008000	Hypothetical protein	37.5	10 / 32 / 0	10.5	None	35
SRAE_X000038800	Hypothetical protein	0	0 / 0 / 0	10.4	None	None
SRAE_2000076800	CAP domain-containing	39.2	11 / 18 / 1	10.4	EC2	14
SRAE_2000515500	Hypothetical protein	2.9	9 / 15 / 0	10.4	None	None
SRAE_X000055700	Hypothetical protein	0	0 / 0 / 0	10.4	None	None
SRAE_1000182600 **(discarded)**	CAP domain-containing	17.8	2 / 14 / 0	10.4	EC1	None
SRAE_X000168400	Astacin	23.8	2 / 7 / 0	10.3	None	None
SRAE_X000169100	Prolyl endopeptidase	0	0 / 0 / 0	10.3	None	None
SRAE_0000081000	Metalloendopeptidase	0	0 / 0 / 0	10.3	None	None
SRAE_0000000600	Hypothetical protein	0	0 / 0 / 0	10.3	None	None
SRAE_X000195900	Hypothetical protein	30.7	2 / 6 / 0	10.3	None	58
SRAE_2000523800	Astacin	2.8	2 / 2 / 0	10.3	EC10	None
SRAE_1000183100 **(discarded)**	CAP domain-containing	20.4	3 / 14 / 1	10.3	EC1	None
SRAE_2000077000	CAP domain-containing	19	6 / 9 / 1	10.2	EC2	14
SRAE_X000226400	CAP domain-containing	2	1 / 1 / 0	10.2	None	None
SRAE_X000066100	Astacin	28.2	18 / 23 / 0	10.2	None	17
SRAE_X000055500	Hypothetical protein	0	0 / 0 / 0	10.2	None	None
SRAE_2000499920	Hypothetical protein	85.9	14 / 52 / 0	10.2	None	None
SRAE_X000191900	Hypothetical protein	0	0 / 0 / 0	10.1	None	33
SRAE_X000222600	Hypothetical protein	30.8	1 / 10 / 0	10.1	None	None
SRAE_2000451600	Transthyretin-like family-containing	20.6	2 / 8 / 0	10.1	None	None
SRAE_X000191800	Hypothetical protein	0	0 / 0 / 0	10.1	None	None
SRAE_2000455000	Astacin	2.6	1 / 2 / 0	10.1	EC8	None
SRAE_0000078700	Hypothetical protein	0	0 / 0 / 0	10	None	None

SRAE_2000455300	Acetylcholinesterase	0	0 / 0 / 0	10	EC8	None
SRAE_X000200700	Hypothetical protein	57.9	3 / 26 / 0	10	None	None
SRAE_2000499200	Hypothetical protein	75.7	8 / 27 / 2	10	None	41
SRAE_2000071300	Hypothetical protein	30.3	8 / 17 / 0	10	None	None
SRAE_X000158300	Acetylcholinesterase	3	3 / 2 / 0	10	None	57
SRAE_2000124300	CAP domain-containing protein	69	17 / 49 / 4	10	EC3	5
SRAE_2000457710	Metallopeptidase, catalytic domain-containing	1.8	2 / 0 / 0	10	None	None
SRAE_2000527500	CAP domain-containing	3.3	3 / 0 / 0	10	EC12	None
SRAE_2000453700	Astacin	5.5	0 / 7 / 0	9.9	EC7	None
SRAE_2000325600	Astacin	0.9	1 / 0 / 0	9.9	EC5	None
SRAE_2000525800 **(discarded)**	Astacin	1.4	0 / 1 / 0	9.9	EC11	None
SRAE_X000055600	Hypothetical protein	0	0 / 0 / 0	9.9	None	None
SRAE_2000482710	Zinc metalloproteinase	17.8	6 / 19 / 0	9.8	None	None
SRAE_0000077800	Hypothetical protein	4.6	0 / 1 / 0	9.8	None	None
SRAE_2000489900	Aspartic peptidase family	0.9	1 / 0 / 0	9.8	None	None
SRAE_2000289800 **(discarded)**	Astacin	0	0 / 0 / 0	9.8	EC11	None
SRAE_2000508100	Hypothetical protein	66	4 / 14 / 2	9.8	None	None
SRAE_2000456300	Acetylcholinesterase	5.2	1 / 8 / 0	9.7	None	None
SRAE_0000071100	Metalloendopeptidase	0	0 / 0 / 0	9.7	None	None
SRAE_0000082200	Trypsin Inhibitor-like	18.1	6 / 19 / 0	9.7	None	None
SRAE_2000126100	Hypothetical protein	8.6	6 / 2 / 0	9.7	FR3R	None
SRAE_X000147300	Astacin	3	3 / 2 / 0	9.7	None	None
SRAE_0000081500	CAP domain-containing protein	5.6	2 / 3 / 0	9.7	None	None

1032

1033 **Supplementary Table 7. The hundred most free-living genes.** Gene gives the gene's designation; Predicted function is the WormBase
1034 ParaSite description of each gene; Coding SNPs per kb is the number of SNPs per kb within the coding sequence of that gene; SNP type
1035 is the absolute number of synonymous (S), nonsynonymous (NS) and STOP codon-causing SNPs; Fold change is the $\log_2$ difference in
1036 expression of the gene between the parasitic female and free-living female morphs taken from Hunt *et al.,* 2016, here shown as positive
1037 values indicating greater expression in the free-living female morph; Expansion cluster is expansion cluster or associated flanking region
1038 gene belongs to, if any; Variable region is as defined in **Supplementary Table 5**.
1039

Gene	Predicted function	Coding SNPs per kb	SNP type (S/NS/STOP)	Fold Change	Expansion cluster	Variable region
SRAE_2000529300	ShKT domain-containing protein	13.5	0 / 4 / 0	11	None	None
SRAE_2000226500	ShKT domain-containing protein	41.5	5 / 17 / 0	10.8	None	None
SRAE_X000147400	Phosphate-regulating neutral endopeptidase	4.8	2 / 5 / 0	10.4	None	None
SRAE_1000161500	DUF148 domain-containing	1.6	0 / 1 / 0	10.3	None	None
SRAE_X000018600	Mucin 18B	2.4	2 / 2 / 0	10.3	None	None
SRAE_X000158400	Astacin-like metalloendopeptidase	1.4	0 / 2 / 0	10.1	None	46
SRAE_2000474600	ShKT domain-containing protein	2.2	0 / 2 / 0	10.1	None	None
SRAE_X000135300	Collagen alpha-5(IV) chain	1	1 / 0 / 0	10	None	None
SRAE_2000463500	Hypothetical protein	5.5	1 / 1 / 1	9.8	None	None
SRAE_2000079600	Transcription factor Sp6	5.3	3 / 1 / 0	8.8	None	None
SRAE_1000062000	Nematode cuticle collagen	5.3	4 / 1 / 0	8.8	None	None
SRAE_2000491300	ShKT domain-containing protein	0	0 / 0 / 0	8.7	None	None
SRAE_1000170700	Hypothetical protein	6.9	8 / 2 / 0	8.6	None	None
SRAE_1000213600	Aspartic peptidase family	2.2	2 / 1 / 0	8.5	None	None
SRAE_2000400600	Saposin-like type B, 1 domain	0	0 / 0 / 0	8.4	None	None
SRAE_2000477400	ShKT domain-containing protein	8.4	1 / 5 / 0	8.4	None	None
SRAE_1000227500	Hypothetical protein	3.5	0 / 2 / 0	8.2	None	None

SRAE_2000292900	GH07323p	1.2	1 / 1 / 0	8	None	None
SRAE_X000034300	Hypothetical protein	8	1 / 5 / 0	8	None	None
SRAE_2000126900	Nematode cuticle collagen	2.1	1 / 1 / 0	7.9	FR4R	None
SRAE_X000032100	Lipase, class 3 family-containing	3.1	2 / 1 / 0	7.9	None	None
SRAE_1000151800	Protein COL-120	4.1	4 / 1 / 0	7.7	None	None
SRAE_X000215700	Hypothetical protein	9.6	2 / 1 / 0	7.7	None	None
SRAE_2000363400	Hypothetical protein	2.8	1 / 0 / 0	7.5	None	None
SRAE_2000434700	Collagen alpha-5(IV) chain	1	0 /1 / 0	7.5	None	None
SRAE_1000352300	Serine/threonine- /dual specificity protein kinase	0.8	1 / 0 / 0	7.4	None	None
SRAE_1000099100	Hypothetical protein	0.7	1 / 0 / 0	7.4	None	None
SRAE_X000100400	Hypothetical protein	0.9	0 / 1 / 0	7.4	None	None
SRAE_1000220400	Hypothetical protein	0	0 / 0 / 0	7.4	None	None
SRAE_2000033400	Heat shock protein Hsp-12.2	0	0 / 0 / 0	7.2	None	None
SRAE_1000228700	Cell death specification protein 2	1.2	1 / 0 / 0	7.2	None	None
SRAE_X000095500	Hypothetical protein	0	0 / 0 / 0	7.2	None	None
SRAE_1000073100	Protein lin-32	0	0 / 0 / 0	7.2	None	None
SRAE_1000271200	MSP domain; PapD-like domain-containing	0	0 / 0 / 0	7.2	None	None
SRAE_2000115300	Metallothionein, family 4, echinoidea-containing	3	0 / 2 / 0	7.1	None	None
SRAE_1000098100	Hypothetical protein	0	0 / 0 / 0	7.1	None	None
SRAE_2000006500	Hypothetical protein	0	0 / 0 / 0	7	None	None
SRAE_2000425600	Hypothetical protein	0	0 / 0 / 0	7	None	None
SRAE_0000045200	von Willebrand factor, type A domain-containing	3.2	10 / 8 / 0	7	None	None
SRAE_1000198200	Glycoside hydrolase	1.2	1 / 1 / 0	7	None	None
SRAE_1000159100	Hypothetical protein	0.7	0 / 1 / 0	6.9	None	None
SRAE_1000268100	Nematode cuticle collagen	0	0 / 0 / 0	6.9	None	None
SRAE_2000473500	Sulfotransferase family	11	5 / 3 / 3	6.9	None	None
SRAE_X000144300	Protein GLF-1	0.6	0 / 1 / 0	6.8	FR14R	None

SRAE_X000086900	Hypothetical protein	7.2	1 / 4 / 0	6.8	None	None
SRAE_1000058300	Hypothetical protein	7.6	3 / 6 / 0	6.8	None	None
SRAE_X000224800	Nematode cuticle collagen	1.9	1 / 1 / 0	6.8	None	None
SRAE_1000033500	Collagen alpha-5(IV) chain	0.9	0 / 1 / 0	6.7	None	None
SRAE_1000004900	Glycoside hydrolase, family 25	1.3	1 / 0 / 0	6.7	None	None
SRAE_1000015400	Lipase EstA/Esterase EstB family-containing	2	1 / 1 / 0	6.7	None	None
SRAE_2000439500	Collagen alpha-5(IV) chain	0	0 / 0 / 0	6.7	None	None
SRAE_X000039100	Brain-specific homeobox protein homolog	0	0 / 0 / 0	6.7	None	None
SRAE_1000049700	Hypothetical protein	0	0 / 0 / 0	6.7	None	None
SRAE_1000036400	Histidine decarboxylase	12	3 / 4 / 0	6.6	None	None
SRAE_2000476800	Hypothetical protein	0	0 / 0 / 0	6.5	None	None
SRAE_2000431300	Nematode fatty acid retinoid binding family-containing	0	0 / 0 / 0	6.5	None	None
SRAE_X000210100	Domain of unknown function DB domain-containing	1.3	1 / 0 / 0	6.4	None	None
SRAE_2000437000	CAP domain-containing protein	12.6	3 / 5 / 0	6.4	None	None
SRAE_X000195000	Si:ch211-105d4.5	0	0 / 0 / 0	6.4	None	None
SRAE_2000145200	Nematode cuticle collagen	0.9	1 / 0 / 0	6.4	None	None
SRAE_2000482000	N-acylethanolamine-hydrolyzing acid amidase	1.7	1 / 1 / 0	6.4	None	None
SRAE_1000115300	Hypothetical protein	1.3	1 / 1 / 0	6.3	None	None
SRAE_2000459400	Acyl-CoA N-acyltransferase domain-containing	0	0 / 0 / 0	6.3	None	None
SRAE_2000468700	Protein dyf-8	0	0 / 0 / 0	6.3	None	None
SRAE_2000214100	Nematode cuticle collagen	1	1 / 0 / 0	6.3	None	None
SRAE_2000481600	MD-2-related lipid-recognition domain	1.9	1 / 0 / 0	6.3	None	None
SRAE_1000158100	Hypothetical protein	2.5	2 / 2 / 0	6.2	None	None

SRAE_0000015000	MD-2-related lipid-recognition domain-containing	3.7	0 / 2 / 0	6.2	None	None
SRAE_2000365700	Glycoside hydrolase, catalytic domain	2.5	0 / 1 / 1	6.2	None	None
SRAE_2000466700	Properdin	5	7 / 4 / 0	6	None	None
SRAE_2000324800	Hypothetical protein	16.2	15 / 5 / 0	6	None	None
SRAE_2000014200	Saposin B domain	2.4	0 / 1 / 0	5.9	None	None
SRAE_1000271800	MSP domain; PapD-like domain-containing	0	0 / 0 / 0	5.9	None	None
SRAE_1000068700	Thrombospondin, type 1 repeat-containing	6.7	4 / 0 / 0	5.9	None	None
SRAE_X000188000	Sphingosine-1-phosphate lyase 1	2.2	2 / 4 / 0	5.8	None	None
SRAE_X000258800	Thioredoxin-like fold domain-containing	0	0 / 0 / 0	5.7	None	None
SRAE_2000009100	Protein-tyrosine phosphatase	1.1	0 / 1 / 0	5.7	None	None
SRAE_0000012300	Hypothetical protein	4.7	0 / 2 / 0	5.7	None	None
SRAE_2000448200	Hypothetical protein	5.6	0 / 2 / 0	5.6	None	None
SRAE_X000101600	Hypothetical protein	5.6	5 / 3 / 0	5.6	None	None
SRAE_2000041300	LDLR class B repeat	0	0 / 0 / 0	5.5	None	None
SRAE_X000083300	Protein CUTL-16	2.1	2 / 1 / 0	5.5	None	None
SRAE_X000079800	Hypothetical protein	0	0 / 0 / 0	5.5	None	None
SRAE_X000138300	Protein mesh	0	0 / 0 / 0	5.4	None	None
SRAE_1000020600	Hypothetical protein	4.3	0 / 2 / 0	5.4	None	None
SRAE_2000476700	Hypothetical protein	0	0 / 0 / 0	5.4	None	None
SRAE_2000347100	Lipase EstA/Esterase EstB family-containing	1	0 / 1 / 0	5.4	None	None
SRAE_2000380600	GPCR, rhodopsin-like	0.9	0 / 1 / 0	5.4	None	None
SRAE_2000052400	Alpha crystallin/Hsp20 domain	1.2	3 / 1 / 0	5.4	None	None
SRAE_X000138500	Lipase, class 3 family-containing	8.8	4 / 4 / 0	5.3	None	None

SRAE_X000166100	Protein CDH-10	3.2	5 / 12 / 0	5.3	None	None
SRAE_1000022400	Epidermal growth factor-like domain	2.7	11 / 7 / 0	5.3	None	None
SRAE_X000157300	Homeobox protein HMX1	2.5	1 / 2 / 0	5.3	None	None
SRAE_X000043300	Proteasomal ubiquitin receptor ADRM1 homolog	6.3	0 / 7 / 0	5.3	None	None
SRAE_2000424300	Fatty-acid amide hydrolase 2	1.8	3 / 0 / 0	5.3	None	None
SRAE_X000098100	Astacin-like metalloendopeptidase	1.2	0 / 2 / 0	5.3	None	None
SRAE_X000095600	Hypothetical protein	4.1	0 / 2 / 0	5.2	None	None
SRAE_2000482100	Hypothetical protein	11.4	6 / 11 / 0	5.2	None	None
SRAE_2000377500	Nematode cuticle collagen	2	2 / 0 / 0	5.2	None	None
SRAE_2000360100	Alpha amylase family;	5	3 / 3 / 0	5.2	None	None

1040

1041 **Supplementary Table 8. *S. ratti* expansion clusters, revised after further inspection of genome assembly in the cluster region.**
1042 Region shows the numbered Flanking Regions (FR) and Expansion Clusters (EC); Gene the genes present within these regions; Predicted
1043 function is the WormBase ParaSite's description of the gene; Coding SNPs per kb is the number of SNPs per kb within the coding sequence
1044 of that gene; SNP type is synonymous (S), non-synonymous (NS) or STOP-causing (STOP); Expression shows whether the gene is
1045 upregulated (with a difference in expression of log_2-fold of at least 1 being considered upregulation) in the parasitic adult female morph
1046 (Parasitic), the free-living adult female morph (Free-living), or not differentially expressed (Same), all taken from Hunt *et al.,* 2016, or
1047 unlisted there.
1048

Region	Gene	Predicted function	Coding SNPs per kb	SNP type (S/NS/STOP)	Expression
FR1L	SRAE_1000180400	Transcriptional regulator ATRX	3.7	6 / 5 / 0	Parasitic
	SRAE_1000180500	Formin	2.8	4 / 5 / 0	Same
	SRAE_1000180600	Hypothetical protein	1.4	0 / 2 / 0	Same
	SRAE_1000180700	Glycosylphosphatidylinositol-mannosyltransferase I	1.7	0 / 1 / 0	Same
	SRAE_1000180800	Hypothetical protein	1.9	1 / 0 / 0	Same
	SRAE_1000180900	Rhodopsin-like	0.7	1 / 0 / 0	Same
	SRAE_1000181000	TPM domain-containing protein	1.4	0 / 1 / 0	Same
	SRAE_1000181100	MIF4-like	1.2	1 / 1 / 0	Same
	SRAE_1000181200	Sodium/potassium-transporting ATPase α subunit	0	0 / 0 / 0	Free-living
	SRAE_1000181300	Hypothetical protein	0	0 / 0 / 0	Free-living
	SRAE_1000181400	Mediator of RNA polymerase II transcription subunit 9	5.2	2 / 0 / 0	Same
	SRAE_1000181500	Serine/threonine-protein kinase Chk1	0.7	1 / 0 / 0	Same
	SRAE_1000181600	Hypothetical protein	1.1	1 / 0 / 0	Same
	SRAE_1000181700	Hypothetical protein	2.7	3 /1 / 0	Same
	SRAE_1000181800	Hypothetical protein	1.2	0 / 1 / 0	Free-living
	SRAE_1000181900	Eukaryotic translation initiation factor 2A	2.5	0 / 4 / 0	Same
	SRAE_1000182000	Hypothetical protein	0	0 / 0 / 0	Same
	SRAE_1000182100	Heme transporter HRG	0	0 / 0 / 0	Same
EC1	SRAE_1000182200	CAP domain-containing	1.1	0 / 1 / 0	Parasitic
	SRAE_1000182300	CAP domain-containing	0	0 / 0 / 0	Parasitic

	SRAE_1000182400	CAP domain-containing	1.2	1 / 0 / 0	Parasitic
	SRAE_1000183300	CAP domain-containing	3.4	2 / 1 / 0	Parasitic
FR1R	SRAE_1000183400	Nanchung	1.4	1 / 2 / 0	Same
	SRAE_1000183500	Hypothetical protein	0	0 / 0 / 0	Free-living
	SRAE_1000183600	SMc04008-like domain-containing	1.4	0 / 3 / 0	Same
	SRAE_1000183700	Hypothetical protein	0	0 / 0 / 0	Unlisted
	SRAE_1000183800	1,2-dihydroxy-3-keto-5-methylthiopentene dioxygenase	0	0 / 0 / 0	Same
	SRAE_1000183900	Transmembrane receptor	7.1	9 / 4 / 0	Parasitic
	SRAE_1000184000	Predicted transmembrane / coiled-coil 2-containing	0.7	0 / 1 / 0	Unlisted
	SRAE_1000184100	Band 7 protein family and Stomatin family-containing	3.2	3 / 0 / 0	Unlisted
	SRAE_1000184200	Basic-leucine zipper domain-containing	2.5	3 / 2 / 0	Unlisted
	SRAE_1000184300	TBC1 domain family member 13	1.6	2 / 0 / 0	Unlisted
	SRAE_1000184400	BTB/POZ domain-containing	0.7	1 / 0 / 0	Unlisted
FR2L	SRAE_2000075900	NHR/GATA-type domain-containing	2.5	4 /2 / 0	Same
	SRAE_2000076000	MIP20649p	3.2	6 / 3 / 0	Same
	SRAE_2000076100	MIP20649p	0.8	1 / 0 / 0	Unlisted
	SRAE_2000076200	Hypothetical protein	5.7	10 / 5 / 0	Free-living
	SRAE_2000076300	Hypothetical protein	2.4	2 / 3 / 0	Parasitic
EC2	SRAE_2000076400	CAP domain-containing	29.8	7 / 13 / 0	Parasitic
	SRAE_2000076600	CAP domain-containing	21.2	3 / 14 / 0	Parasitic
	SRAE_2000076700	CAP domain-containing	60.4	11 / 39 / 0	Parasitic
	SRAE_2000076800	CAP domain-containing	39.2	11 / 18 / 1	Parasitic
	SRAE_2000076900	CAP domain-containing	36.8	6 / 25 / 0	Parasitic
	SRAE_2000077000	CAP domain-containing	19	6 / 9 / 1	Parasitic
	SRAE_2000077100	CAP domain-containing	14	6 / 6 / 0	Parasitic
	SRAE_2000077200	UDP-glucosyltransferase	12.7	12 / 8 / 0	Parasitic
	SRAE_2000077300	CAP domain-containing	17.4	5 / 10 / 0	Parasitic

	SRAE_2000077400	CAP domain-containing	13	4 / 7 / 0	Parasitic
	SRAE_2000077500	CAP domain-containing	4.4	2 / 4 / 0	Same
FR2R	SRAE_2000077600	Hypothetical protein	10	8 / 14 / 0	Same
	SRAE_2000077700	BTB/POZ domain-containing	7.9	1 / 4 / 1	Unlisted
	SRAE_2000077800	Hypothetical protein	2.9	1 / 0 / 0	Unlisted
	SRAE_2000077900	Protein kinase-like domain-containing	2.1	1 / 2 / 0	Unlisted
	SRAE_2000078000	Ubiquitin-conjugating enzyme, E2 domain	4.5	2 / 0 / 0	Same
	SRAE_2000078100	WH2 domain-containing	5.9	3 / 0 / 0	Same
	SRAE_2000078200	Casein kinase II subunit beta	8.3	2 / 3 / 0	Same
	SRAE_2000078300	Hypothetical protein	0	0 / 0 / 0	Unlisted
	SRAE_2000078400	Hypothetical protein	0	0 / 0 / 0	Same
	SRAE_2000078500	Serine/threonine-protein kinase haspin	11.1	7 / 9 / 0	Same
	SRAE_2000078600	PDZ domain-containing	1.4	0 / 1 / 0	Unlisted
	SRAE_2000078700	CAP domain-containing	15.2	5 / 10 / 0	Parasitic
	SRAE_2000078800	Hypothetical protein	1.4	4 / 0 / 0	Same
FR3L	SRAE_2000123100	Transcription elongation factor SPT5	0.4	0 / 1 / 0	Same
	SRAE_2000123200	Armadillo-like helical domain -containing	1.3	3 / 3 / 0	Same
	SRAE_2000123300	Hypothetical protein	0	0 / 0 / 0	Unlisted
	SRAE_2000123400	Gamma-aminobutyric acid receptor subunit beta	2	3 / 0 / 0	Same
	SRAE_2000123500	Hypothetical protein	6.1	2 / 1 / 0	Unlisted
	SRAE_2000123600	Phosphodiesterase	0.9	2 / 0 / 0	Same
	SRAE_2000123700	Glycosyl transferase	3.4	1 / 4 / 0	Same
	SRAE_2000123800	Tyrosine-protein kinase	0	0 / 0 / 0	Unlisted
	SRAE_2000123900	Bax inhibitor 1-related family-containing	0	0 / 0 / 0	Unlisted
	SRAE_2000124000	Bloom syndrome protein	2	3 / 6 / 0	Free-living
	SRAE_2000124100	Protein lethal(2)essential for life	7.8	4 / 1 / 0	Parasitic
	SRAE_2000124200	Hypothetical protein	14.5	5 / 21 / 0	Parasitic
EC3	SRAE_2000124300	CAP domain-containing	69	17 / 49 / 4	Parasitic
	SRAE_2000124400	CAP domain-containing	43.3	8 / 30 / 1	Parasitic

	SRAE_2000124500	CAP domain-containing	50.9	11 / 33 / 2	Parasitic
	SRAE_2000124600	CAP domain-containing	8.7	3 / 5 / 0	Parasitic
	SRAE_2000124700	CAP domain-containing	5.2	0 / 4 / 1	Parasitic
	SRAE_2000124800	CAP domain-containing	6.5	4 / 2 / 0	Parasitic
	SRAE_2000124900	CAP domain-containing	6.6	2 / 4 / 0	Parasitic
FR3R	SRAE_2000126100	Hypothetical protein	8.6	6 /2 / 0	Parasitic
	SRAE_2000126200	Hypothetical protein	50	3 / 17 / 1	Unlisted
	SRAE_2000126290	Hypothetical protein	10.7	3 / 7 / 0	Unlisted
	SRAE_2000126300	Hypothetical protein	14.1	6 / 7 / 0	Parasitic
	SRAE_2000126400	Hypothetical protein	11.8	3 / 7 / 1	Parasitic
	SRAE_2000126500	Hypothetical protein	0	0 / 0 / 0	Parasitic
	SRAE_2000126600	CAP domain-containing	18.5	6 / 11 / 0	Parasitic
	SRAE_2000126700	Hypothetical protein	3.6	1 / 2 / 0	Same
	SRAE_2000126800	Serine/threonine-protein phosphatase	0.5	0 / 1 / 0	Unlisted
	SRAE_2000126900	Nematode cuticle collagen	2.1	1 / 1 / 0	Free-living
	SRAE_2000127000	Hypothetical protein	8.5	3 / 7 / 0	Unlisted
	SRAE_2000127100	Hypothetical protein	2.5	1 / 1 / 0	Unlisted
	SRAE_2000127200	Flavin-containing monooxygenase	2.9	2 / 2 / 0	Same
	SRAE_2000127300	Serine/threonine-protein kinase RIO1	2.6	3 / 1 / 0	Same
	SRAE_2000127400	Hypothetical protein	1.9	2 / 2 / 0	Same
FR5L	SRAE_2000325100	IA-2 ortholog	2	2 / 5 / 0	Same
	SRAE_2000325200	Hypothetical protein	4.7	0 / 1 / 0	Unlisted
	SRAE_2000325300	Integrator complex subunit 9	0.5	0 / 1 / 0	Same
	SRAE_2000325400	Hypothetical protein	0	0 / 0 / 0	Unlisted
	SRAE_2000325500	UDP-glucuronosyltransferase	3.8	2 / 4 / 0	Free-living
EC5	SRAE_2000325600	Astacin-like metalloendopeptidase	0.9	1 / 0 / 0	Parasitic
	SRAE_2000326000	Astacin-like metalloendopeptidase	7.6	3 / 7 / 0	Parasitic
FR5R	SRAE_2000326100	Epidermal growth factor-like domain-containing	0.6	1 / 1 / 0	Free-living

FR6L	SRAE_2000450300	UDP-glucosyltransferase	5.7	2 / 7 / 0	Parasitic
EC6	SRAE_2000450400	Astacin-like metalloendopeptidase	1.9	1 / 2 / 0	Parasitic
	SRAE_2000450500	Astacin-like metalloendopeptidase	4	1 / 4 / 0	Parasitic
	SRAE_2000450600	Astacin-like metalloendopeptidase	6.5	2 / 6 / 0	Parasitic
	SRAE_2000450700	Astacin-like metalloendopeptidase	22.3	7 / 25 / 0	Parasitic
FR6R	SRAE_2000450800	Nematode fatty acid retinoid binding	5.5	3 / 0 / 0	Unlisted
	SRAE_2000450900	Hypothetical protein	5.3	1 / 5 / 0	Unlisted
	SRAE_2000451000	Hypothetical protein	22.2	6 / 3 / 0	Parasitic
FR7L	SRAE_2000452400	Hypothetical protein	3.6	3 / 0 / 0	Unlisted
	SRAE_2000452500	ATP-binding cassette sub-family D member 4	2.3	3 / 1 / 0	Free-living
	SRAE_2000452600	ATP-binding cassette sub-family D member 4	1.1	1 / 1 / 0	Parasitic
	SRAE_2000452700	Hypothetical protein	1.7	1 / 2 / 0	Unlisted
	SRAE_2000452800	Hypothetical protein	1.8	3 / 0 / 0	Unlisted
	SRAE_2000452900	Hypothetical protein	0	0 / 0 / 0	Unlisted
	SRAE_2000453000	Hypothetical protein	0	0 / 0 / 0	Same
	SRAE_2000453100	Hypothetical protein	20.9	7 / 10 / 0	Parasitic
EC7	SRAE_2000453200	Astacin-like metalloendopeptidase	9.6	3 / 8 / 0	Parasitic
	SRAE_2000453300	Astacin-like metalloendopeptidase	2.6	0 / 3 / 0	Parasitic
	SRAE_2000453400	Sulfotransferase family-containing	0	0 / 0 / 0	Unlisted
	SRAE_2000453500	Astacin-like metalloendopeptidase	2.5	0 / 3 / 0	Parasitic
	SRAE_2000453600	Astacin-like metalloendopeptidase	0	0 / 0 / 0	Parasitic
	SRAE_2000453700	Astacin-like metalloendopeptidase	5.5	0 / 7 / 0	Parasitic
	SRAE_2000453800	Astacin-like metalloendopeptidase	34.8	15 / 26 / 0	Parasitic
	SRAE_2000453900	Astacin-like metalloendopeptidase	5.1	4 / 2 / 0	Parasitic
FR7R	SRAE_2000454000	Zinc metalloproteinase	3.4	3 / 1 / 0	Unlisted
	SRAE_2000454100	Hypothetical protein	3.7	7 / 4 / 0	Free-living
	SRAE_2000454200	Hypothetical protein	0	0 / 0 / 0	Same

	SRAE_2000454300	Sulfotransferase	4.2	4 / 0 / 0	Same
	SRAE_2000454400	Sulfotransferase	1.8	2 / 0 / 0	Same
	SRAE_2000454500	Estradiol 17-beta-dehydrogenase 12	0	0 / 0 / 0	Parasitic
	SRAE_2000454600	Alpha-(1,3)-fucosyltransferase C	3.1	0 /3 / 0	Unlisted
	SRAE_2000454700	Glycosyl transferase, family 14-containing	2.3	1 / 2 / 0	Same
FR8L	SRAE_2000454800	Cytochrome P450 4V2	1.3	1 / 1 / 0	Same
EC8	SRAE_2000454900	Acetylcholinesterase	1.2	2 / 0 / 0	Parasitic
	SRAE_2000455000	Astacin-like metalloendopeptidase	2.6	1 / 2 / 0	Parasitic
	SRAE_2000455100	Hypothetical protein	1.6	1 / 0 / 0	Parasitic
	SRAE_2000455200	CAP domain-containing	0	0 / 0 / 0	Parasitic
	SRAE_2000455300	Acetylcholinesterase	0	0 / 0 / 0	Parasitic
FR8R	SRAE_2000455400	Hypothetical protein	0	0 / 0 / 0	Unlisted
	SRAE_2000455500	Hypothetical protein	0	0 / 0 / 0	Same
	SRAE_2000455600	Zona pellucida domain-containing	0.9	0 / 1 / 0	Unlisted
	SRAE_2000455700	Hypothetical protein	0	0 / 0 / 0	Free-living
	SRAE_2000455800	Hypothetical protein	0	0 / 0 / 0	Unlisted
FR9L	SRAE_2000497000	Hypothetical protein	1.4	5 / 4 / 0	Free-living
EC9	SRAE_2000497100	Astacin-like metalloendopeptidase	5.2	1 / 5 / 0	Parasitic
FR9R	SRAE_2000497600	Cad96Cb	4.5	9 / 0 / 0	Parasitic
	SRAE_2000497700	Zinc finger, RING/FYVE/PHD-type domain-containing	1.5	1 / 0 / 0	Parasitic
	SRAE_2000497800	Protein lethal(2)essential for life	0	0 / 0 / 0	Parasitic
FR10L	SRAE_2000522800	Trypsin Inhibitor-like, cysteine rich domain-containing	22.7	10 / 5 / 0	Parasitic
	SRAE_2000522900	Glycosyl transferase, family 14-containing	4.3	2 / 4 / 0	Unlisted
	SRAE_2000523000	Transthyretin-like family-containing	9.1	3 / 1 / 0	Parasitic

	SRAE_2000523100	7TM GPCR, (Sre) family-containing	0	0 / 0 / 0	Unlisted
	SRAE_2000523200	7TM GPCR, (Sre) family-containing	4.3	0 / 2 / 0	Unlisted
	SRAE_2000523300	Hypothetical protein	1.4	0 / 1 / 0	Unlisted
	SRAE_2000523400	Nuclear hormone receptor	3.9	4 / 1 / 0	Same
	SRAE_2000523500	Proteinase inhibitor I25	0	0 / 0 / 0	Free-living
	SRAE_2000523600	Carboxylic ester hydrolase	3.4	2 / 4 / 0	Unlisted
EC10	SRAE_2000523700	Astacin-like metalloendopeptidase	5.2	1 / 5 / 0	Parasitic
	SRAE_2000523800	Astacin-like metalloendopeptidase	2.8	2 / 2 / 0	Parasitic
	SRAE_2000523900	Astacin-like metalloendopeptidase	26.1	8 / 29 / 1	Parasitic
	SRAE_2000524000	Astacin-like metalloendopeptidase	4	1 / 4 / 0	Parasitic
FR12L	SRAE_2000526900	Importin-beta	2.2	4 / 2 / 0	Same
	SRAE_2000527000	Hypothetical protein	14.3	8 / 17 / 0	Unlisted
EC12	SRAE_2000527100	CAP domain-containing	71.1	9 / 54 / 1	Parasitic
	SRAE_2000527200	CAP domain-containing	18.6	1 / 15 / 1	Parasitic
	SRAE_2000527300	CAP domain-containing	4.6	2 / 2 / 0	Parasitic
	SRAE_2000527400	CAP domain-containing	5.5	2 / 3 / 0	Unlisted
	SRAE_2000527500	CAP domain-containing	3.3	3 / 0 / 0	Parasitic
	SRAE_2000527600	CAP domain-containing	2.2	0 / 2 / 0	Parasitic
	SRAE_2000527700	CAP domain-containing	1.1	0 / 1 / 0	Parasitic
FR12R	SRAE_2000527800	Hypothetical protein	18.5	2 / 10 / 0	Unlisted
	SRAE_2000527900	Hypothetical protein	41.5	9 / 17 / 0	Unlisted
	SRAE_2000528000	Hypothetical protein	1.8	0 / 1 / 0	Unlisted
	SRAE_2000528100	Hypothetical protein	3	3 / 4 / 0	Unlisted
FR14L	SRAE_X000143400	Ferric-chelate reductase 1	10.1	5 / 3 / 0	Unlisted
	SRAE_X000143500	Hypothetical protein	7.1	7 / 9 / 0	Same
	SRAE_X000143600	1x GPCR, rhodopsin-like, 7TM domain-containing	0.7	1 / 0 / 0	Same
	SRAE_X000143700	Hypothetical protein	4.1	3 / 1 / 0	Same

EC14	SRAE_X000143800	Astacin-like metalloendopeptidase	15.5	8 / 9 / 1	Parasitic
	SRAE_X000143900	Astacin-like metalloendopeptidase	18.3	8 / 13 / 2	Parasitic
	SRAE_X000144000	Astacin-like metalloendopeptidase	7.2	4 / 5 / 0	Parasitic
	SRAE_X000144100	Astacin-like metalloendopeptidase	2.4	0 / 3 / 0	Parasitic
	SRAE_X000144200	Astacin-like metalloendopeptidase	39.5	24 / 24 / 1	Parasitic
	SRAE_X000144210	Astacin-like metalloendopeptidase	21.5	6 / 21 / 0	Parasitic
FR14R	SRAE_X000144220	Hypothetical protein	9.4	4 / 4 /0	Same
	SRAE_X000144300	Amine oxidase domain-containing	0.6	0 / 1 / 0	Free-living
EC15	SRAE_X000146800	Astacin-like metalloendopeptidase	29.3	16 / 21 / 0	Parasitic
	SRAE_X000146900	Astacin-like metalloendopeptidase	47.5	25 / 34 / 0	Free-living
FR15R	SRAE_X000146950	Hypothetical protein	3.2	1 / 0 / 0	Unlisted
	SRAE_X000147000	Hypothetical protein	5.1	0 / 1 / 0	Parasitic
	SRAE_X000147100	Hypothetical protein	6.3	2 / 1 / 0	Unlisted
	SRAE_X000147200	Hypothetical protein	26.9	15 / 22 / 0	Parasitic

1049

1050 **Supplementary Table 9. dN/dS ratios of expansion clusters and their flanking regions.**
1051 The dN/dS ratio for genes in expansion clusters and in parentheses the number of genes,
1052 N. We calculated dN/dS ratios by analysing parasites from clades 1 and 3 (**Figure 3**),
1053 treating each as separate populations.
1054

Expansion cluster	Expansion cluster mean dN/dS ratio (N)	Flanking region mean dN/dS ratio (N)
2	0.257 (1)	2.088 (2)
3	0.454 (5)	0.735 (6)
6	1.373 (1)	0.408 (1)
7	3.419 (2)	0.278 (3)
14	0.322 (3)	1.242 (1)

1055

1056 **Supplementary Table 10. Sampling sites and times.**
1057

Site (code)	Coordinates	Type
Cardiff (CA)	51°29'54"N 3°07'25"W	Industrial
Avonmouth (AM)	51°30'43"N 2°40'15"W	Industrial
Long Ashton (LA)	51°26'08"N 2°38'41"W	Farm
Season	**Sampling start date**	**Sampling End date**
Spring	2.2017	3.2017
Summer	6.2017	6.2017
Autumn	9.2017	11.2017
Winter	12.2017	2.2018

1058

1059

SUPPLEMENTARY FIGURES

Supplementary Figure 1. Frequency distribution of the number of *S. ratti* infective larvae isolated from infected rat faecal pellets. Uninfected pellets (N = 178) are not shown. The x-axis is in increments of 20 larvae, with only the upper limit shown, and only alternate increments labelled.

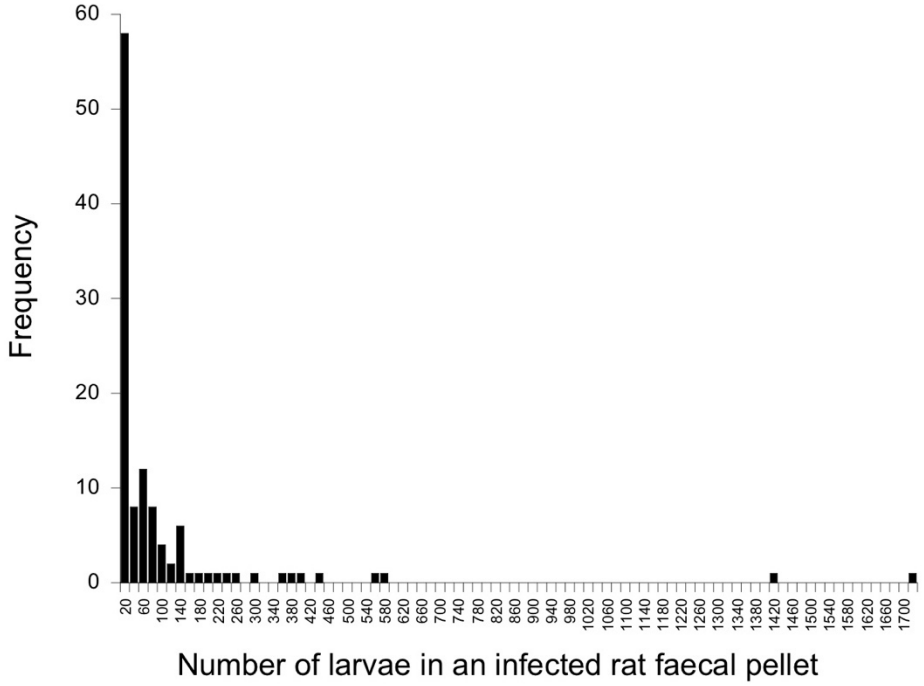

Supplementary Figure 2. Histogram of Φ relatedness values among 90 *S. ratti* larvae. The x-axis is in increments of 0.05 with only the upper limit shown.

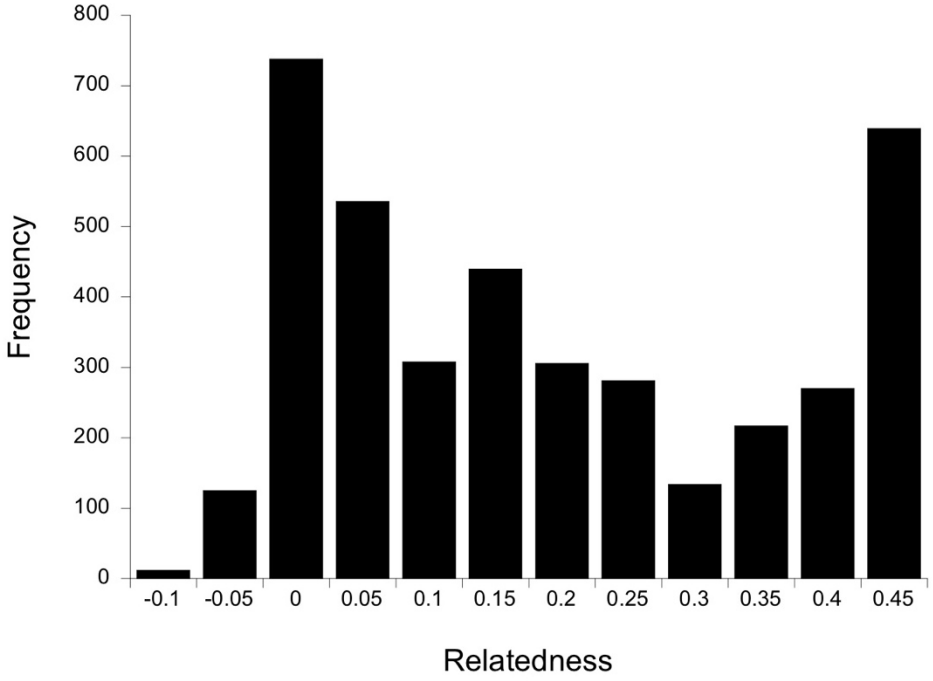

1072 **Supplementary Figure 3. The frequency distribution of the pairwise number of SNP**
1073 **differences among the 90 parasites.** The x-axis is in categories of 10,000, save for the
1074 first three which are 0-1,000, 1,000-5,000, 5,000-10,000; in all the lower end of the range is
1075 shown. The frequency is 1 in the first category.
1076

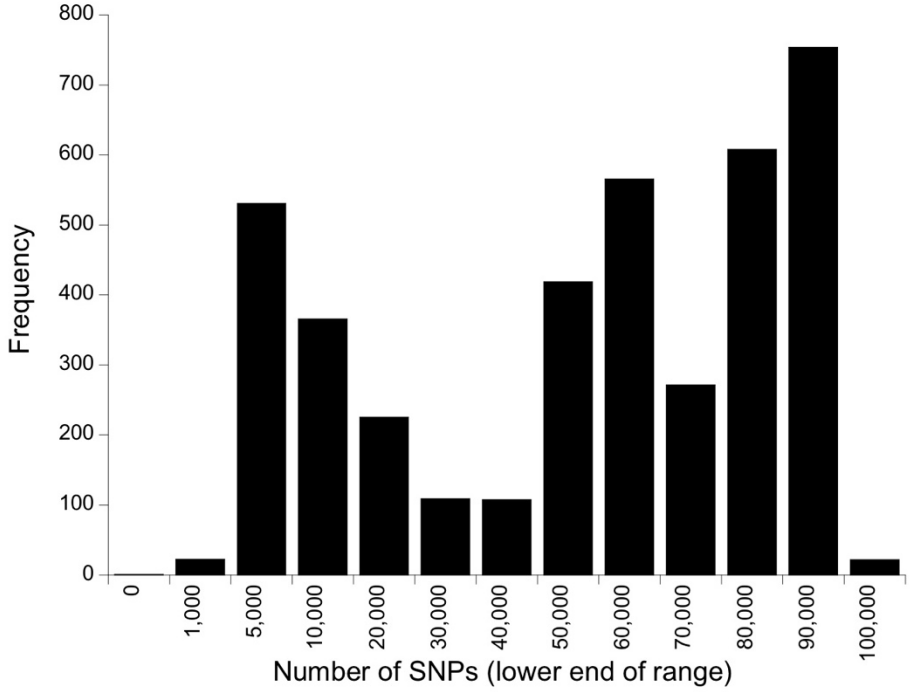

1077
1078

1079 **Supplementary Figure 4. Maximum likelihood trees of the 90 parasites.** In each tree,
1080 the support for each node is shown, and the clade membership of the worm is shown by the
1081 coloured dots, which correspond to the neighbour-joining tree (**Figure 3**). Trees are
1082 calculated based on analysis of chromosome 1 only, part 1 of chromosome 2, part 2 of
1083 chromosome 2, part 1 of the X chromosome and part 2 of the X chromosome. In all the scale
1084 bar is in units of substitutions per site.
1085

Chromosome 1

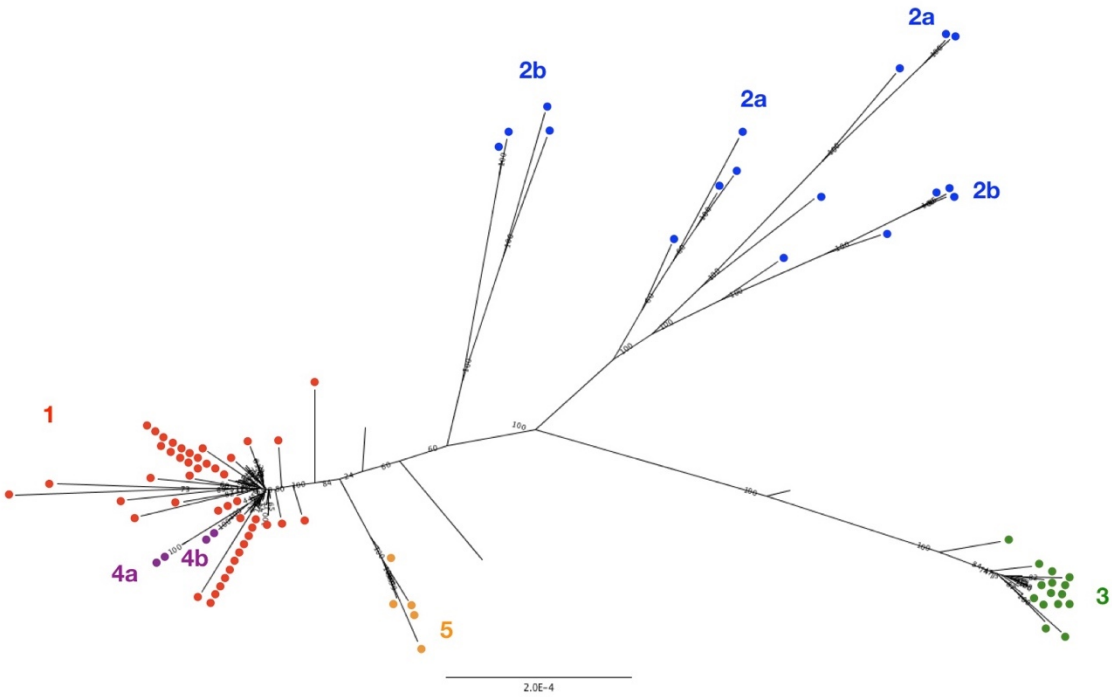

1086

Chromosome 2, part 1

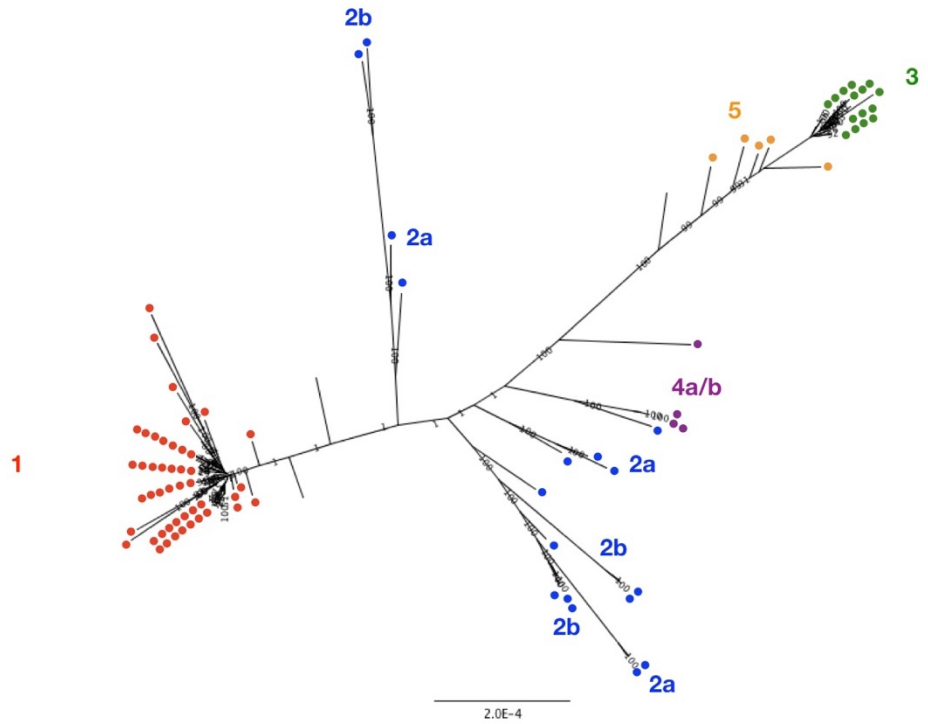

1087
1088

Chromosome 2, part 2

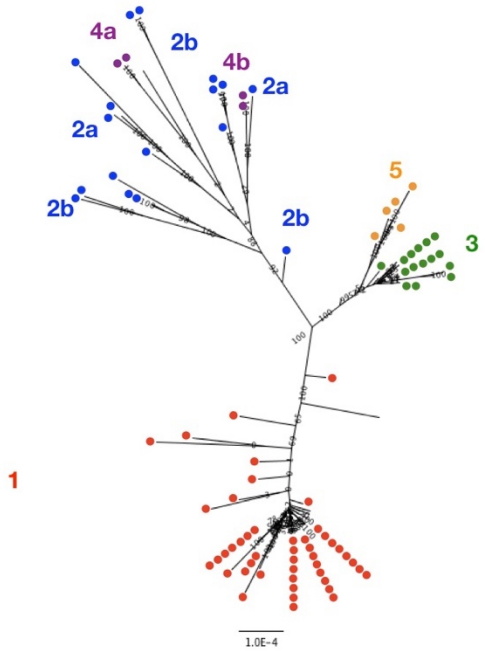

1089
1090

1091

Chromosome X, part 1

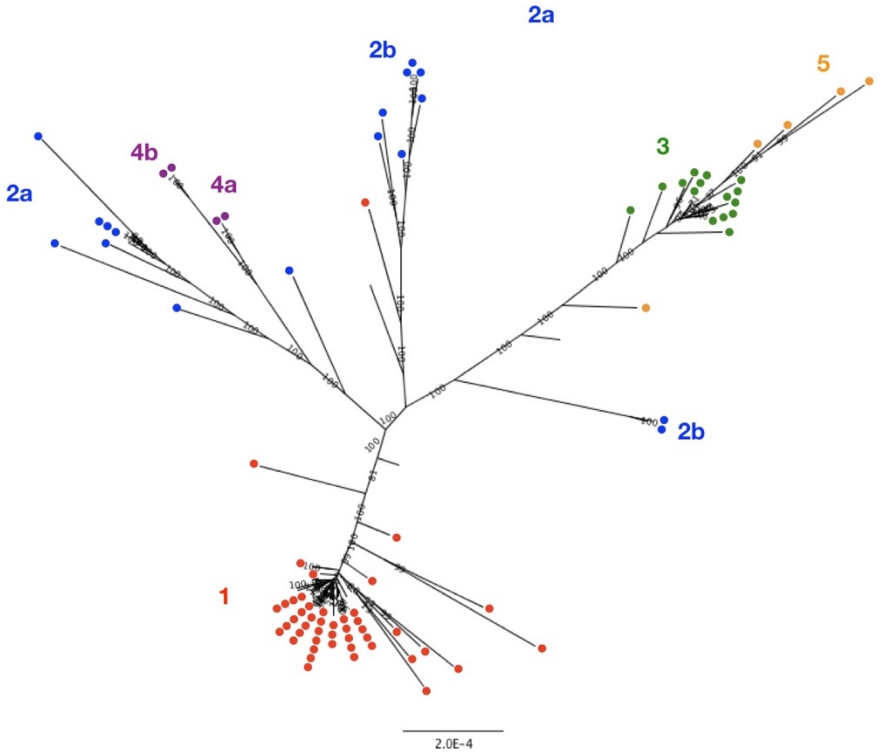

1092
1093

Chromosome X, part 2

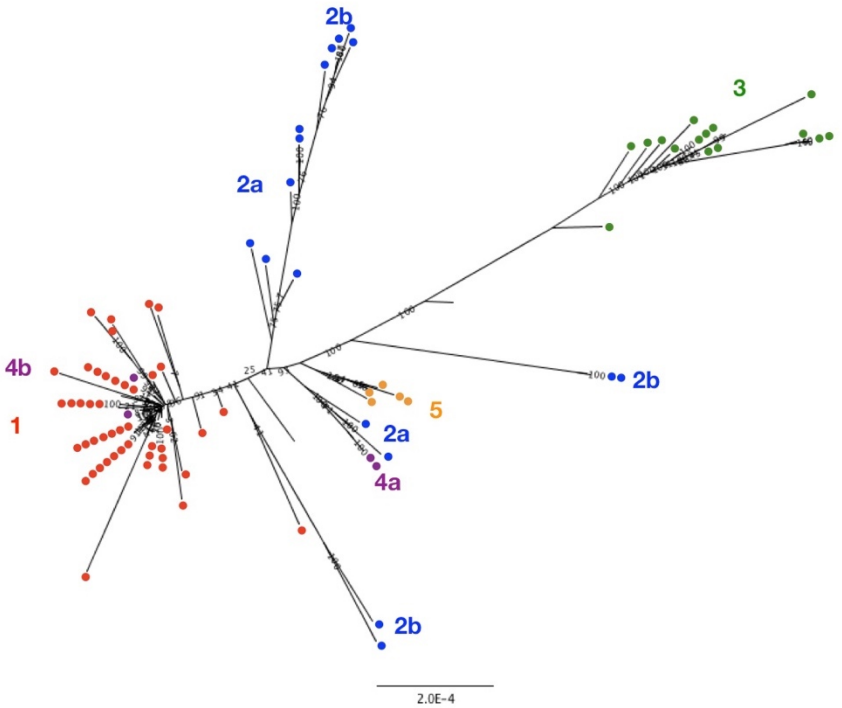

1094

1095 **Supplementary Figure 5. ADMIXTURE analysis of the 90 parasites.** The ADMIXTURE
1096 diagrams are shown for K = 2, 3, 4, 5 (with cross validation errors of 0.22965, 0.16255,
1097 0.16335, 0.16136, respectively). For K = 6, only five groups are detected. All diagrams have
1098 the same right to left order of worms, which is shown in a Table at the end of the figure.
1099

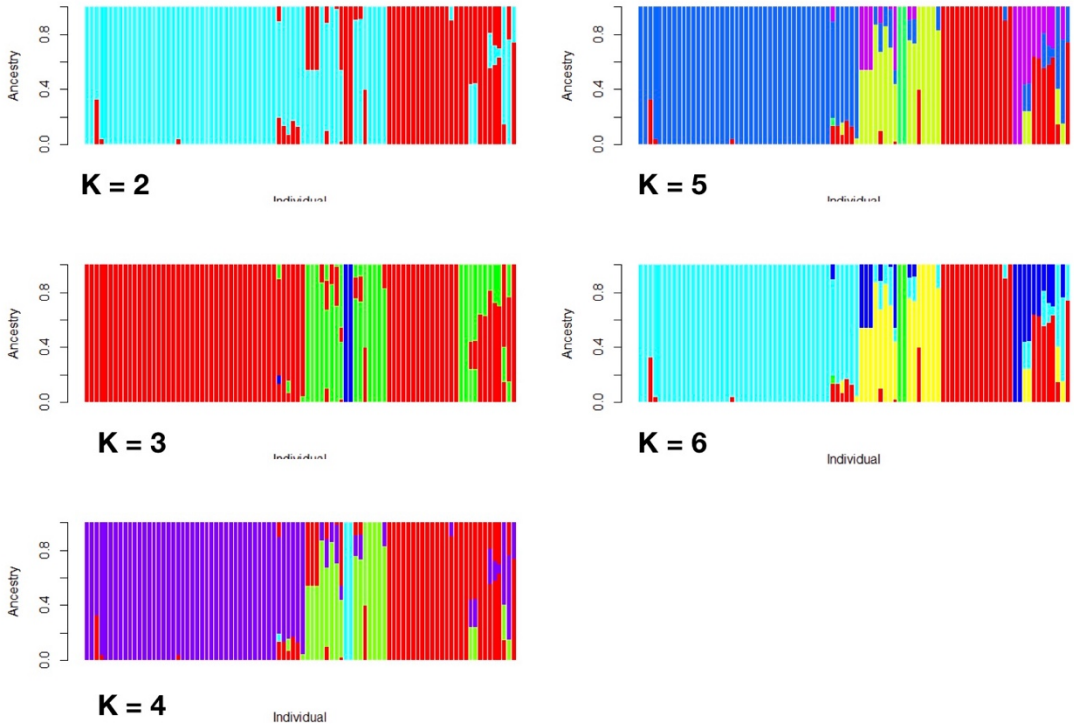

1100
1101

Position in ADMIXTURE diagram	Worm designation	NJ tree clade membership
Far left	CA273_8	1
	CA273_30	1
	CA275_47	1
	LA217_14	1
	LA219_13	1
	LA222_45	1
	LA223_8	1
	LA223_29	1
	LFA14_5	1
	LA315_1	1
	LA315_4	1
	LA316_4	1
	LA316_5	1
	LA317_2	1
	LA319_5	1

	LA319_8	1
	AM99_8	1
	AM99_21	1
	AM100_37	1
	AM190_17	1
	AM194_1	1
	AM242_30	1
	AM252_62	1
	AM253_77	1
	AM280_49	1
	AM282_1	1
	AM282_67	1
	AM283_1	1
	AM283_2	1
	AM283_3	1
	AM283_4	1
	AM283_5	1
	AM284_59	1
	AM284_60	1
	AM284_61	1
	AM286_88	1
	AM286_92	1
	AM287_67	1
	AM288_1	1
	AM288_2	1
	AM291_93	1
	AM292_2	1
	AM293_2	1
	AM294_2	1
	AM296_4	1
	AM299_79	1
	CA338_1	2a
	LA217_5	2a
	LA319_3	2a
	LA320_1	2a
	AM245_61	2a
	AM253_6	2a
	AM287_65	2a
	AM293_94	2b
	CA273_38	2b
	CA275_20	2b
	CA338_4	2b
	CA338_6	2b
	LA320_11	2b

	AM99_31	2b
	AM100_35	2b
	AM100_50	2b
	AM294_4	2b
	CA273_10	3
	CA273_26	3
	CA275_11	3
	CA275_51	3
	LA315_3	3
	LA319_6	3
	LA320_5	3
	AM99_19	3
	AM99_30	3
	AM187_14	3
	AM258_25	3
	AM281_5	3
	AM282_63	3
	AM296_1	3
	AM298_2	3
	AM187_12	4a
	AM287_58	4a
	AM114_2	4a
	AM287_56	4a
	AM105_9	5
	AM280_56	5
	AM294_1	5
	AM295_1	5
	AM296_2	5
	AM292_3	Not in clade
	CA338_2	Not in clade
Far right	AM296_5	Not in clade

1103 **Supplementary Figure 6. PCA analysis of *S. ratti* parasites.** Projections of principal components (PC) 1 and 2 of the 90 parasites from
1104 the three samples sites and the 10 isofemale lines, where PCs 1 and 2 explained 91% of the variance. Individuals are coloured according
1105 to (A) sampling site and (B) neighbour-joining dendrogram clades (**Figure 3**) with the colour coding scheme shown in each panel.

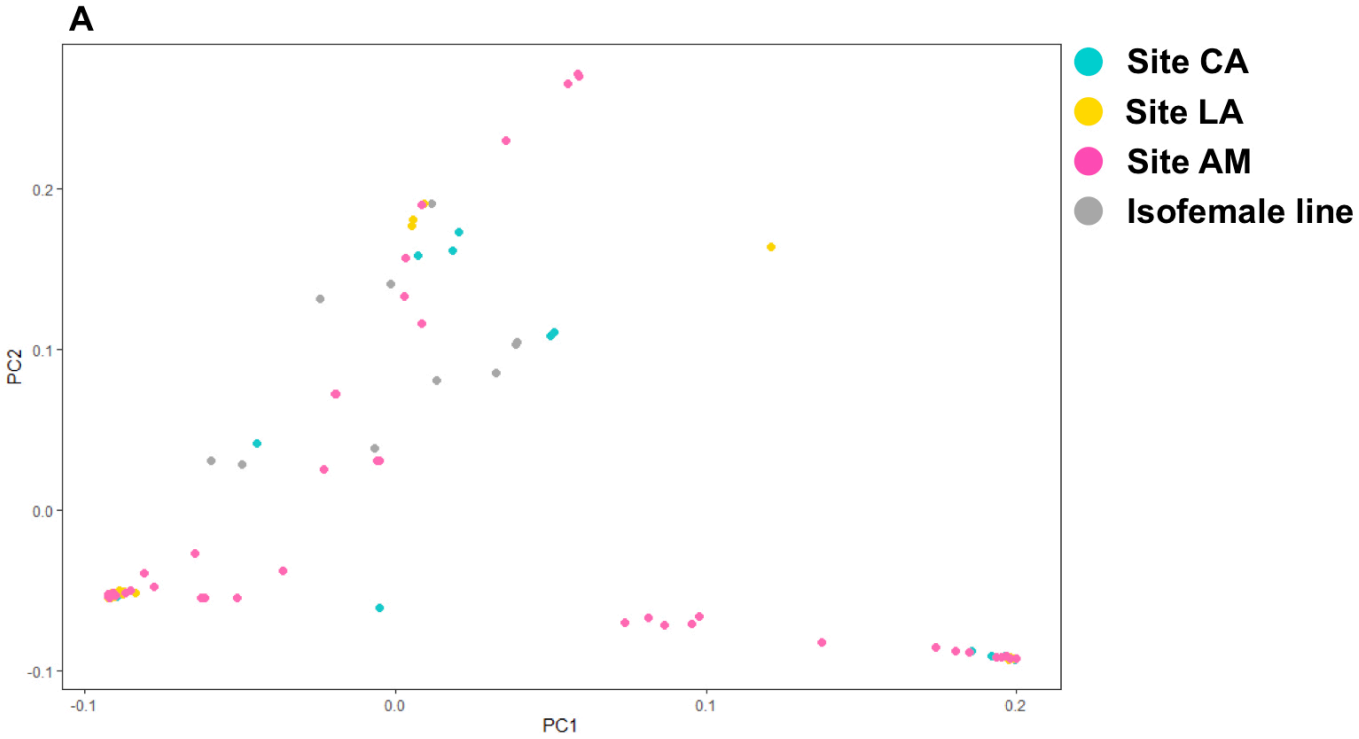

1106
1107
1108

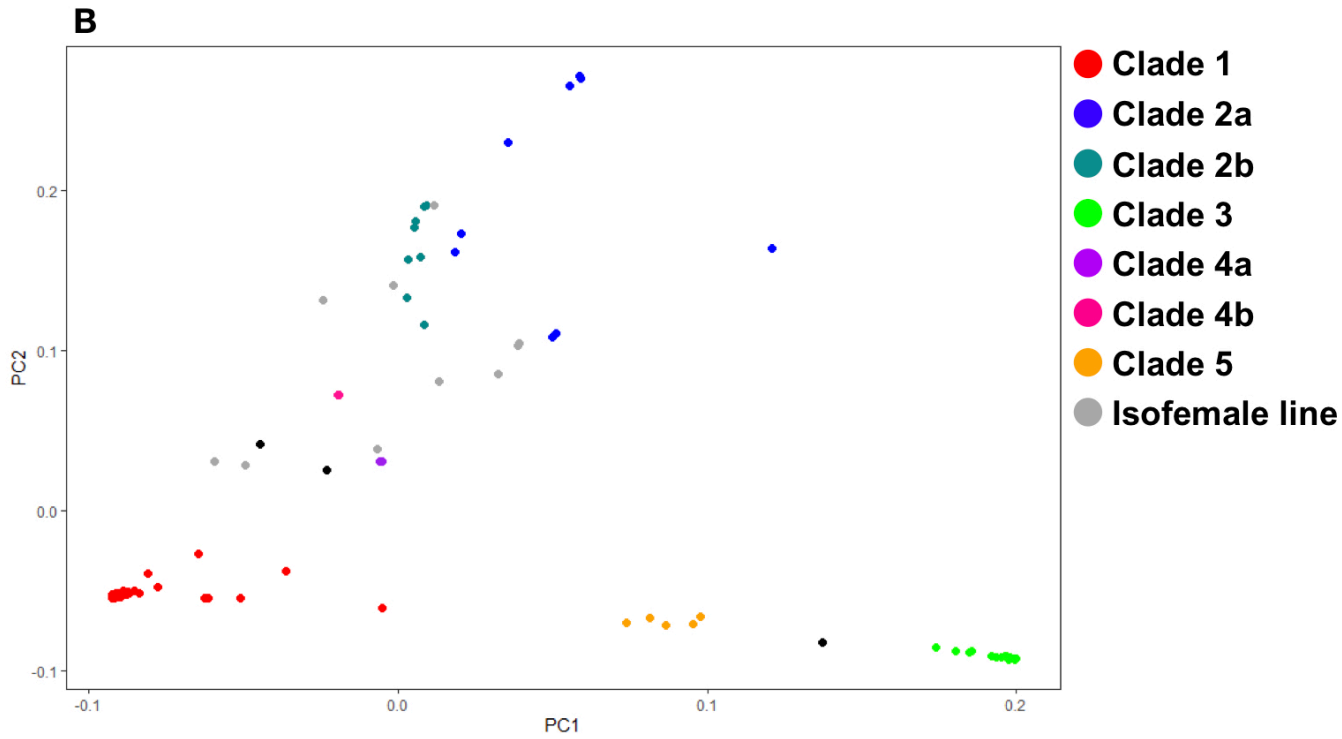
B
Clade 1
Clade 2a
Clade 2b
Clade 3
Clade 4a
Clade 4b
Clade 5
Isofemale line
PC2
PC1
0.2
0.1
0.0
-0.1
-0.1
0.0
0.1
0.2

1109
1110

1111 **Supplementary Figure 7. Minimum spanning *S. ratti* mitochondrial haplotype maps.** Individual pellets are shown by their sampling
1112 site (AM, CA, LA) and the number preceding the underscore; the number after the underscore is the unique identifier of that worm.
1113 Haplotypes represented by multiple individuals are denoted by single letters. Four mitochondrial clades (A – D) are evident. Individual
1114 worms are coded either by the sampling site from which they were obtained or by the nuclear clade to which they belong (**Figure 3**).
1115 Mitochondrial clades A, B and C contained individuals from all 3 sampling sites, though at different rates. Mitochondrial clade A contains
1116 all individuals from nuclear clades 3 and 5 as well as one individual from nuclear clade 2b. Mitochondrial clade B contains individuals from
1117 nuclear clades 1, 2a and 4b. Mitochondrial clade C contains only individuals from nuclear clade 2b. The two individuals of nuclear clade
1118 4a appear as intermediate between mitochondrial clades B and C in the haplotype map and so are designated as minor mitochondrial
1119 clade D.
1120

1121

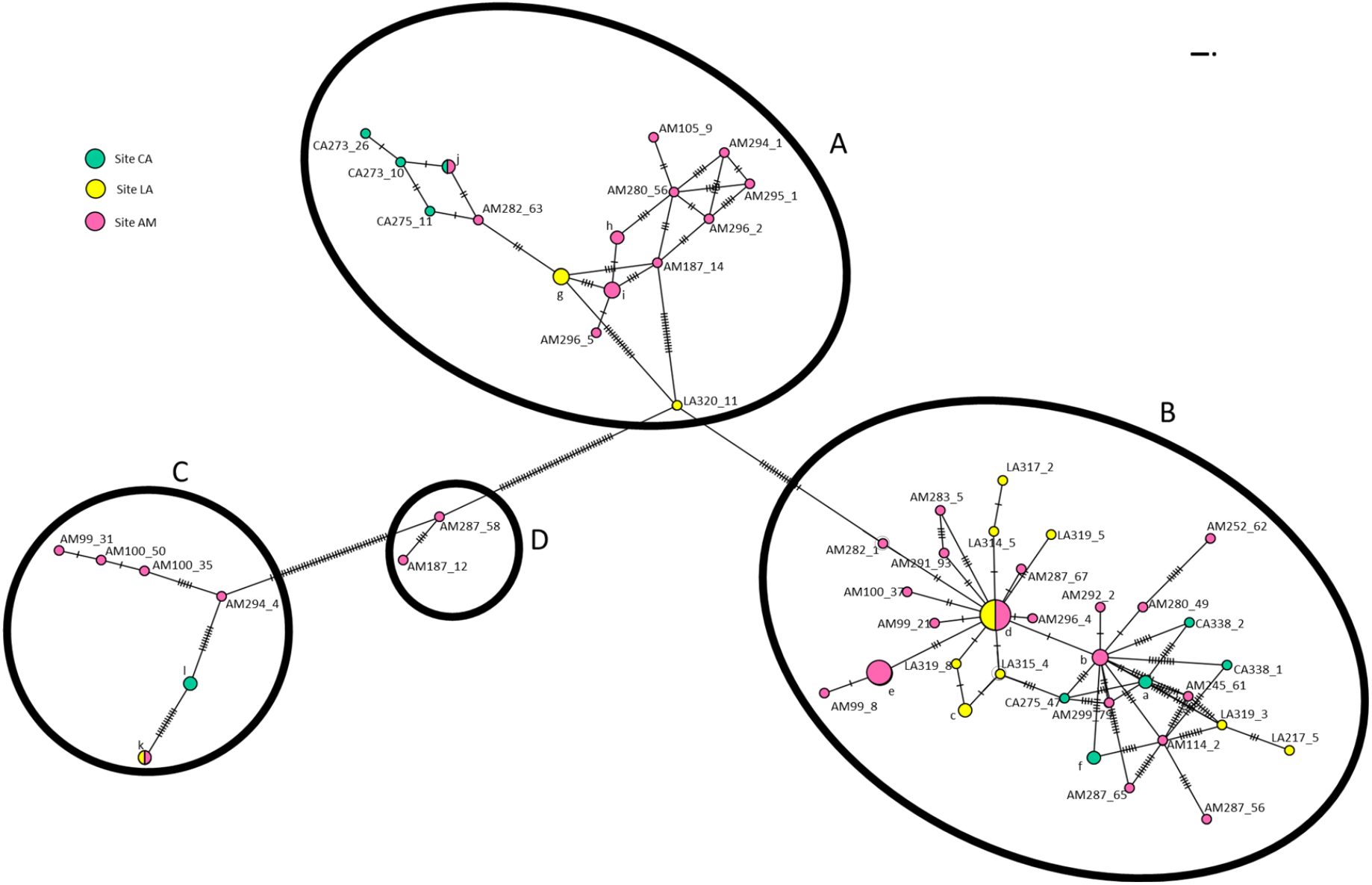

1122
1123

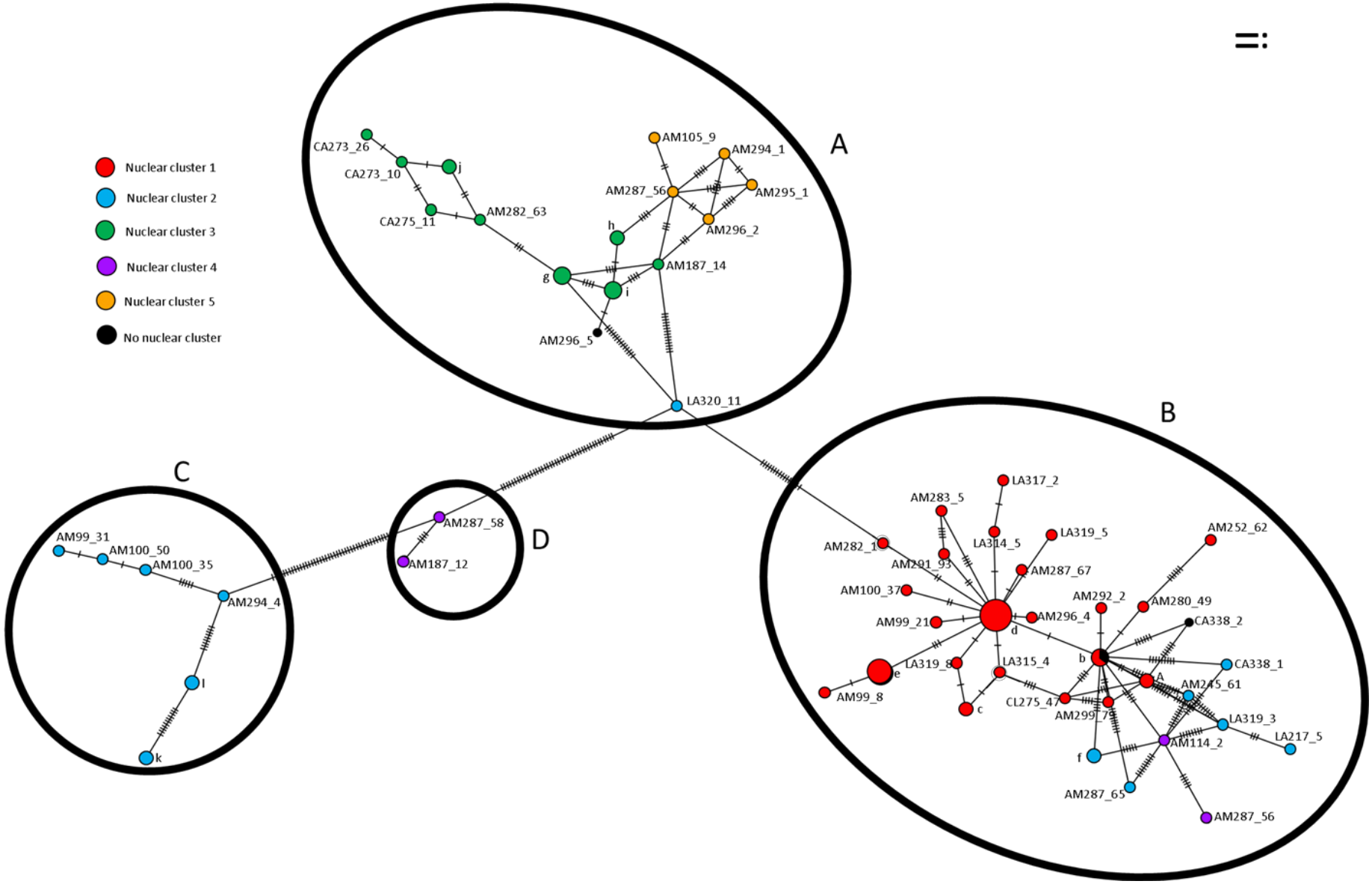
Nuclear cluster 1
Nuclear cluster 2
Nuclear cluster 3
Nuclear cluster 4
Nuclear cluster 5
No nuclear cluster
A
B
C
D
CA273_26
CA273_10
CA275_11
AM282_63
j
h
g
i
AM105_9
AM294_1
AM287_56
AM295_1
AM296_2
AM187_14
AM296_5
LA320_11
AM99_31
AM100_50
AM100_35
AM294_4
l
k
AM287_58
AM187_12
LA317_2
AM283_5
LA319_5
AM252_62
AM282_1
LA314_5
AM291_93
AM287_67
AM100_37
AM292_2
AM280_49
AM99_21
AM296_4
CA338_2
d
b
CA338_1
LA319_8
LA315_4
e
A
AM245_61
AM99_8
CL275_47
c
AM299_79
LA319_3
LA217_5
AM114_2
f
AM287_65
AM287_56

1124

Supplementary Figure 8. Ritland and Lynch pairwise relatedness values of rats within sampling sites. The x-axis is in increments of 0.1, with only the upper limit shown. At each site there is a right-hand skew to these distributions; Shapiro-Wilkes test for normality statistics W = 0.89 for site AM, W = 0.9. for site CA and W = 0.87 for site LA, P > 0.0001 in all cases.

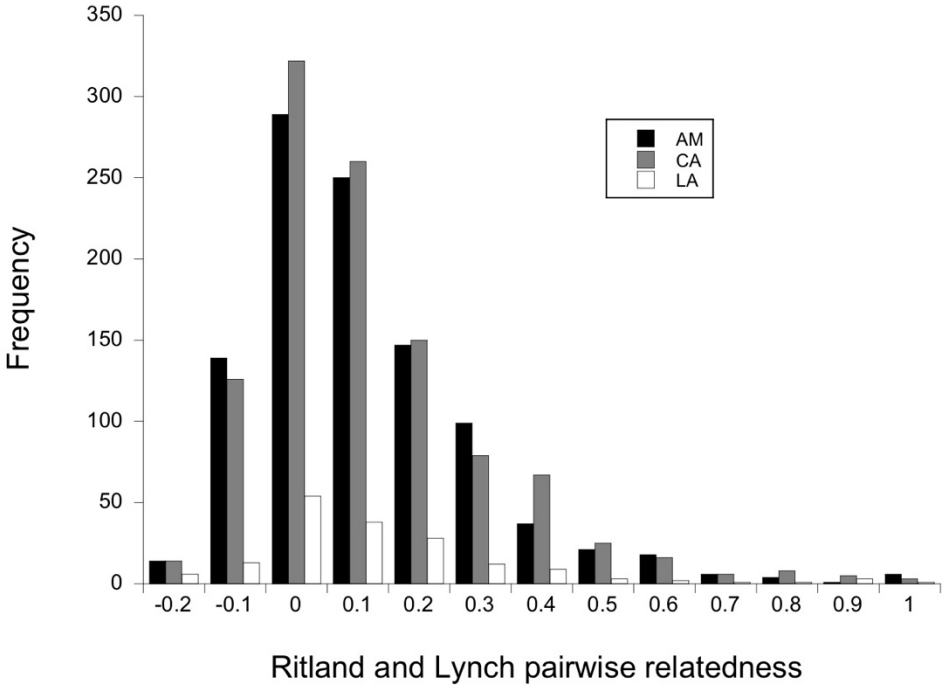

Supplementary Figure 9. *S. ratti* neighbour-joining dendrograms of 10 isofemale lines and 90 larvae collected from the three sample sites. Isofemale lines are prefixed by ED (**Supplementary Table 4**). Five of the isofemale lines (derived from parasites collected from the southern UK in 1989-90, and Japan in 1990) are within clade 2b, which is the most diverse of the clades, but the other 5 isofemale lines are in clades 1, 2a and 4.

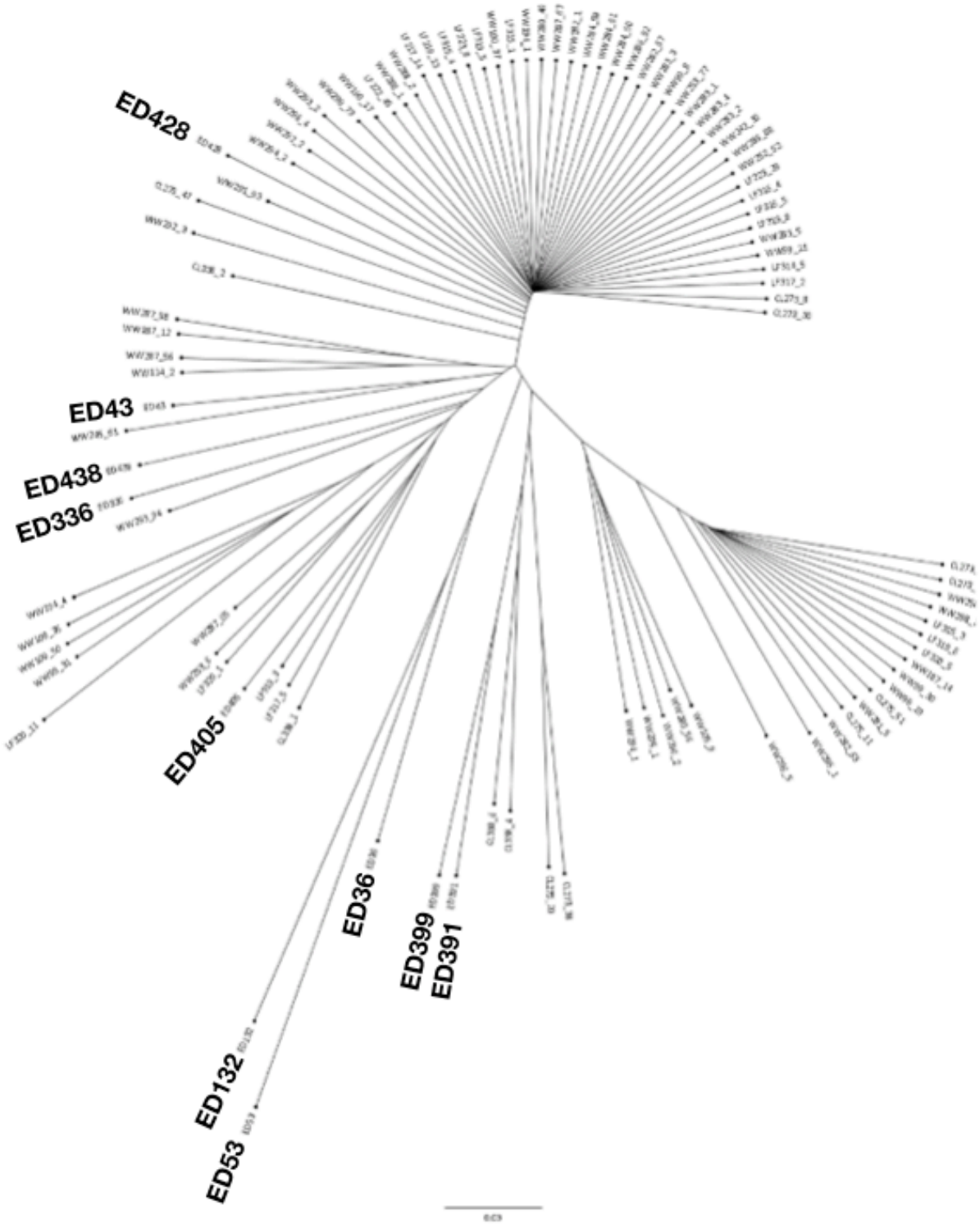

1141 **Supplementary Figure 10. Linkage disequilibrium in the *S. ratti* genome.** LD shown as
1142 r^2 values. X1 and X2 are the largest and second largest X chromosome scaffolds,
1143 respectively.
1144

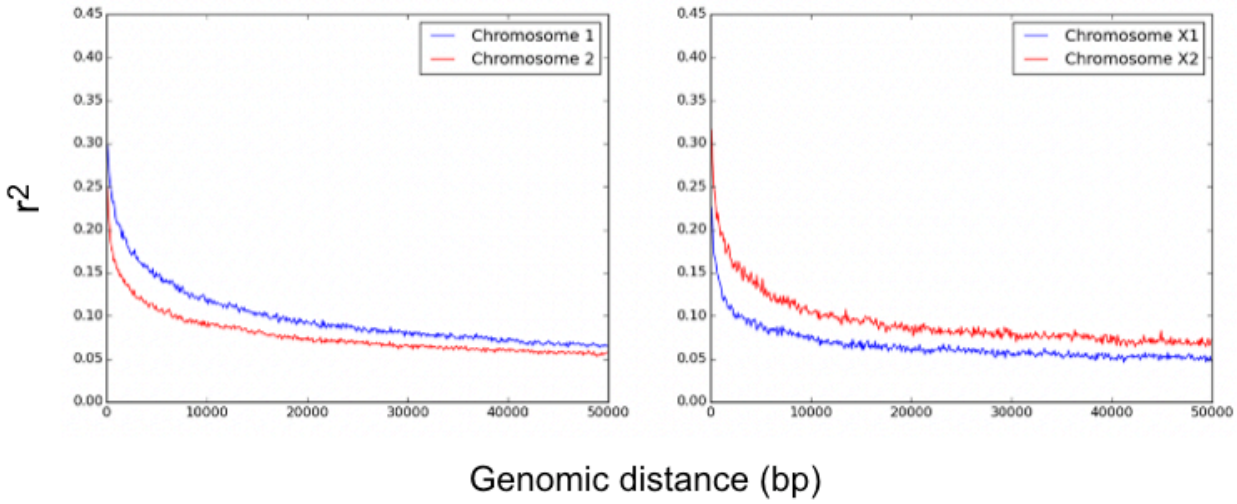

1145
1146

1147 **Supplementary Figure 11. Linkage disequilibrium in the *S. ratti* genome for clade 1**
1148 **and 3 parasites.** LD is shown as r^2 values for (A) clade 1 and (B) clade 3 parasites. X1 and
1149 X2 are the largest and second largest X chromosome scaffolds, respectively.
1150

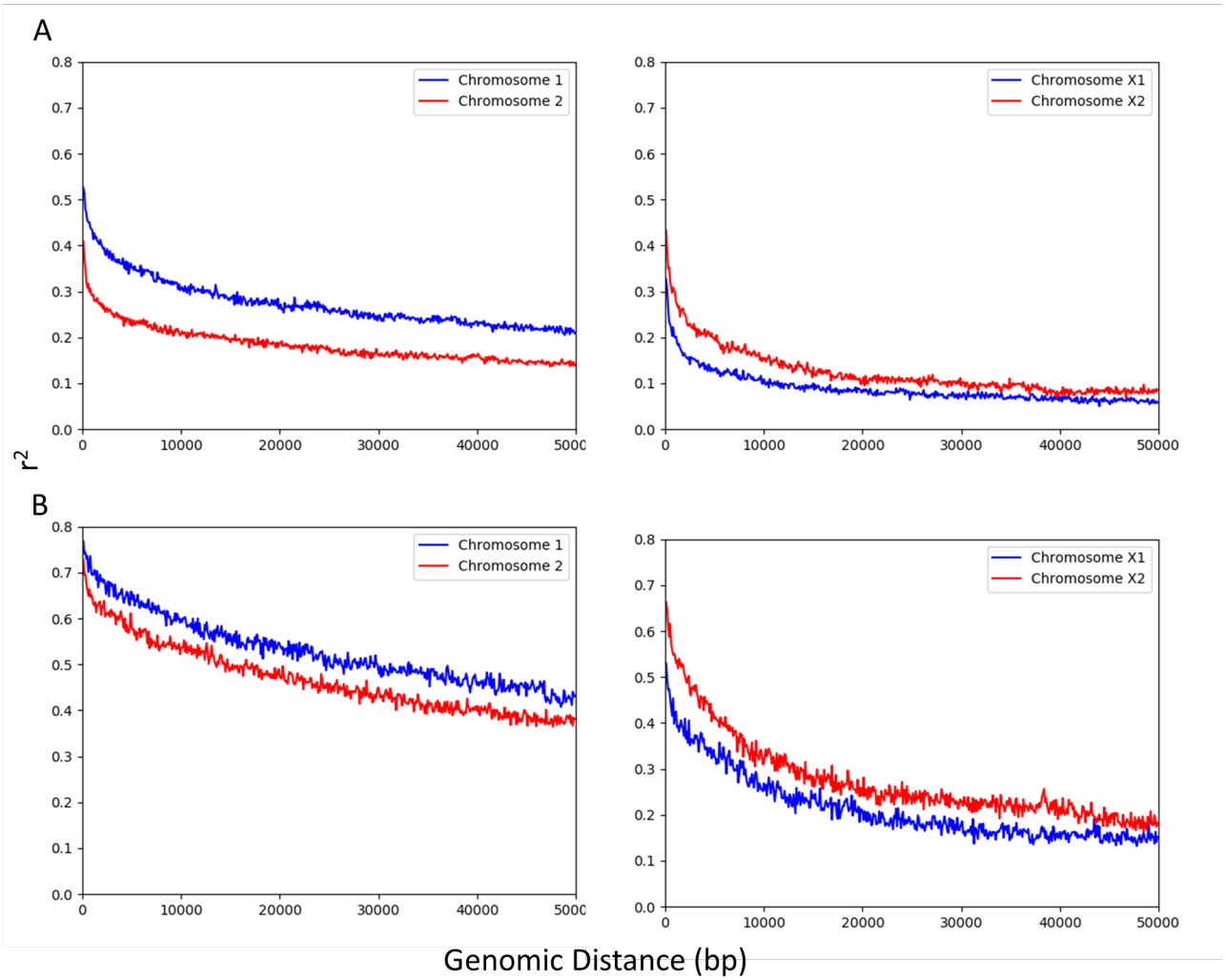

1151
1152

1153 **Supplementary Figure 12. Heatmaps of linkage disequilibrium in the *S. ratti* genome**
1154 **for clade 1 and 3 parasites.** LD is shown as r^2 values on a coloured scale for (A) clade 1
1155 and (B) clade 3. X1 and X2 refer to the largest and second largest scaffolds of the X
1156 chromosome, respectively. The inserts enlarge regions to show areas of high LD.
1157

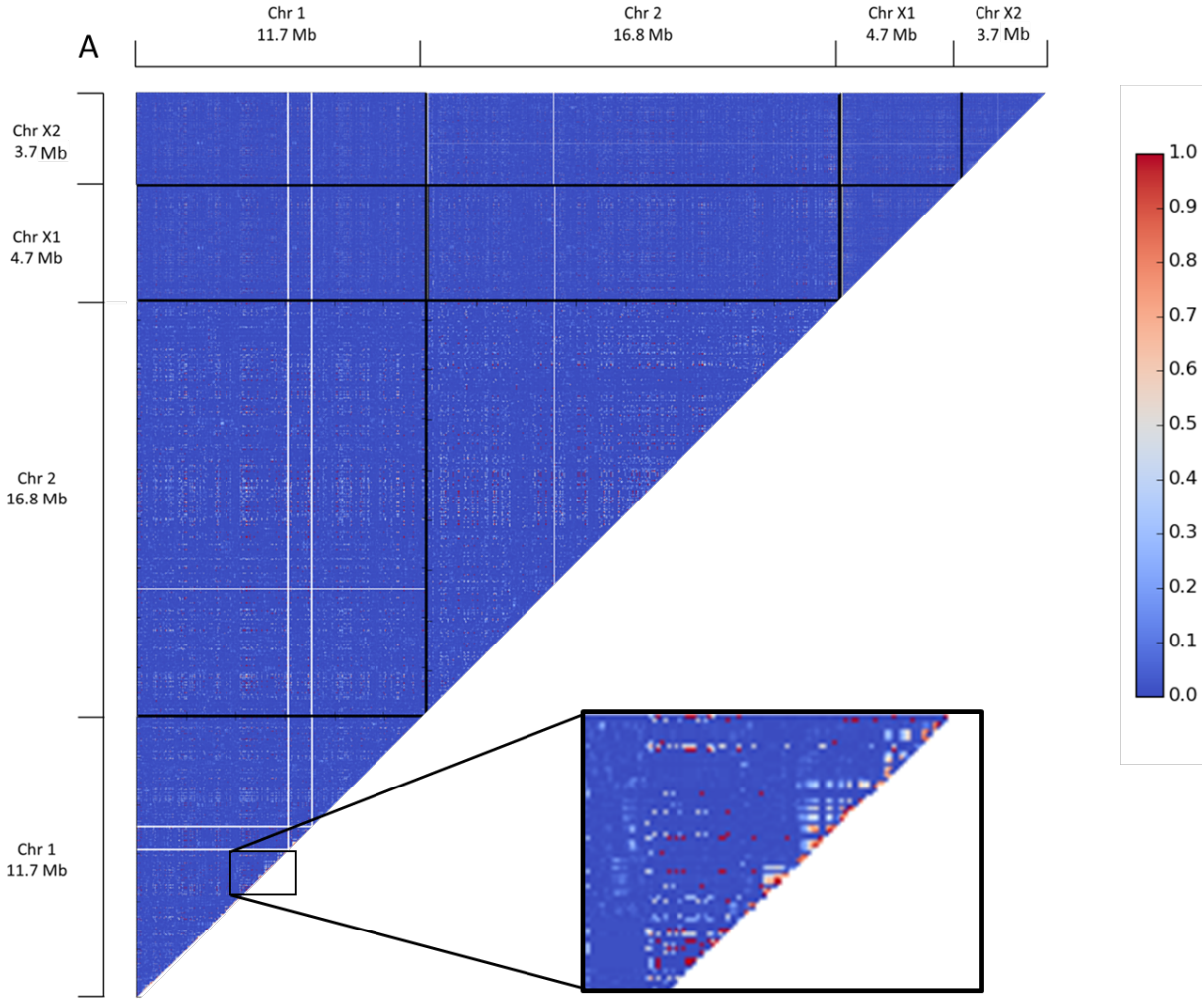

1158

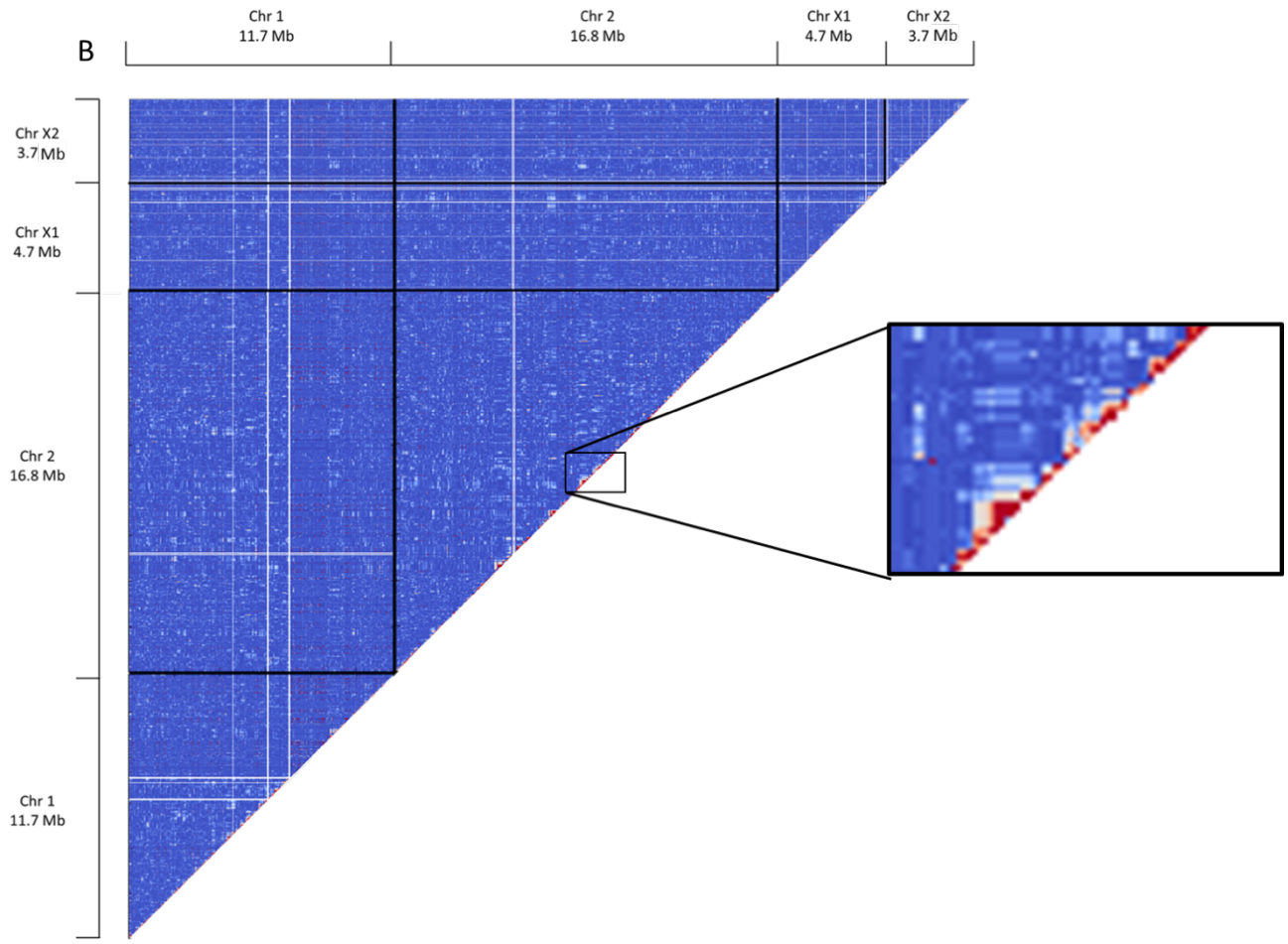
B
Chr 1
11.7 Mb
Chr 2
16.8 Mb
Chr X1
4.7 Mb
Chr X2
3.7 Mb
Chr X2
3.7 Mb
Chr X1
4.7 Mb
Chr 2
16.8 Mb
Chr 1
11.7 Mb

Supplementary Figure 13. Heatmaps of linkage disequilibrium in the *S. ratti* genome. Phasing of genotypes was carried out by Beagle (above the diagonal) or Shapeit (below the diagonal). X1 and X2 refer to the largest and second largest scaffolds of the X chromosome, respectively. Vertical and horizontal white lines in chromosome 1 represent two megabase long tracts of Ns that separate the three X chromosome scaffolds, whose genomic order is not known.

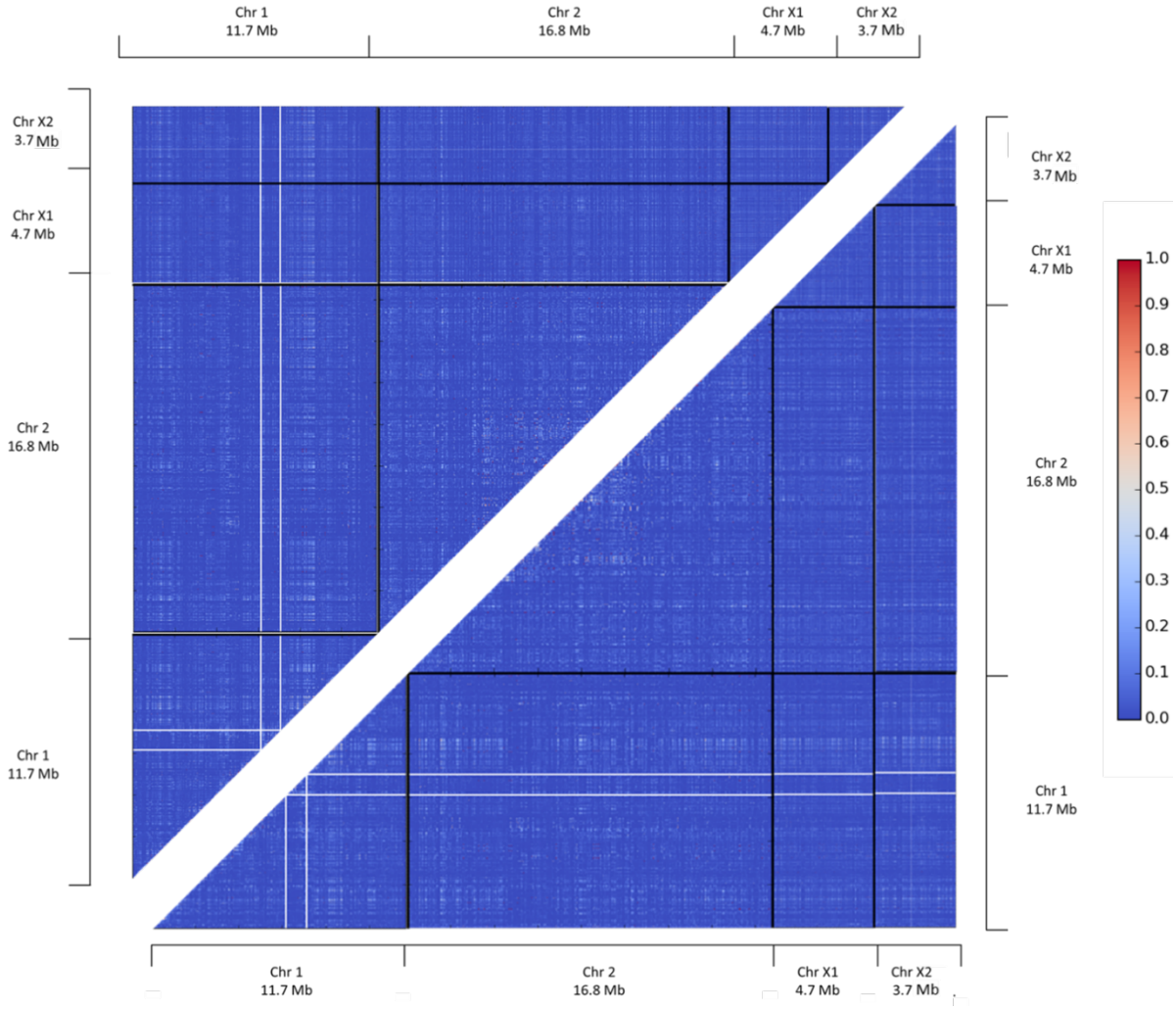

1170 **Supplementary Figure 14. The distribution of SNPs across the *S. ratti* genome.** The distribution of SNPs for all 90 parasites for
1171 discrete, 10 kb windows, each represented by a vertical bar, for chromosomes 1, 2 and the two scaffolds of the X chromosome.
1172

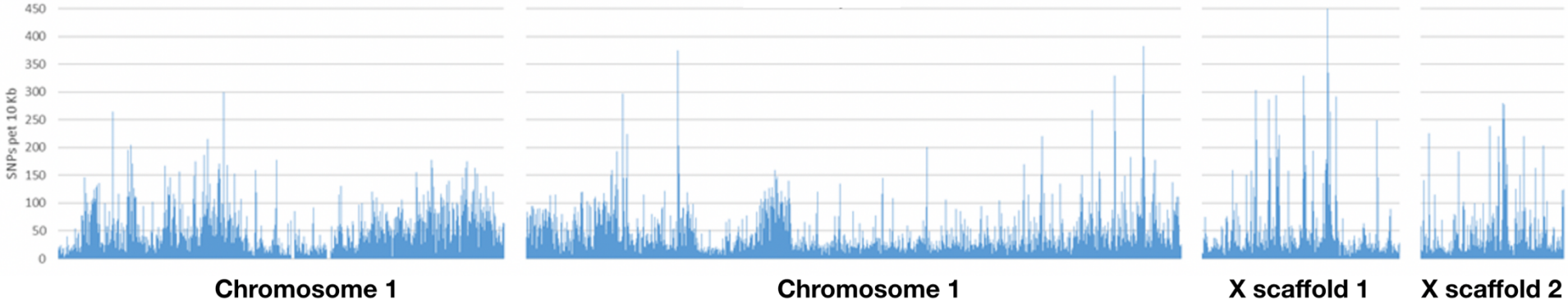

1173
1174

Supplementary Figure 15. Neighbour-joining dendrograms based on five expansion clusters. Clusters, 6, 7, 8, 12 and 14 are the clusters from which no genes were excluded due to concerns about genome assembly. Each tree was calculated based on the entire sequence from the start to the end of each cluster (excluding flanking regions). Clades (1 – 5) and sub-clades (2a and 2b, 4a and 4b) are defined based on the whole genome dendrogram (**Figure 3**). Individual parasites are marked with circles coloured according to their (sub-)clade in the whole genome dendrogram. Branch lengths are relative such that the distance between the two most distant individuals is 1, and so absolute distance differs among the panels.

Expansion Cluster 6

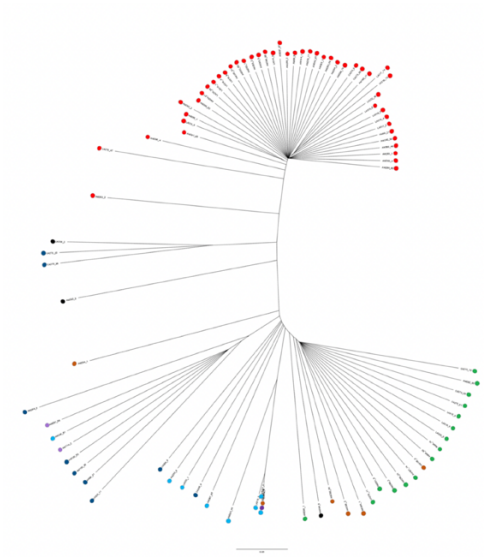

Expansion Cluster 7

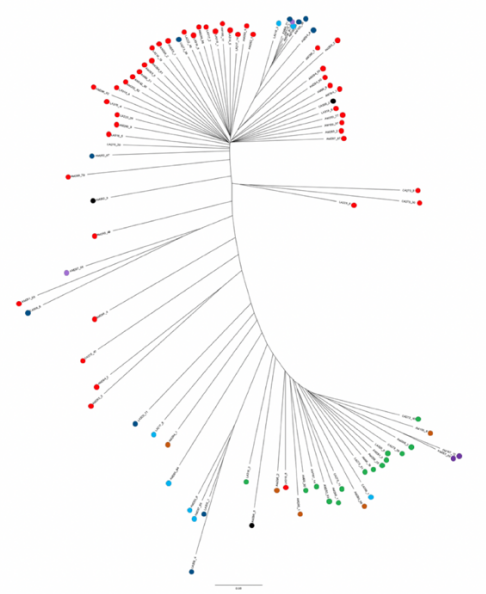

Expansion Cluster 8

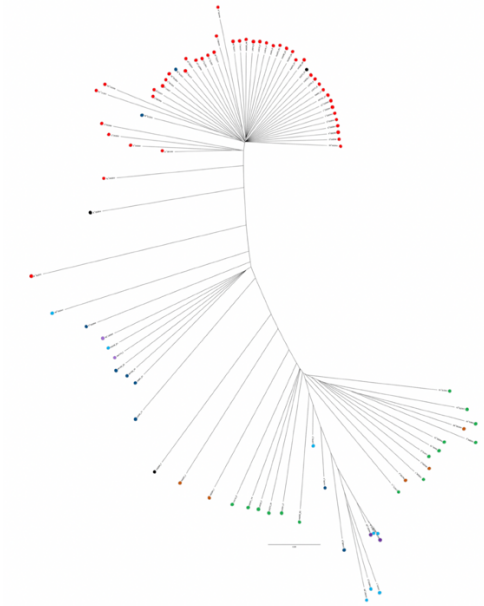

Expansion Cluster 12

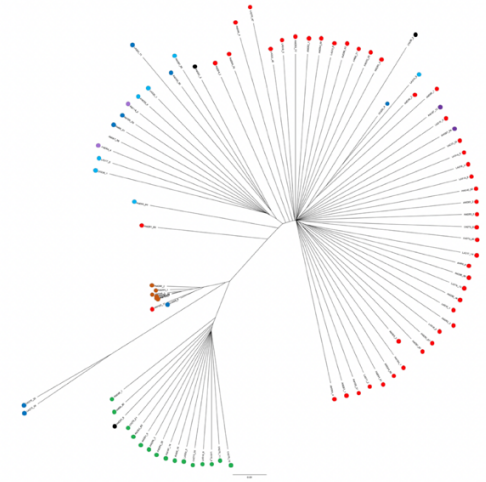

Expansion Cluster 14

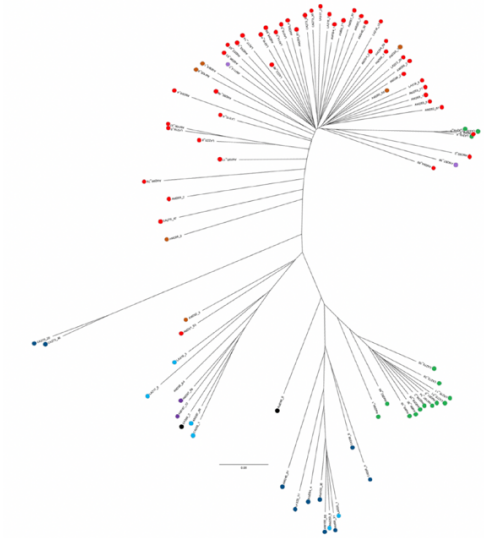

1190 **Supplementary Figure 16. Correlation of read depth and GC content for 90 *S. ratti***
1191 **larvae**. GC content is measured in non-overlapping 10 kb regions. Correlation ρ = 0.783, *df*
1192 = 4,008, P < 0.00001.
1193

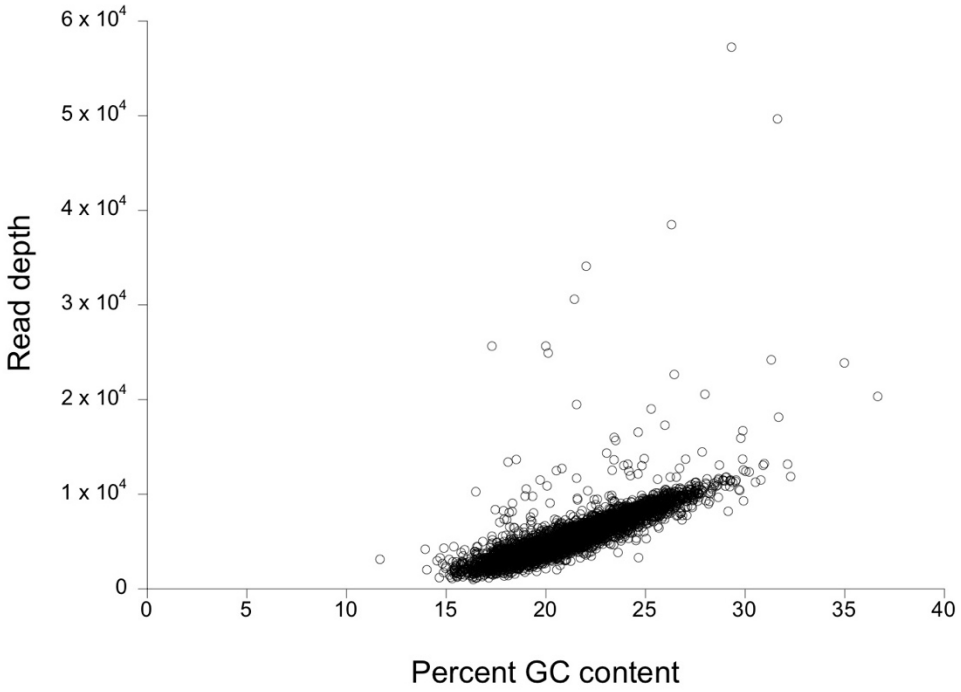

1194